

Republic of Iraq
Ministry of Higher Education
and Scientific Research
Al-Nahrain University
College of Science
Department of Chemistry



Investigation of Thermal Properties for some Ionic Liquids containing Urea and Acetamide

A Thesis

Submitted to the College of Science/Al-Nahrain University as a partial
fulfillment of the requirements for the Degree of Master of Science in
Chemistry

By:

Huda Salam Abid

B.Sc. Chemistry / College Sciences / Al-Nahrain University

Supervised by:

Dr. Hadi M. A. Abood

(Assist. Prof.)

May 2015

Rajab 1436

Supervisor Certification

I certify that this thesis entitled "Investigation of Thermal Properties for some Ionic Liquids containing Urea and acetamide" under my supervision at the College of Science/Al-Nahrain University as partial fulfillment of the requirements for the Degree of Master of Science in Chemistry.

Signature:

Name: Assist. Prof. Dr. Hadi M. A. Abood

Date: 16 \ 2 \ 2015

In view of the available recommendation, I forward this **thesis** for debate by the examining committee.

Signature:

Name: Nasreen Raheem Jber

Scientific Degree: Assist. Prof. Dr.

Head of Chemistry Department

College of Science

Al-Nahrain University

Date: 16 \ 2 \ 2015

Committee Certification

We, the examining committee certify that we read this thesis entitled "Investigation of Thermal Properties for some Ionic Liquids containing Urea and acetamide" in its contents and that in our opinion, it is accepted for the Degree of Master of Science in Chemistry.

Signature:

Name: **Mahasin F. Alias**

Scientific Degree: Prof. Dr.

Date: \ \ 2015

(Chairman)

Signature:

Name: **Rashed T. Rasheed**

Scientific Degree: Assist. Prof. Dr.

Date: \ \ 2015

(Member)

Signature:

Name: **Ammar J. Alabdali**

Scientific Degree: Lect. Dr.

Date: \ \ 2015

(Member)

Signature:

Name: **Hadi M. A. Abood**

Scientific Degree: Assist. Prof. Dr.

Date: \ \ 2015

(Member/Supervised)

I, hereby certify upon the decision of the examining committee.

Signature:

Name: **Hadi M. A. Abood**

Scientific Degree: Assist. Prof. Dr.

Dean of the College of Sciences

Date: \ \ 2015

بِسْمِ اللَّهِ الرَّحْمَنِ الرَّحِيمِ

﴿اللَّهُ لَا إِلَهَ إِلَّا هُوَ الْحَيُّ الْقَيُّومُ لَا تَأْخُذُهُ سِنَّةٌ وَلَا نَوْمٌ لَهُ مَا فِي السَّمَاوَاتِ وَمَا فِي الْأَرْضِ

مَنْ ذَا الَّذِي يَشْفَعُ عِنْدَهُ إِلَّا بِإِذْنِهِ يَعْلَمُ مَا بَيْنَ أَيْدِيهِمْ وَمَا خَلْفَهُمْ وَلَا يُحِيطُونَ بِشَيْءٍ مِّنْ

عِلْمِهِ إِلَّا بِمَا شَاءَ وَسِعَ كُرْسِيُّهُ السَّمَاوَاتِ وَالْأَرْضَ وَلَا يَئُودُهُ حِفْظُهُمَا وَهُوَ الْعَلِيُّ الْعَظِيمُ﴾.

صَدَقَ اللَّهُ الْعَظِيمُ

آية (255) سورة البقرة

الأهداء

الى من أضاء بعلمه عقل غيره وهدى بالجواب الصحيح حيرة سائله, فأظهر
بسماحته تواضع العلماء وبرحابته سماحة العارفين, الى أستاذي الفاضل
المشرف على رسالتي (أ.م.د. هادي محمد علي عبود) المحترم أدامه الله منهلًا
للعلم والمعرفة.

الى من علمني أن اصمد أمام الصعاب, إلى من علمني العطاء,

إلى من أحمل أسمه بكل افتخار ... (والدي الحنون)

إلى معنى الحب والحنان والتفاني, إلى بسمة الحياة وسر الوجود,
إلى من كان دعائها سر نجاحي وحنانها بلسم جراحي, إلى أغلى الحبايب ...
(أمي الحبيبة)

الى من بهم أكبر وعليهم أعتد وبهم استمد عزتي وإصراري, الى من
بوجودهم أكتسب قوة لا حدود لها... (إخوتي الأحبة)

الى الاخوات اللواتي لم تلدهن أمي, الى من كانوا معي على طريق النجاح
والخير, الى من اوجدهم الله لي, وعلمني أن لا أضيعهم
... (قريباتي وصديقاتي العزيزات)

Acknowledgement

First of all, Thanks to ALLAH for his blesses. The honor is mine to express my sincere thanks and gratitude to my supervisor Dr. Hadi M. A. Abood for suggestion this project, advice, continuous encouragement, his valuable guidance and sustained efforts throughout my study.

Sincere thanks are due to the Chemistry Department, Al-Nahrain University and to Staff of the department, specially the head of the department Dr. Nasreen Raheem Jber and M. Widad Mohammed Shaaban.

A great thanks are gone to the Physics Department, Al-Nahrain University especially to Dr. Hassan N. Hashim.

My deepest thanks and appreciation to my lovely family, for their patience with me, their financial and moral support.

Finally, sincere thanks and deep respect go to all my doctors in chemistry department for their support. Thanks to all my friends for their help and support.

Huda 2015

Summary

Characterization of some room temperature ionic liquids (RTILs) as candidates for thermal storage media and heat transfer fluids in thermal applications were investigated. Five ionic liquids prepared from ammonium alum $[\text{NH}_4\text{Al}(\text{SO}_4)_2 \cdot 12\text{H}_2\text{O}]$ pronounced S, as inorganic salt with urea $[\text{NH}_2\text{CONH}_2]$ pronounced U, or acetamide $[\text{CH}_3\text{CONH}_2]$ pronounced A, as organic compounds, and aluminum nitrate $[\text{Al}(\text{NO}_3)_3 \cdot 9\text{H}_2\text{O}]$ pronounced N with urea or acetamide compounds in different mole ratios were investigated alone and with addition of some improving materials to study their synergetic effect using thermo-gravimetric analysis (TGA), Differential Scanning Calorimetry (DSC), X-ray diffraction (XRD), Fourier Transform Infrared (FTIR) spectroscopy and conductivity measurements. Thermo-physical properties such as enthalpy ΔH , heat capacity C_p and thermal energy storage capacity were determined. It was found that hydrated aluminum nitrate:acetamide (1:22 mole ratio, AN2IL) alone and hydrated ammonium aluminum sulfate:urea (1:5 mole ratio, USIL) alone or with addition of some materials characterized with high density, chemical stability, heat capacity, thermal energy storage capacity and wide temperature range. The results indicated that ionic liquids alone or with addition of some materials could be considered as a promising candidate for liquid thermal storage media and heat transfer fluids.

Studying the synergetic effect by addition of some alkali metal hydroxide (NaOH) with hydrated aluminum nitrate:urea (1:1.2 mole ratio, UNIL) and KOH with hydrated ammonium aluminum sulfate:urea (1:5 mole ratio, USIL) ionic liquids increased thermal energy storage capacity of these ionic liquids, while the addition of NaOH to hydrated aluminum nitrate:acetamide (1:22

mole ratio, AN2IL) gave less thermal stability and storage capacity of ionic liquid.

Also addition of alkaline earth metal oxide MgO, CaO to hydrated ammonium aluminum sulfate:urea (1:5 mole ratio, USIL) and BaO to hydrated aluminum nitrate:urea (1:1.2 mole ratio, UNIL) decreased thermal stability, heat capacity and thermal energy storage capacity than ionic liquid alone.

Moreover, addition of transition metal oxide ($\text{VOSO}_4 \cdot 5\text{H}_2\text{O}$, CuO and ZnO) to hydrated ammonium aluminum sulfate:urea (1:5 mole ratio, USIL) increased thermal stability and storage capacity of hydrated ammonium aluminum sulfate:urea (1:5 mole ratio, USIL), while the addition of NiO to hydrated ammonium aluminum sulfate:urea (1:5 mole ratio, USIL) only improve thermal stability of ionic liquid.

Contents

	Subject	Page
Abstract.		I
Contents.		III
List of Figures.		V
List of Tables.		X
Abbreviations.		XII
Notations.		XIII

Chapter One Introduction

1.1 Introduction.	1
1.2 Some thermal and physical properties of ionic liquids.	3
1.3 Important applications of ionic liquids.	9
1.4 Heat storage materials.	11
1.4.1 Rocks.	12
1.4.2 Water.	14
1.4.3 Organic materials.	15
1.4.4 Thermal oils.	16
1.4.5 Molten salts.	17
1.4.6 Ionic liquids.	18
1.5 Thermal analysis.	23
1.5.1 Simultaneous thermal analysis (STA).	24
1.5.2 Thermogravimetric analysis (TGA).	24
1.5.3 Differential Scanning Calorimetry (DSC).	27

1.5.4 Determination of thermo-physical properties.	28
1.6 Aim of the work.	32

Chapter Two Experimental Part

2.1 Chemicals.	33
2.2 Experimental methods.	34
2.2.1 Preparation of Room Temperature Ionic Liquids (RTILs).	34
2.2.1.1 Ionic liquid preparation with acetamide.	34
2.2.1.2 Ionic liquid preparation with urea.	34
2.2.2 Added salts to ionic liquids.	35
2.3 Instruments and measurements.	36
2.3.1 Simultaneous thermal analysis (STA).	36
2.3.2 X-Ray Diffraction (XRD).	36
2.3.3 Fourier Transform Infrared Spectroscopy (FTIR).	36
2.3.4 Conductivity, Density and Freezing Point measurements.	37

Chapter Three Results and Discussion

3.1 Thermal Analysis (TGA/DTG & DSC), ATR-FTIR spectroscopy and X-ray diffraction (XRD) of Ionic Liquids.	38
3.1.1 ATR-FTIR spectroscopy, thermal decomposition behavior X-ray diffraction (XRD) of hydrated ammonium aluminum sulfate:acetamide (ASIL).	39
3.1.2 ATR-FTIR spectroscopy, thermal decomposition behavior X-ray diffraction (XRD) of hydrated ammonium aluminum	46

sulfate:urea (USIL).	
3.1.3 ATR-FTIR spectroscopy, Thermal decomposition behavior and X-ray diffraction (XRD) of hydrated aluminum nitrate:acetamide (ANIL, 1:2.4 mole ratio) and (AN2IL, 1:22 mole ratio).	52
3.1.4 ATR-FTIR spectroscopy, Thermal decomposition behavior and X-ray diffraction (XRD) of hydrated aluminum nitrate:urea (UNIL).	63
3.2 Thermo-physical properties of ionic liquids.	68
3.2.1 Thermal properties.	68
3.2.2 Conductivity (κ).	71
3.2.3 Density (ρ).	73
3.2.4 Enthalpy (ΔH).	74
3.2.4 Heat capacity (C_p) and thermal energy storage capacity (E).	75
3.3 Addition of some materials to ionic liquids (ILs).	80
3.3.1 Addition of alkali metal hydroxide to ILs.	80
3.3.2 Addition of alkaline earth metal oxide to ILs.	86
3.3.3 Addition of transition metal oxide to ILs.	92
Conclusion.	99
Future Work.	101
References.	102

List of Figures

Figure No.	Description	Page No.
1-1	A general STA chart.	24
1-2	A general TGA/DTG curve.	25
1-3	TGA/DTG for calcium oxalate.	27
1-4	A general DSC thermogram.	28
1-5	DSC measurement of specific heat capacity. (a) baseline (empty), (b) sample and (c) reference.	29
3-1	FTIR of (hydrated ammonium aluminum sulfate: acetamide, ASIL with 1:5 mole ratio) (black line), hydrated ammonium aluminum sulfate (blue line) and urea (red line).	40
3-2	Thermogravimetric Analysis TGA (1), Differential Thermal Analysis DTG (2), Differential Scanning Calorimeter DSC (3) of (hydrated ammonium aluminum sulfate: acetamide, ASIL with 1:12 mole ratio) heated from room temperature to 500 °C at 10 °C/min.	43
3-3	X-ray diffraction of (hydrated ammonium aluminum sulfate:acetamide, ASIL with 1:12 mole ratio) after heating it from room temperature up to 500 °C.	44
3-4	FTIR of (hydrated ammonium aluminum sulfate: acetamide, ASIL with 1:12 mole ratio) (black line) and (red line) after heating it to 500 °C.	46
3-5	FTIR of (hydrated ammonium aluminum sulfate:urea, USIL with 1:5 mole ratio) (black line), hydrated	47

	ammonium aluminum sulfate (blue line) and urea (red line).	
3-6	Thermogravimetric Analysis TGA (1), Differential Thermal Analysis DTG (2), Differential Scanning Calorimeter DSC (3) of (hydrated ammonium aluminum:urea, USIL with 1:5 mole ratio) heated from room temperature to 517 °C at 10 °C/min.	50
3-7	X-Ray diffraction of (hydrated ammonium aluminum sulfate:urea, USIL with 1:5 mole ratio) after heating to 500 °C.	50
3-8	FTIR of (hydrated ammonium aluminum sulfate:urea, USIL with 1:5 mole ratio) (black line) and (red line) after heating it to 500 °C.	52
3-9a	FTIR of (hydrated aluminum nitrate:acetamide, ANIL with 1:1.2 mole ratio) (black line), hydrated aluminum nitrate (blue line) and acetamide (red line).	54
3-9b	FTIR of (hydrated aluminum nitrate:acetamide, AN2IL with 1:22 mole ratio) (black line), hydrated aluminum nitrate (blue line) and acetamide (red line).	55
3-10	Thermogravimetric Analysis TGA (1), Differential thermal Analysis DTG (2), Differential scanning calorimeter DSC (3) of (hydrated aluminum nitrate:acetamide, ANIL with 1:2.4 mole ratio) heated from room temperature to 495 °C at 10 °C/min.	59
3-11	Thermogravimetric Analysis TGA (1), Differential thermal Analysis DTG (2), Differential scanning calorimeter DSC (3) of (hydrated aluminum nitrate:	60

	acetamide, AN2IL with 1:22 mole ratio) heated from room temperature to 495 °C at 10 °C/min.	
3-12	X-ray diffraction of (hydrated aluminum nitrate: Acetamide, AN2IL with 1:22 mole ratio) after heating it up to 500 °C.	62
3-13	FTIR of (hydrated aluminum nitrate: Acetamide, ANIL with 1:2.4 mole ratio) (black line) and (red line) after heating it up to 500 °C.	62
3-14	FTIR of (hydrated aluminum nitrate: Acetamide, AN2IL with 1:22 mole ratio) (black line) and (red line) after heating it up to 500 °C.	63
3-15	FTIR of (hydrated aluminum nitrate:urea, UNIL with 1:1.2 mole ratio) (black line), hydrated aluminum nitrate (blue line) and urea (red line).	64
3-16	Thermogravimetric TGA (1), Differential thermal Analysis DTG (2), Differential scanning calorimeter DSC (3) of (hydrated aluminum nitrate: urea, UNIL with 1:1.2 mole ratio) heated from room temperature to 471 °C at 10 °C/min.	66
3-17	X-Ray diffraction of (hydrated aluminum nitrate:urea, UNIL with 1:1.2 mole ratio) after heating to 500 °C	67
3-18	FTIR of (hydrated aluminum nitrate:urea, UNIL with 1:1.2 mole ratio) (black line) and (red line) after heating to 500 °C.	68
3-19	Conductivity (mS/cm) of (a): hydrated aluminum nitrate:urea, UNIL with 1:1.2 mole ratio, (b): hydrated ammonium aluminum sulfate: urea, USIL with 1:5 mole	73

	ratio), (c): hydrated ammonium aluminum sulfate:acetamide, ASIL with 1:12 mole ratio and (d): hydrated aluminum nitrate:acetamide, ANIL with 1:2.4 mole ratio versus temperature up to 70 °C.	
3-20	DSC thermogram in μV for; (1): baseline, (2): reference material (Al_2O_3), (3): hydrated ammonium aluminum sulfate:acetamide, ASIL with 1:12 mole ratio, (4): hydrated ammonium aluminum sulfate:urea, USIL with 1:5 mole ratio, (5): hydrated aluminum nitrate:acetamide, ANIL with 1:2.4 mole ratio, (6): hydrated aluminum nitrate:acetamide, AN2IL with 1:22 mole ratio, (7): hydrated aluminum nitrate:urea, UNIL with 1:1.2 mole ratio at 10 °C/min.	78
3-21	TGA/ DSC of (hydrated aluminum nitrate:urea, UNIL with 1:1.2 mole ratio) (blue color) and with addition of sodium hydroxide (red color) at 10 °C/min.	81
3-22	TG/DSC of (hydrated aluminum nitrate:acetamide, AN2IL with 1:22 mole ratio) (blue color) and with addition of sodium hydroxide in (red color) at 10 °C/min.	83
3-23	TG/DSC of (hydrated ammonium aluminum sulfate:urea, USIL with 1:5 mole ratio) (blue color) and with addition of potassium hydroxide (red color) at 10 °C/min.	85
3-24	TG/DSC of (hydrated ammonium aluminum sulfate:urea, USIL with 1:5 mole ratio) (blue color) and with addition of magnesium oxide (red color) at 10 °C/min.	87
3-25	TG/DSC of (hydrated ammonium aluminum sulfate:urea, USIL with 1:5 mole ratio) (blue color) and with addition	89

	of calcium oxide (red color) at 10 °C/min.	
3-26	TG/DSC of (hydrated aluminum nitrate:urea, UNIL with 1:1.2 mole ratio) (blue color) and with addition of barium oxide(red color) at 10 °C/min.	91
3-27	TGA/DSC of (hydrated ammonium aluminum sulfate: urea, USIL with 1:5 mole ratio) (blue color) and with addition of nickel oxide in red color (red color) at 10 °C/min.	93
3-28	TGA/DSC of (hydrated ammonium aluminum sulfate: urea, USIL with 1:5 mole ratio) (blue color) and with addition of copper oxide in red color(red color) at 10 °C/min.	95
3-29	TGA/DSC of (hydrated ammonium aluminum sulfate: urea, USIL with 1:5 mole ratio) (blue color) and with addition of zinc oxide in red color(red color) at 10 °C/min.	96
3-30	TGA/DSC of (hydrated ammonium aluminum sulfate: urea, USIL with 1:5 mole ratio) (blue color)and with addition of vanadyl sulfate pentahydrate in red color(red color) at 10 °C/min.	98

List of Tables

Table No.	Description	Page No.
1-1	Heat capacity of some important heat storage materials with their temperature range.	12
1-2	Some physical properties of imidazolium based ionic liquids.	19

1-3	Thermo-physical characteristic of tetrabutylammonium based ionic liquids.	20
1-4	Thermal characteristics of tetraethylammonium based ionic liquids.	20
2-1	Specification of the chemicals.	33
3-1	FTIR vibration frequencies of hydrated ammonium aluminum sulfate:acetamide, ASIL with 1:12 mole ratio.	40
3-2	X-ray data of the product of (hydrated ammonium aluminum sulfate:acetamide, ASIL with 1:12 mole ratio) heated up to 500°C compared with $Al_2(SO_4)_3$ standard data.	45
3-3	FTIR vibration frequencies of hydrated ammonium aluminum sulfate:urea, USIL with 1:5 mole ratio.	48
3-4	X-ray data of the product of (hydrated ammonium aluminum sulfate:urea, USIL with 1:5 mole ratio) heated up to 500°C compared with $NH_4Al(SO_4)_2$ standard data.	51
3-5	FTIR vibration frequencies of hydrated aluminum nitrate: acetamide, ANIL with 1:2.4 and AN2IL with 1:22 mole ratios.	55
3-6	FTIR vibration frequencies of hydrated aluminum nitrate: urea, UNIL with 1:1.2 mole ratio.	64
3-7	Thermo-physical properties of five room temperature ionic liquids.	70
3-8	Conductivity (\bar{k}) and PH of five room temperature ionic liquids.	72
3-9	Enthalpy (ΔH) and entropy (ΔS) of five room temperature ionic liquids.	75
3-10	A comparison of reported heat capacities (C_p), densities (ρ),	77

	temperature range (°C) and thermal energy storage capacities (E) of some heat storage materials compared with ionic liquids present work.	
3-11	Thermal characteristics of ionic liquids with some alkali metal hydroxide.	81
3-12	Thermal characteristics of ionic liquids with some alkaline earth metal oxide.	86
3-13	Thermal characteristics of (hydrated ammonium aluminum sulfate:urea, USIL with 1:5 mole ratio) with some transition metal oxide.	92

Abbreviations

Abbreviation	Name
ILs	Ionic Liquids
RTILs	Room Temperature Ionic Liquids
SAIL	Hydrated ammonium aluminum sulfate:acetamide in 1:12 mole ratio
USIL	Hydrated ammonium aluminum sulfate:urea in 1:5 mole ratio
ANIL	Hydrated aluminum nitrate:acetamide in 1:2.4 mole ratio
AN2IL	Hydrated aluminum nitrate:acetamide in 1:22 mole ratio
UNIL	Hydrated aluminum nitrate:urea in 1:1.2 mole ratio

[C ₂ MIm] ⁺	1-ethyl-3-methylimidazolium
[BF ₄]	tetrafluoroborate
[PF ₆] ⁻	hexafluorophosphate
[Tf ₂ N] ⁻	bis(trifluorosulfonyl)imide
CF ₃ SO ₃ ⁻	trifluoromethylsulfonate
[C ₂ EIm] ⁺	1-ethyl-3-ethylimidazolium
[C ₄ EIm] ⁺	1-butyl-3-ethylimidazolium
[C ₂ MIm] ⁺	1-ethyl-3-methylimidazolium
[C ₄ MIm] ⁺	1-butyl-3-methylimidazolium
[C ₈ MIm] ⁺	1-octyl-3-methylimidazolium
[CH ₃ SO ₃] ⁻	Methane sulfonate
[CF ₃ CO ₃] ⁻	Trifluoroacetate
[C ₃ F ₇ CO ₂] ⁻	Perfluorobutanoate
[(CF ₃ SO ₂) ₂ N] ⁻	1,1,1-trifluoro-N-[(trifluoromethylsulfonyl)] ⁻
[C ₄ MP] ⁺	N-butyl-N-methyl-pyrrolidinium
[MMC ₃ Im]	1-2-dimethyl-3-propylimidazolium
[RMIm]	1-Alkyl-3-methylimidazolium
[N(CN) ₂] ⁻	Dicyanamide anion
[1C ₆ -2C ₃ -3,5C ₂ py]	1-hexyl-2-propyl-3,5-diethylpyridinium salt
TFA	Trifluoroacetate
[C ₈ MIm]	1-octyl-3-methylimidazolium
[C ₁₆ CPTS]	<i>N</i> -hexadecyl-ε-caprolactam Cation-Based Toluene- <i>p</i> -sulfonate
[N ⁺ ₄₄₄₄]	tetrabutylammonium cation

Notations

Symbols	Name	Units
E	Thermal energy storage density	kJ/m^3
ρ	density	kg/m^3
C_p	specific heat capacity	kJ/K.kg
$C_p(s)$	specific heat of the sample	kJ/K.kg
$C_p(r)$	specific heat of the reference	kJ/K.kg
ΔT	change in temperature	K
Mwt	Molecular weight	g/mol
m	Weight	mg
M(s)	mass of the sample	mg
M(r)	mass of the reference	mg
H(s)	differential potential (in μV) of the signal between the base line and the sample	μV
H(r)	differential potential (in μV) of the signal between the baseline and reference	μV
ΔH	Latent heat, enthalpy	kJ/kg
ΔH_f	heat of fusion	kJ/kg
ΔS	Entropy	$\text{kJ/kg.}^\circ\text{C}$
ΔG	Gibbs free energy	kJ/kg
D	crystallite size	nm
\hat{k}	conductivity	mS.cm^{-1}
k	constant	

λ	wave length of X-ray	Å°
β	full width of diffraction peak at half maximum (FWHM) intensity	
θ	Bragg angle	degree

Chapter One
Introduction

Chapter One

Introduction

1.1 Introduction:-

The early history of ionic liquids began in 1888, when ethanolanmonium nitrate (mp 52-55 °C) was reported by Gabriel^[1]. Later in 1914, one of the earlier known room temperature ionic liquids was $[\text{C}_2\text{H}_5\text{NH}_3][\text{NO}_3]$, excogitated by Walden^[2]. He viewed the physical properties of ethyl ammonium nitrate, $[\text{C}_2\text{H}_5\text{NH}_3][\text{NO}_3]$, which had a melting point of 12 °C produced from the reaction of concentrated nitric acid with ethylamine.

In 1951 Hurly and Weir declared that a room temperature ionic liquid could be prepared by mixing and warming 1-ethylpyridinium chloride with aluminum chloride^[3]. In 1970s and 1980s Osteryoung *et al.* and Hussy *et al.* carried extensive studies on organic chloride- aluminum chloride ambient temperature ionic liquid and the first major review of room temperature ionic liquids was published^[4]. The ionic liquids based on aluminum chloride $[\text{AlCl}_3]$ can be considered as the first generation of room temperature ionic liquids. The hygroscopic nature of AlCl_3 based ionic liquids has delayed the development in their use. In multiple science applications they have to be prepared and handled under inert gas atmosphere. Thus, the synthesis of air and water stable ionic liquids, which are considered as the second generation of ionic liquids attracted further interest in the use of ionic liquids in various fields^[5].

In 1992, Wilkes and Zaworotko confessed the first air and moisture stable ionic liquids based on 1-ethyl-3-methylimidazolium $[\text{C}_2\text{MIm}]^+$ cation with either tetrafluoroborate $[\text{BF}_4]^-$ or hexaflourophosphate $[\text{PF}_6]^-$ as anions like

$[\text{C}_2\text{MIm}]^+[\text{BF}_4]^-$, was prepared via metathesis of $[\text{C}_2\text{MIm}]^+\text{I}^-$ with $\text{Ag}[\text{BF}_4]$ in methanol. Unlike the chloroaluminate ionic liquids, these ionic liquids should be prepared and safely stored out off an inert atmosphere. Generally, these ionic liquids are water stable, however, the exposure for a moisture to long time may cause some change in their physical and chemical properties^[6].

In 2006 several scientists, e.g. Welton, Wasserscheid, MacFarlane, Endres, and others, came in this field having a strong impact in offering the ionic liquids in many applications. They focused on the syntheses and characteristics of environmentally friendly ionic liquids as green solvents. They measured and established physicochemical characteristics for many ionic liquids with the aim of providing data to start evaluating the use of ionic liquids in a variety of processes. Also, they work on the development of new materials from cellulose employing ionic liquids^[7].

Wasserscheid is an active member of the ionic liquids community concentrated on the preparation and characterization of ionic liquids for use in the biphasic catalysis. For example, he could show that the use of hexafluorophosphate ionic liquids give selective, biphasic oligomerization of ethylene to 1-olefins. Together with Welton; they edited important book entitled "ionic liquids in synthesis", which proffers the synthesis and physicochemical properties of ionic liquids as well as their use in catalysis, polymerization, organic and inorganic synthesis^[8]. MacFarlane has prepared a new air and water stable ionic liquids to employing such ionic liquids as indicators for sensing and displaying an environmental parameter like humidity. This process was controlled by the color change of the ionic liquids where they are synthesized with either a colored cation or anion, so that the ionic liquids themselves are indicators. Also, he has published many papers on the use of ionic liquids in electropolymerization and in the batteries^[9,10].

1.2 Some Thermal and Physical properties of ionic liquids:-

1.2.1 Melting point:

As a class, ionic liquids have been defined to have melting points less than 100 °C and most of them are liquids at room temperature. Both cations and anions share to the low melting point of ionic liquid. The increase in anion size result in a decrease in melting point^[8]. Another example, the melting point of [C₂MIm]⁺ type ionic liquid with different anions such as [BF₄]⁻ and [Tf₂N]⁻ are 15 °C and -3 °C^[11], respectively. Cations size and the symmetry make an important effect on the melting points of ionic liquids. Large cations and increased asymmetric substitution leads to a melting point reduction^[8].

1.2.2 Density:

In general ionic liquid are denser than water with values ranging from 1 to 1.6 g/ml and their densities decrease with increase in the length of the alkyl chain in the cation. For example, the density in ionic liquids composed of substituted imidazolium cation and CF₃SO₃⁻ anions decrease from 1.39 g/ml for [C₂MIm]⁺ to 1.33 g/ml for [C₂EIm]⁺, to 1.29 g/ml for [C₄MIm]⁺ and to 1.27 g/ml for [C₄EIm]⁺^[12], the densities of ionic liquid are also affected by the identity of anions. Another example, the densities of 1-butyl-3-methyl imidazolium type ionic liquids with various anions, such as BF₄⁻, PF₆⁻, and Tf₂N⁻ are 1.12 g/ml, 1.21 g/ml, and 1.43 g/ml, respectively. The order of increasing density for ionic liquid consisted of a single anions is: [CH₃SO₃]⁻ = [BF₄]⁻ [CF₃CO₃]⁻ < [C₃F₇CO₂]⁻ < [(CF₃SO₂)₂N]⁻^[13,14].

1.2.3 Conductivity:

Ionic liquids have relatively good ionic conductivities compared with those of organic solvents/electrolyte systems (up to 10 mScm^{-1})^[8,11]. At high temperature of e.g. $200 \text{ }^\circ\text{C}$ a conductivity of 0.1 mScm^{-1} can be achieved for some systems.

However, at room temperature their conductivities are usually lower than those of concentrated aqueous electrolyte. Upon the fact that ionic liquids are consisted only of ions, it could be exerted that ionic liquids have elevated conductivities. This was not the case, yet the conductivity of any solution relies not only on the number of charge carrier but also their mobility^[15]. The large constituent ions of ionic liquids decrease the ion mobility which cause in lower conductivities. Moreover ion pair formation and/or ion aggregation results in conductivity reduction^[11].

The conductivity of ionic liquid is inversely related to their viscosity. Hence ionic liquids of higher viscosity show lower conductivity. Increasing the temperature increase conductivity and reduce viscosity^[13].

1.2.4 Viscosity:

Generally, ionic liquids are more viscous than popular molecular solvents and their viscosities are ranging from 10 mPas to about 500 mPas at room temperature. The viscosities of some common air and water stable ionic liquid at room temperature are: 312 mPas for $[\text{C}_4\text{MIm}]^+ \text{PF}_6^-$ ^[16], 154 mPas for $[\text{C}_4\text{MIm}]^+ \text{BF}_4^-$; 52 mPas for $[\text{C}_4\text{MIm}]^+ \text{Tf}_2\text{N}^-$,^[11] 85 mPas for $[\text{C}_4\text{MP}]^+ \text{Tf}_2\text{N}^-$. The viscosity of ionic liquid is demonstrated, by Vander Waals forces and hydrogen bonding. Electrostatic forces may also play significant role. Alkyl chain lengthening in the cation resulted in an increase in viscosity as a result of stronger Van der Waals forces between cations resulting in increase the

energy needed for molecular motion. Also, the ability of anions to form hydrogen bonding has an obvious effect on viscosity. The fluorinated anions as BF_4^- and PF_6^- form viscous ionic liquid due to the formation of hydrogen bonding^[16]. In general, all ionic liquids exhibit a significant decrease in viscosity as the temperature increases^[17].

1.2.5 Thermal stability:

Ionic liquid can be thermally stable up to temperature of 450 °C. The thermal stability of ionic liquid is limited by the strength of their hetero atom-carbon and their heteroatom–hydrogen bonds^[18]. Wilkes et al. reported that the ionic liquids 1-ethyl-3-methyl imidazolium tetrafluoro borate $[\text{C}_2\text{MIm}][\text{BF}_4]$, 1-butyl-3-methyl imidazolium tetrafluoro borate $[\text{C}_4\text{MIm}][\text{BF}_4]$, and 1-2-dimethyl-3-propyl imidazolium bis(trifluorosulfonyl) imide $[\text{MMC}_3\text{Im}][\text{Tf}_2\text{N}]$ are stable up to temperature of 445 °C, 423 °C, and 457 °C, respectively^[19].

Thermogravimetric analysis indicates high thermal stability for many ILs, generally up to 350 °C. Such high temperatures are only tolerated by most liquids for a short time. For example, after 10 h, even at temperatures as low as 200 °C, $[\text{RMIm}][\text{PF}_6]$ and 1-decyl-3-methylimidazolium triflate show an appreciable mass loss. Long time exposure to such high temperature inevitably leads to decomposition. The ILs with low thermal stability are $[\text{C}_2\text{MIm}][\text{X}]$, where $\text{X} = [\text{Tf}_2\text{N}]^-$ and Br^- ^[20]. Phosphonium ILs with $[\text{Tf}_2\text{N}]^-$ or $[\text{N}(\text{CN})_2]^-$ anions decompose completely to volatile products in a single step. The degradation products indicate that Hofmann elimination process and/or dealkylation reactions occurred. Conversely, ILs based on nitrogen cations do not decompose completely^[21]. The start of thermal decomposition is furthermore similar for the different cations but appears to decrease as the

anion hydrophilicity increases. It has been suggested that the stability dependency on the anion is in the order $[\text{PF}_6]^- > [\text{Tf}_2\text{N}]^- > [\text{BF}_4]^- > \text{halides}$.

An increase in cation size, at least from 1-butyl to 1-octyl, does not offer large effect [22]. Commonly most of the ionic liquids have extremely low vapor pressures. This allows removing water by simple heating under vacuum. Water contents below 1 ppm are quite easy to achieve with most of the liquid [23].

1.2.6 Volatility:

Ionic liquids (ILs) are actual nonvolatile in the sense at near ambient temperatures, their vapor pressure is negligible [24]. For typical ILs, normal boiling temperatures (T_b), which related to the vapor pressure of ILs at one atmosphere, cannot be experimentally determined as ILs decomposes at a lower temperature. It has nevertheless been reported that ILs can be distilled at 200–300 °C but under significantly reduced pressure and at very low distillation rate ($<0.01 \text{ gh}^{-1}$). Vapor pressure of ILs remains, however, negligible at near ambient conditions; thus, for all practical purposes, they may be considered as nonvolatile solvents [25]. On the whole, the negligible volatility of these ILs denotes that air pollution by gaseous release is not a concern. ILs are considered as nonvolatile and, consequently, nonflammable at ambient and higher temperatures. However, the potential release of IL vapors (or decomposition products) must be considered when ILs are used at high temperatures [2].

1.2.7 Electrochemical window:

The electrochemical window is an important character and plays a key role in using ionic liquids in electrodepositing of metals and semiconductors. By

definition, the electrochemical window is the electrochemical potential range in which the electrolyte is neither reduced nor oxidized at an electrode [26]. This value indicates the electrochemical stability of solvents. As known, the electrodeposition of elements and compounds in water is limited by its low electrochemical window of only about 1.2 V, versus, ionic liquids have significantly larger electrochemical windows, e.g., 4.15 V for $[\text{C}_4\text{MIm}]^+\text{PF}_6^-$ at a platinum electrode, 4.10 V for $[\text{C}_4\text{MIm}]^+\text{BF}_4^-$ [27] and 5.5 V for $[\text{C}_4\text{MP}]^+\text{Tf}_2\text{N}^-$ at a glassy carbon electrode. In general, the broad electrochemical windows of ionic liquids have opened the door to electrodeposited metals and semiconductors at room temperature which were olden obtained only from high temperature molten salts. For example, Al, Mg, Si, Ge, and rare earth elements can be obtained from room temperature ionic liquids. The thermal stability of ionic liquids permits to electrodeposits Ta, Nb, V, Se and presumably many other ones at elevated temperature [16].

1.2.8 Heat Capacity:

Heat capacity refers to the amount of energy per molecule that a compound can store by increasing temperature. Generally this energy is stored in translational, vibrational and rotational modes. Thus higher heat capacity expected to found in materials with greater number of atoms in its composition [28]. The values of heat capacities of 24 ILs, pyridinium-based, imidazolium, and ammonium ILs were presented. The high value ($766 \text{ J mol}^{-1} \text{ K}^{-1}$ at 298 K) was observed for 1-hexyl-2-propyl-3,5-diethylpyridinium salt, $[\text{1C}_6\text{-2C}_3\text{-3,5C}_2\text{py}][\text{Tf}_2\text{N}]$. Also it was found that heat capacity increases linearly with increasing molar mass for these compounds that are comprised of a limited number of different atoms [30].

1.2.9 Heat of Fusion (ΔH):

It is the amount of thermal energy that a material must absorb or release in order to change its phase from solid to liquid and vice versa. These values can be straight away calculated from the area included in the DSC melting endotherm. High values of heat of fusion lead to more efficient thermal energy storage devices TESDs^[30]. Certain ionic liquids possessing liquid crystalline behavior can have multiple values of heat of fusion ranged from 100 kJ.mol⁻¹ to 200 kJ.mol⁻¹. These values correspond to the morphological change in the material occurring in the same phase. The changes usually occur in a narrow temperature range. Thus it is possible to use ILs as thermal energy storage TES devices. While using ILs as TESD, the summation of small heat changes occurring in the neighborhood of the phase change temperature can be considered as effective heat of fusion^[31].

1.2.10 Hygroscopic:

The water content has an impact on the viscosity of the ionic liquid. Viscosity measurement determines that ionic liquids become less viscous with rise water content. Hydrolysis problems may also occur^[3]. Moisture sensitivity and the difficulty of separation of products owning heteroatom from the ionic liquid infect. In order to progress chemistry of ionic liquids, and increase the robustness of processes, water-stable ionic liquids have been found to be hydrophobic but yet readily dissolve many organic molecules ^[32].

1.2.11 The color:

The high quality ionic liquid has been showed to be colorless, but they are not 100 % pure. Generally, the color of less pure ionic liquids ranges from yellowish to orange. The formation of the color was resulted from using raw materials with color or excessive heating through the synthesis of imidazolium salt. Several precautions for synthesis of colorless ionic liquid

has been described. A procedure to remove the color from impure ionic liquid using acidic alumina (Al_2O_3) and activated charcoal has also been suggested [8].

1.3 Important applications of Ionic Liquids:-

Ionic liquids (ILs), considered to be a relatively recent magical chemical due to their unique properties, have a large diverse applications in all field of the chemical industries. The most important applications are:

1.3.1 Homogeneous and heterogeneous catalyst:-

For some applications, ionic liquids exhibit the better benefit of both homogeneous and heterogeneous catalysts. Because of chosen ionic liquids could be immiscible with the reactants and products and the catalysts still soluble.

This has the advantages of a solid for immobilizing the catalyst, with the advantages of a liquid for permitting the catalyst to mobilize freely [33-35].

1.3.2 Biological reactions media:-

Enzymes are stable in ionic liquids, opening the probability of ionic liquids to be applied in biological reactions. Synthesis of pharmaceuticals is an example of such application [34,35].

Ionic liquid-water biphasic systems were widely studied and applied as new energy-storage processes for condensation, separation, extraction and of biopolymers [36]. Mainly stabilization and solubilization of proteins in isolated hydrophobic ionic liquid phase more than aqueous phase could lead to the interesting application of ionic liquids for product separation systems and/or continuous enzymatic reaction.

1.3.3 Removing of metal ions:-

In another application, Davis and Rogers were designed and synthesized a number of novel ionic liquids to eliminate cadmium and mercury from pollutant water. When these water immiscible ionic liquids become in contact with pollutant water, they arrest the metal ions outside of water and insulate them in the ionic liquid^[37].

1.3.4 Purification of gases:-

Ionic liquids can selectively dissolve and remove gases and might be applied for air purification on spaceships and submarines, it was found that aluminum chloride-urea ionic liquid effective in carbon dioxide capture^[38]. RTILs had a special potential as designer solvents in the gas capturing and can be used in CO₂/CH₄ and ethylene (C₂H₄)/ethane (C₂H₆) isolations. RTILs can be used as a basis for development substituent strong absorption solvents. Generally, pattern ionic liquids with fluorine-constituent anions, such as BF₄, PF₆, Tf₂N, TFA, gave the higher CO₂ absorption capacity. The highest CO₂ solubility was performed with the ionic liquid [C₂MIm][NTf₂], with a molar fraction of 0.23 at 303 K. The large gas capacity of this ionic liquid might be belonged to weaker anion-cation interaction, which permits a large interaction with ions of the liquid and the gas solute^[39].

1.3.5 Heat storage media:-

Ionic liquids had excellent technical features for the applications as liquid heat transfer fluids and thermal storage media. The features include high heat capacity, high chemical stability, wide liquid temperature range, high density, non-volatility and high storage density. For example C₈MImPF₆ ionic liquid, have storage density of 378 MJ/m³ and liquid temperature range from (-75 to 416) °C^[40], also it is found that [C₄MIm][Tf₂N] ionic liquid have some advantages over other ILs. The calculated sensible heat storage density for [C₄MIm][Tf₂N] was more than 170 MJ/m³ when the inlet and outlet region

temperature were 210 °C and 310 °C. It is found that these ionic liquids were suitable for application as heat-transfer fluids and they are over present commercial heat transfer fluids due to low vapor pressure, wide liquid temperature range and ability to store essential sensible heat [41].

1.4 Heat Storage materials:-

The demand and supply gap for energy sources increased day by day. Moreover, the fact that "energy can neither be created nor destroyed" has led in focused of some scientific research in the direction of storing the different forms of energy using various heat storage materials. Heat storage materials are materials with the ability to store energy and then release it in a continuous manner, which were chosen on the basis of several limited physical, chemical and economic properties [41,42].

Recently, various conventional and unconventional compounds were studied to demonstrate their capability to store thermal energy. Such materials had their melting points within the usable temperature range and hence known as phase changing materials (PCMs) [43].

Several thermophysical, chemical and economic assets were desired of an ideal phase change material to be used as heat storage materials. It is expected that PCMs would have high value of density, heat capacity, thermal conductivity and heat of fusion [3,44]. There were a large range of various materials which could be used for thermal storage. One of the most significant physical parameters of a thermal storage was its storage capacity and temperature range. These two parameters determine the volume and suitability of the storage for an application, respectively [44,45]. Table (1-1) gave a summary of the storage capacity and temperature range of some important storage materials.

Table (1-1): Heat capacity of some important heat storage materials with their temperature range^[41].

Heat storage materials	Heat capacity (kJ/K.kg)	Temperature range(°C)
Water	1.6 at 100 °C	0 – 100
Rock as Granite	0.76	-
Ethylene glycol	2.1 at 100 °C	-37 - 110
Thermal oil	1.90	-30 - 300
Molten salts as 50% KNO ₃ + 7%NaNO ₃ + 43% NaNO ₂	1.56	142 - 540
Ionic liquid	2.50	-75 - 416

1.4.1 Rocks:-

Energy can be stored at low and intermediate temperatures by heating rocks held in isolated containers. This type of storage was used often for temperatures up to 100 °C connected with solar air heaters since rocks could be heated by just blowing air within the spaces between the rocks (if liquid is used in the collectors, a more developed heat-exchange mechanism will be required). Rock storage could be simple and inexpensive, but designing an optimum system might be difficult since the performance efficiency is affected by the volume, shape, specific heat, density and other characteristics for the used rocks^[45].

Direct contact between the solid storage medium and heat transfer fluid is required to minimize the expense of heat exchange of a solid storage medium. Using rocks as thermal storage^[46] provides several advantages:

1. Rocks are non-flammable and not toxic.
2. Rocks had low cost.
3. Rocks can behave as both heat transfer surface and heat storage medium.

4. Heat transfer between air and a rock surface was good, arise from very large heat transfer area with effective thermal conductance of the rock hill was low, due to the low area for a touching between the rocks. Then the heat lost from the hill is small.

The main disadvantages of using rocks as heat storage are associated with the larger air mass flow rates and surface area needed due to the lower volumetric heat capacity and thermal conductivity of air as compared to those of thermo-oils, molten salts or other heat transfer fluids proposed. These drawbacks translate into higher pressure drops and concomitant energy penalties. Energy densities for a concrete-based thermal storage system have been estimated at 22 kWh/m³, resulting in 50,000 m³ sized storage for a 50 MW parabolic trough power plant with 1100 MWh_{th} storage capacity^[47].

The difficulties and limitations relative to liquids can be avoided by using solid materials for storing thermal energy as sensible heat. However, larger amounts of solids are required compared with using water, a rise from the fact that solids, in general, shown less storing capacity than water. The cost of the storage media per unit energy stored is, anyway, still agreeable for rocks.

The use of rocks as heat storage is more limited due to their low heat capacity (~0.9 kJ/kg/K), low thermal conductivity (~6.6 W/m/K), and unknown response to long-term thermal cycling^[48]. The presence of a confined aquifer, an impermeable cap rock, compatible underground water regime, high porosity, and high permeability of the rock formation^[49].

1.4.2 Water:-

For most industrial applications, water is the most popular heat transfer fluid and the use of water as the storage medium for liquid systems has been the dominant approach and is likely to remain so for at least a decade^[50,51]. It

has high specific heat capacity, high latent thermal energy (ΔH), high density, high thermal conductivity, moderate viscosity and wide availability with low environmental impact. In contrast, the use of rocks as sensible heat storage is more limited due to their low heat capacity, low thermal conductivity, and unknown response to long-term thermal cycling^[49].

In most solar heating and hot water systems they use an insulated hot water tank located in the building equipment room or buried in the ground. It may also be possible to store very large amounts of low temperature thermal energy by pumping hot water into contained underground aquifers. Water storage tanks were made from a diverse of materials such as concrete, steel and fiberglass. The tanks were suitably insulated by mineral wool, glass wool or polyurethane resulting in high cost^[43], but the biggest difficulties for use water as a heat transfer fluid was the limited range of temperature above which it could be used. Theoretical liquid range is between 0 °C and 100 °C, but the practical temperature range of water applied as heat transfer fluid was much less than 100 °C, because of the high vapor pressure at near boiling point. The extension of the application temperature range to below freeze point can be accomplished by using antifreeze (e.g., ethylene glycol water mixture), but the extension over the boiling point of the aqueous system is extremely difficult. High pressure is needed to keep water in the liquid state when the temperature is over 100 °C, which could cause very high costs for the related pressure vessels and pipes. High temperature water (over 100 °C) was suggested for many industrial applications^[52,53], but corrosiveness and volume expansion at high temperature are its major downsides for thermal applications so it is not suitable as a heat transfer fluid nor thermal media for a solar energy power plant.

Water storage is probably not an attractive option for storage above 150 to 200 °C since the pressure required would greatly increase the cost and danger of operating such systems.

1.4.3 Organic Compounds:-

Organic compounds can also be used for storing energy as latent heat (ΔH). These materials have the advantage of relatively high heats of fusion, and few of the materials examined present problems of supercooling or high vapor pressures. Unfortunately, some of the most attractive organic materials under consideration e. g., paraffins^[54] have a relatively large volume change upon melting nearly 10 % in some cases, are flammable, and can cause stress cracking if the containment vessel is not constructed from a material as strong as steel. Experimental paraffin storage systems, however, have been operated successfully. Other materials suitable for heating include artificial spermaceti manufactured by Lipo Chemicals and paraffin wax possibly mixed with carbon tetrachloride. These materials melt in the range of 58 to 60 °C, and have heats of fusion on the order of 200 to 210 kJ kg⁻¹^[55].

Organic materials can be classified as phase change materials (PCM), and it can be subdivided into paraffin and non-paraffin compounds. Paraffin compounds are among the most reliable in latent heat storage (ΔH) systems due to their availability, cost, and safeness. They also have a wide range of melting points, are chemically inert (stable below 500 °C), and exhibit volume change upon melting on the order of 10 %^[48]. The latent heat of fusion (ΔH) of paraffins is about 200 kJ/kg. For a mass density ρ 850 kg/m³, the approximate energy density (E) of paraffin is 170 MJ/m³. However, paraffin compounds have low thermal conductivity and are chemically incompatible with some plastic containers^[49].

1.4.4 Thermal Oils:-

Heat transfer oils are used in sensible heat storage systems for intermediate temperatures ranging from 100 to 300 °C as Dowtherm and Therminol. Some of the sensible heat storage systems utilize a mixture of rocks and a heat-transfer fluid such as Therminol^[49].

All heat transfer oils share a common set of problems are low decomposition temperature, low density, inflammability, high vapor pressure, harmfulness, and low chemical stability,^[56] and they all degrade with time^[52]. Their degradation is increased rapidly if they are operated above their recommended temperature limits for any length of time. This degradation requires a filtering system and means that the relatively expensive oils must be continually replaced. The oils also can present safety problems, since they can be ignited by open flames at temperatures in the range of 165 °C (fire point) and have a high enough vapor pressure to sustain combustion at temperatures in the range of 550 °C to 600 °C ignition temperature, This means that great care should be taken to ensure that the material is not overheated, dikes will be needed to prevent the material from spreading if a leak should occur. Some systems require an inert gas (such as nitrogen) over the liquids in the tanks to inhibit reactions which might degrade the storage material^[57].

A further limitation to the use of heat transfer oils is their cost. For these reasons, they could be seriously considered to use only for small storage systems^[58].

1.4.5 Molten Salts:-

A molten salt heat transfer medium was commercialized in 1937^[59]. A number of molten inorganic salts were considered for their high temperatures 300 °C and above. One is an eutectic mixtures composed of 7 % NaNO₃, 40 % NaNO₂ and 53 % KNO₂ by weight which is available in trade name of 'Hitec'. Hitec has a melting point of 145 °C and could be used up to a temperature of 425 °C. Over this temperature; decomposition and oxidation appear to take place^[60]. A good candidate alternative molten salt formulation also available at a reasonable cost is a commercial ternary molten salt mixture known as Hitec-XL, an eutectic mixture of 48 % Ca(NO₃)₂, 7 % NaNO₃, 45 % KNO₃ (by weight), has freezing point of about 120 °C and stable to temperatures around 500 °C^[61]. Another molten salt was taken in to account for high temperature storage is NaOH, that had a melting point of 320 °C and can be used for temperatures up to 800 °C. Anyway, it is highly corrosive and there was a difficulty in containing it at higher temperatures storage in a parabolic trough plant^[62].

Due to the avoidance of high pressure, the wall thickness of the piping and the pump casings, heat exchangers, and other items of equipment were much lower than those required for high pressure steam systems operating in this temperature range. One problem is that the heat exchanger system has to be preheated to ensure that liquid metal and molten salts remain liquid. When the temperature is not high enough, molten salts freeze and cause operation problems. Although there are some operation problems as described above, the molten salts have been used in cracking units in the petroleum refining industry. The reason is that there is no better heat transfer medium available^[61,62].

Currently molten salt is used as liquid storage media. The main problems for molten salt media is its high melting point (e.g. 220 °C). The high melting point could lead to molten salt freezing in evening or cold weather, causing high operating costs^[40].

1.4.6 Ionic Liquids:-

Ionic liquids are liquid salts consist solely of ions (cations and anions) have melting point of 100 °C or below and considered as green solvents^[63]. Ionic liquids have a couple of unique features that open the door for the development of new highly specialized applications^[64,65]. Based on the experimental results, it's found that ionic liquids have excellent technical properties for the applications as liquid heat transfer fluids and thermal storage media in a solar thermal power plant^[66]. These properties include high heat capacity, wide liquid temperature range, and high density, on the other hand the combination of very low vapor pressure, good heat capacity, wide usable temperature range and great thermal stability of ionic liquids permit of their using as heat transfer media under vacuum or very low pressures^[67], another properties contribute to the qualification of ionic liquids as heat transfer fluids and liquid thermal storage media were high chemical stability, non-volatility, high storage density, non-harmfulness, and non-flammable^[68].

The use of ionic liquids as thermal fluids was first suggested by Rogers *et al.* in 2001^[40]. They studied a number of ionic liquids based on imidazolium cations with a variety of inorganic anions such as [C₄MIm][PF₆], [C₄MIm][BF₄], [C₄MIm][Tf₂N], [C₄MIm][(CF₃SO₂)₂N], [C₈MIm][BF₄], [C₈MIm][PF₆], and found that they have advantages of high density, low viscosity, non-volatility, wide liquid temperature range, high chemical

stability, high heat capacity, and high storage density ,Table(1-2) offer some of these properties^[40,41].

Table (1-2): Some physical properties of imidazolium based ionic liquids.

Ionic liquid	Melting Point (°C)	Decomposition point (°C)	Density at 25 °C (kg/m ³)	Viscosity at 25°C(mPa s)
[C ₄ mIm][PF ₆]	4	390	1370	312
[C ₄ mIm][BF ₄]	-75	407	1119	219
[C ₄ mIm][Tf ₂ N]	-89	402	1429	54.2
[C ₈ mIm][PF ₆]	-75	416	1400	-

These properties make ionic liquids excellent candidates as heat transfer fluids for solar thermal power plant system but economic application cost of ionic liquids as heat transfer fluids and liquid thermal storage media needs to further investigation^[41].

In 2010, Bhatt *et al.*^[28] study thermal energy storage capacity of some phase changing materials and ionic liquids and after a rigorous study of their properties, they unable to place ionic liquids in the final list as heat storage material due to lack of information of properties of some ionic liquids. But, in 2013 Bhatt and G. Kuldip found seven ionic liquids (ILs) based on tetrabutylammonium cation [N⁺₄₄₄₄] and inorganic anions, have good thermophysical characteristics to use as thermal energy stored materials for their applications in a solar cooker, Table(1-3) show these properties more clearly^[69].

Table (1-3): Thermo-physical characteristics of tetrabutylammonium based ionic liquids.

ILs	T _m (°C)	ρ (kg/m ³)	ΔH (kJ/kg)	C _p (kJ/kg.°C)
[N ⁺ ₄₄₄₄][BF ₄ ⁻]	71	1291	253.75	1.00
[N ⁺ ₄₄₄₄][PF ₆ ⁻]	71	1234	155.00	0.40
[N ⁺ ₄₄₄₄][BrO ₃ ⁻]	86	1050	153.71	0.30
[N ⁺ ₄₄₄₄][NO ₃ ⁻]	98	1195	144.00	1.50
[N ⁺ ₄₄₄₄][SCN ⁻]	110	1143	253.00	0.20
[N ⁺ ₄₄₄₄][Br ⁻]	102	1039	193.00	2.00
[N ⁺ ₄₄₄₄][I ⁻]	44	1279	113.00	2.70

Recently, Bhatt and G. Kuldip^[43] made further investigation on eight ionic liquid salts based on tetraethylammonium cation [N⁺₂₂₂₂] with inorganic anions like BF₄⁻, NO₃⁻, NO₂⁻, SCN⁻, BrO₃⁻, IO₃⁻, PF₆⁻ and HCO₃⁻. They found that these ionic liquids ILs deserve a consideration to replace the traditional materials used as thermal energy storage TES, due to unique properties of storing and releasing a significant amount of thermal energy in both solid and molten phases, as illustrated in Table(1-4).

Table (1-4): Thermal characteristics of tetraethylammonium based ionic liquids^[43].

ILs	T _m (°C)	T _{dec.} (°C)	ρ (kg/m ³)	C _p (kJ/kg°C)	ΔH (kJ/kg)
[N ⁺ ₂₂₂₂][HCO ₃]	74	170	1145	1.60	142.26
[N ⁺ ₂₂₂₂][BF ₄ ⁻]	91	190	1132	1.00	102.08
[N ⁺ ₂₂₂₂][PF ₆ ⁻]	82	170	1074	1.40	132.00
[N ⁺ ₂₂₂₂][BrO ₃ ⁻]	46	180	1153	0.70	118.00
[N ⁺ ₂₂₂₂][NO ₃ ⁻]	115	190	1029	0.90	137.44
[N ⁺ ₂₂₂₂][NO ₂ ⁻]	58	180	1023	1.50	157.17
[N ⁺ ₂₂₂₂][SCN ⁻]	62	160	1057	1.10	127.67
[N ⁺ ₂₂₂₂][IO ₃ ⁻]	53	180	1162	1.70	147.29

Now days, they are being studied for their use in the fields of thermal energy storage, solar power plant, solar cell^[70] and heat transfer fluids^[71]. Nucleating agents such as copper and graphite powder have been used for releasing the stored energy from super cooled ionic liquids^[72].

The efficacy of ionic liquids as thermal fluids determined by comparing the properties of ionic liquids with an existing thermal fluid, and by comparing properties with the specific needs of a device or technology^[43]. The matrix of properties determined so far indicate that ionic liquids are attractive candidates for heat transfer and storage. Properties of material that may be compared with the ionic liquids are: composition, freezing point, moisture content, viscosity, density, heat of fusion, decomposition temperature, electric conductivity, use range of temperature, cost and appearance. A set of thermal fluid target specifications for thermal trough technology was promulgated by the National Renewable Energy Laboratory. Ionic liquid properties that may be compared now with those targets are: latent heat storage density, sensible heat storage density, freezing point, thermal stability, vapor pressure, viscosity, cost. But they lack in quantitative data on materials compatibilities.

The most commonly used ILs $[\text{C}_4\text{MIm}][\text{PF}_6]$ and $[\text{C}_4\text{MIm}][\text{BF}_4]$ were known to decompose in the presence of water and as a result phosphoric and hydrofluoric acids were produced. Therefore, both toxicity and ecotoxicity provided data which give metabolism and degradability of ionic liquids were also required to label them as green solvents or study their environmental impact^[74].

Ionic liquids contain PF_6^- and BF_4^- anions were reported to be decomposed in the presence of water, giving of HF. Wasserscheid et al. referred that ionic liquids containing halogen anions generally showed poor

stability in water and also form toxic and corrosive fumes such as HCl and HF^[75]. Therefore, they suggested the use halogen-free and relatively hydrolysis stable anions for example octylsulfate compounds. The degree of hydroscopic character and interaction between water and ionic liquids were strongly dependent on anions. The quantity of water absorbed was higher in the BF_4^- and lower in PF_6^- . However, $[\text{Tf}_2\text{N}]^-$ showed much more water stability and having the advantage of an increased hydrophobic property. Ionic liquids which are water immiscible tend to absorb moisture from the atmosphere^[76].

The FTIR studies explained that the water molecules absorbed from the air were mostly found in the free state and bonded via H-bonding with the PF_6^- and BF_4^- anions. The presence of water might have great effect on the reactivity of ionic liquids^[74,77].

The newly synthesized ionic liquids were much stable than the old halogenoaluminated systems. The new ionic liquid alum such as $(\text{NH}_4\text{Al}(\text{SO}_4)_2 \cdot \text{XH}_2\text{O})$, $\text{Al}_2(\text{SO}_4)_3 \cdot \text{XH}_2\text{O}$ and $\text{AlK}(\text{SO}_4)_2 \cdot \text{XH}_2\text{O}$ with urea considered useful as a green solvent because these have low vapor pressure and stable to air or moisture. New types of ionic liquids were prepared from alum sulfate $(\text{AlNH}_4(\text{SO}_4)_2 \cdot 12\text{H}_2\text{O})$ instead of aluminum chloride with urea salt^[78]. These ionic liquids much stable than chloroaluminate ionic liquids, offering relatively cheaper, easily prepared ionic liquids with promising similar properties. As this is green ionic liquid as it expected to be used in variable process such as metal coating as it offer good media for some insoluble compounds in aqueous media to be dissolve easily in this ionic liquid such as silver sulfate^[79].

Another room temperature ionic liquids based on alum of the type $\text{Al}_2(\text{SO}_4)_3 \cdot \text{XH}_2\text{O}$, $\text{AlNH}_4(\text{SO}_4)_2 \cdot \text{XH}_2\text{O}$ and $\text{AlK}(\text{SO}_4)_2 \cdot \text{XH}_2\text{O}$ with urea or Acetamide and hydrated aluminum nitrate $\text{Al}(\text{NO}_3)_3 \cdot \text{XH}_2\text{O}$ with urea^[80] or Acetamide for its ease of handling ,cheaper ,greener and incorporating of these compounds in variable industrial applications such as water purification. The ionic liquids chosen have the advantages of being stable towards air and moisture.

1.5 Thermal Analysis:-

Thermal analysis is defined as an analytical experimental technique which investigates the physical properties of a sample as a function of temperature or time under controlled conditions. This definition is broad and the following techniques are referred to conventionally as thermal analysis, i.e. thermogravimetry (TG), differential thermal analysis (DTA), differential scanning calorimetry (DSC)^[81,82].

Most common is the simultaneous thermal analysis (STA) apparatus as the combination of thermogravimetric analysis (TGA) and differential scanning calorimetry (DSC)^[83].

1.5.1 Simultaneous Thermal Analysis (STA):-

The STA combines two analytical techniques together. It combines TGA and DSC. Simultaneously the STA collects the data of both heat flow from DSC and weight loss from TGA. The STA Simultaneous Thermal Analyzer applies leading border sensor technology to give high accuracy and quality results^[83].

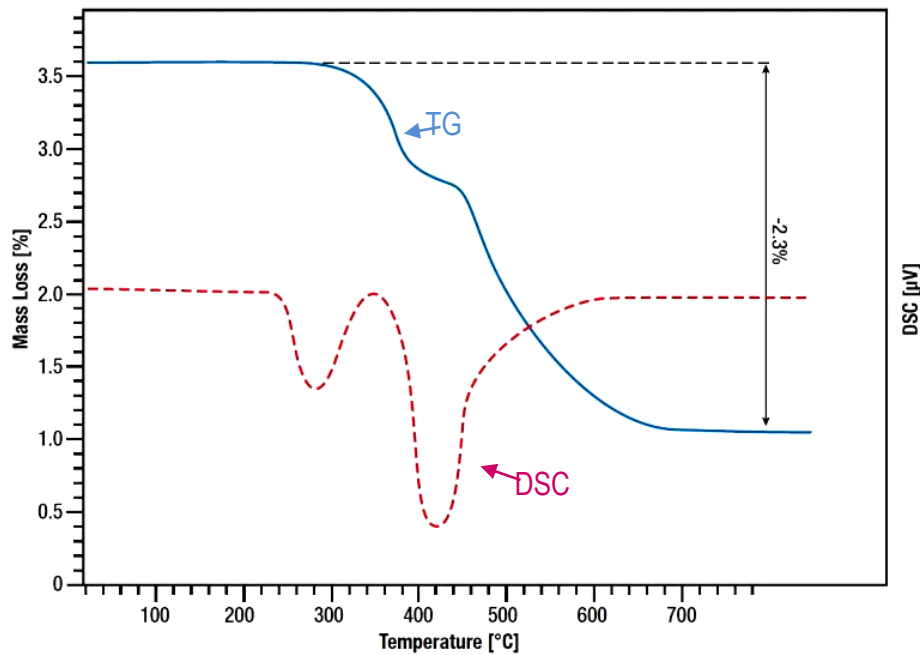


Figure (1-1): A general STA chart.

1.5.2 Thermo-gravimetric Analysis (TGA):-

Thermo-gravimetry study changes in the mass of a sample under a controlled temperature program. The temperature program is most often a linear increase in temperature^[84]. TGA is originally quantitative, and so an extremely powerful thermal technique, but do not gives direct chemical information and the ability for analyzing the volatile products through a weight loss is of great value. Applications ability of TGA to create fundamental quantitative information from almost any class of materials, had lead to its widespread used in field of science and technology. Mainly the key application areas were thermal stability; related materials could be compared at elevated temperatures through the required atmosphere and can help to elucidate decomposition mechanisms.

1.5.2.1 Data Analysis:-

Thermogram: is graph of mass versus temperature. Sometimes given as percent of original mass (m %) [85].

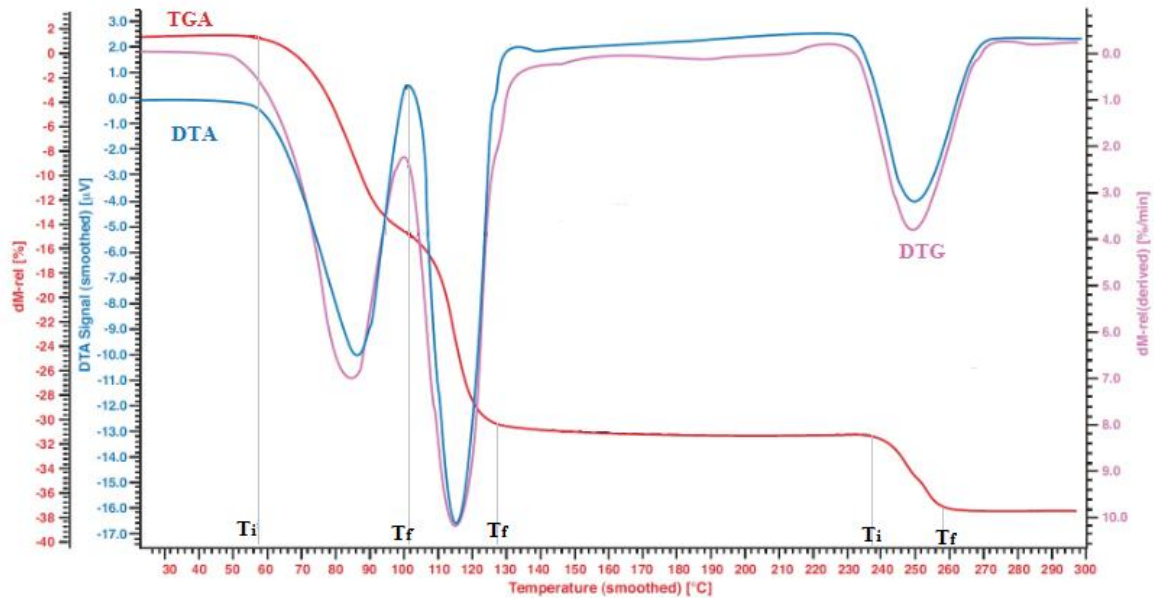


Figure (1-2): A general TGA/DTG curve.

In a TGA curve of one decomposition stage, there were two characteristic temperatures; the initial T_i and the final temperature T_f (see Fig. 1-2). T_i is known as the lowest temperature at which the onset of a mass change can be detected by thermo-balance working under particular conditions and T_f as the final temperature in which the specific decomposition appear to be complete. The difference $T_f - T_i$ is termed as reaction time [86].

TGA curves of a pure compound are a property of that compound. Using TGA curve we could relate the mass changes to the stoichiometry included. This could often directly lead to the quantitative analysis of the samples that their quantitative composition was known [87].

For further illustration, weight loss detected by TG can be calculated depending on two important factors weight lost percent and temperature at that point; weight lost percent can be calculated using molecular weight of each fraction divided to the original molecular weight of the sample, for example if there are three stages at which sample undergoes three decomposition steps then there must be three fractions from the original sample are lost so each weight will become^[87,88]:

$$\text{First weight loss \%}(m_1) = \frac{\text{Mwt of fraction}}{\text{Mwt of sample}} * 100 \quad \dots(1.1)$$

$$\text{Second weight loss \%}(m_2) = \frac{\text{Mwt of fraction}}{\text{Mwt of sample}} * 100 \quad \dots(1.2)$$

$$\text{Third weight loss \%}(m_3) = \frac{\text{Mwt of fraction}}{\text{Mwt of sample}} * 100 \quad \dots(1.3)$$

The resulted calculation then compared with measured values found by TG analysis. Both boiling points of vapors and weight loss percents enable us to estimate fractions (gases) liberated through decomposition process.

Now see example how TG curve could be used for thermal stability comparison between materials (qualitative interpretation). Predict product efficiency and enhance product quality. The thermal decomposition of calcium oxalate monohydrated ($\text{CaC}_2\text{O}_4 \cdot \text{H}_2\text{O}_{(s)}$), involve three decomposition stages^[86,89,90]:-

Calculated weight loss percent will be:

$$m_1 = \frac{\text{Mwt of } \text{H}_2\text{O}}{\text{Mwt of } \text{CaC}_2\text{O}_4 \cdot \text{H}_2\text{O}} * 100 = \frac{18 \text{ g} \cdot \text{mol}^{-1}}{146 \text{ g} \cdot \text{mol}^{-1}} * 100 = 12.3 \%$$

$$m_2 = \frac{\text{Mwt of } \text{CO}}{\text{Mwt of } \text{CaC}_2\text{O}_4 \cdot \text{H}_2\text{O}} * 100 = \frac{28 \text{ g} \cdot \text{mol}^{-1}}{146 \text{ g} \cdot \text{mol}^{-1}} * 100 = 19.2 \%$$

$$m_3 = \frac{\text{Mwt of } CO_2}{\text{Mwt of } CaC_2O_4 \cdot H_2O} * 100 = \frac{44 \text{ g. mol}^{-1}}{146 \text{ g. mol}^{-1}} * 100 = 30.1 \%$$

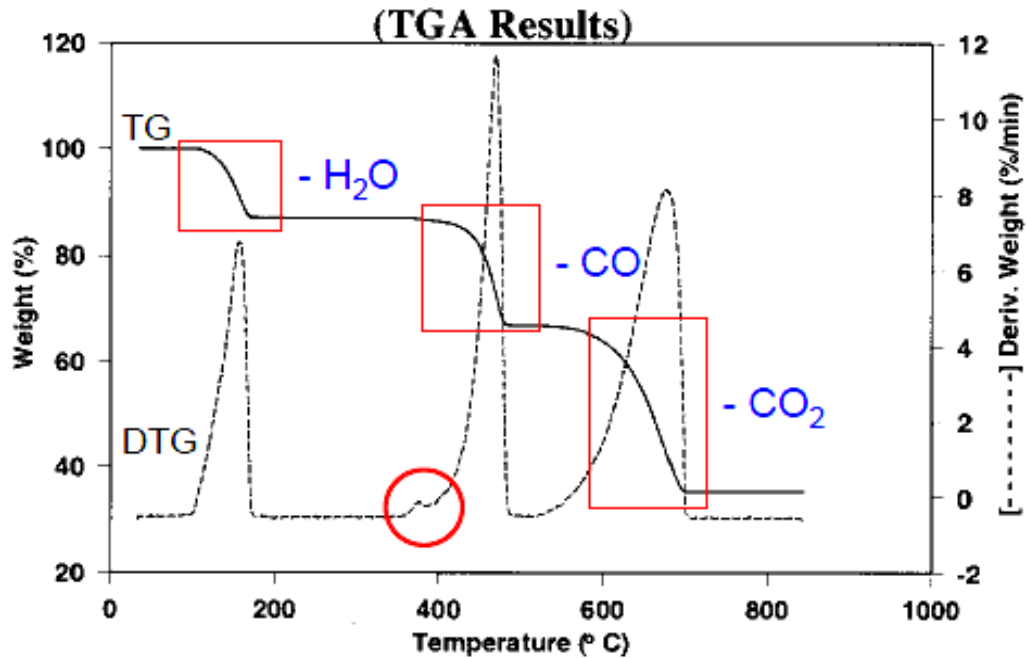


Figure (1-3): Reference TG/DTG of calcium oxalate.

Interpretation data analysis will be

1. Stage: Dehydration: $CaC_2O_4 \cdot H_2O_{(s)} \rightarrow CaC_2O_4_{(s)} + H_2O_{(g)}$
Mass change found (calculated): -11.89% (-12.3%)
2. Stage: Building carbonate: $CaC_2O_4_{(s)} \rightarrow CaCO_3_{(s)} + CO_{(g)}$
Mass change found (calculated): -19.42% (-19.2%)
3. Stage: Decarbonation: $CaCO_3_{(s)} \rightarrow CaO_{(s)} + CO_2_{(g)}$
Mass change found (calculated): -30.44% (-30.1%)

1.5.3 Differential Scanning Calorimetry (DSC):-

Differential Scanning Calorimetry (DSC) is most popular thermal analysis technique, DSC measures endothermic and exothermic transitions as a

function of temperature^[87,90], in endothermic transition heat flows into a sample as a result of either heat capacity (heating) or some endothermic process (glass transition, melting, evaporation, etc.). While in exothermic transitions heat flows out of the sample as a result of either heat capacity (cooling) or some exothermic process (crystallization, cure, oxidation, etc.)^[91] as showed in Figure (1-4). DSC used to characterize polymers, pharmaceuticals, foods/biologicals, organic chemicals and inorganics^[92-95]. DSC is able to provide all the thermodynamic parameters of a conformational transition.

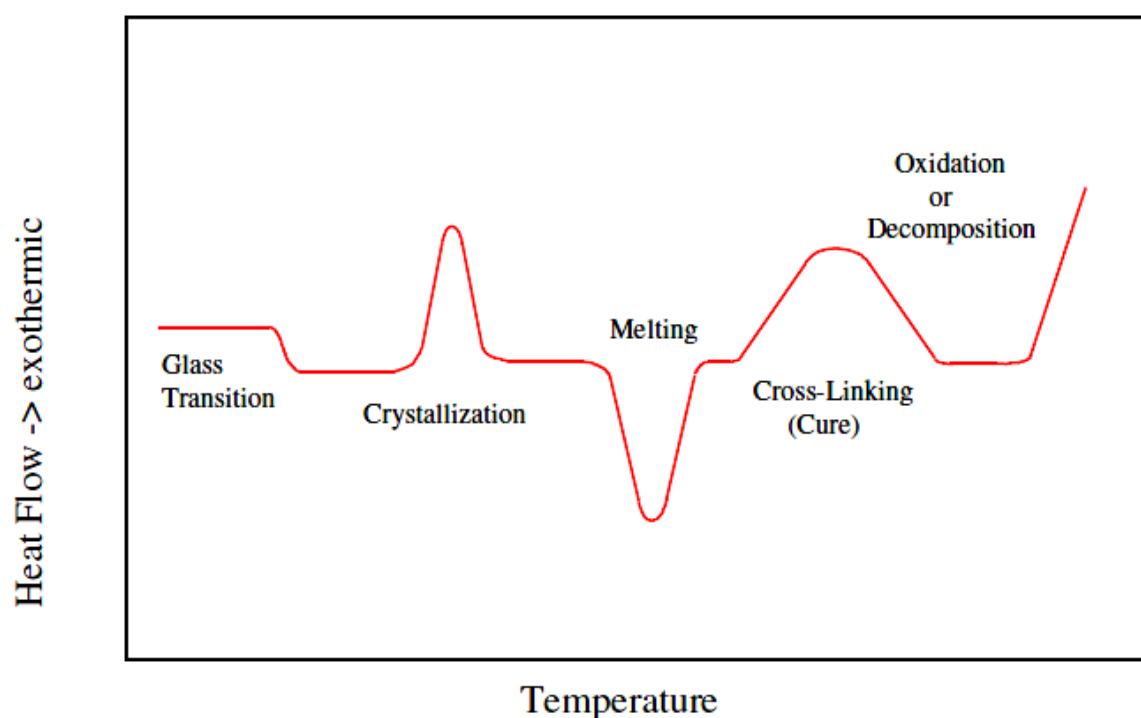


Figure (1-4): A general DSC thermogram.

1.5.4 Determination of thermo-physical properties:-

1. Heat Capacity, Enthalpy and Entropy:-

Specific heat capacity (C_p) is a material property describing the energy required to induce a certain change in the temperature of a unit mass of the

material^[96]. Measurement of this quantity, a differential scanning calorimeter (DSC) may be used. The DSC measures specific heat capacity by heating a sample and measuring the temperature difference between the sample and a reference^[97]. Three measurements are necessary for calculating specific heat. First a “Baseline” is recorded. This is the response with both crucibles empty, yielding a signal bias inherent in the system. Next is a reference test, in which a sample with a well defined specific heat is tested for comparison to an experimental sample. Finally, an experimental sample is tested. The “Baseline” allows removal of system bias from the data, while the reference test allows calculation of the specific heat of the experimental sample as a ratio of the reference material specific heat^[98,99].

The specific heat capacity of the sample was calculated by equation (1.4) from the DSC data obtained (a, b and c in Figure 1-5).

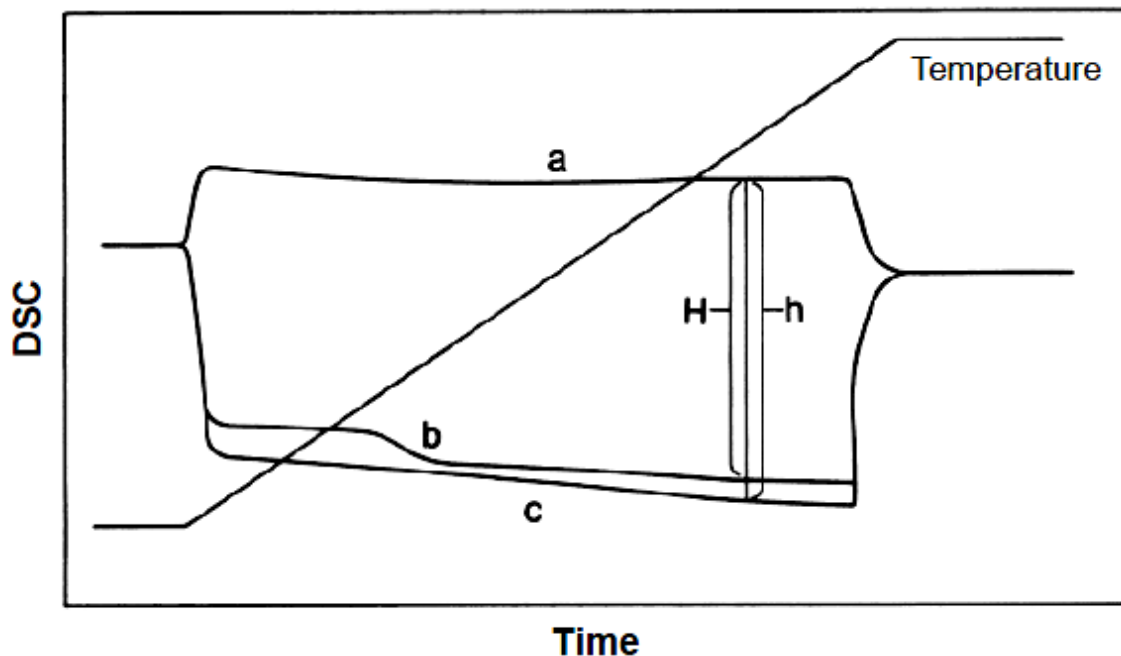


Figure (1-5) DSC measurement of specific heat capacity, (a) base line (empty), (b) sample and (c) reference.

$$Cp(s) = \frac{H(s)*M(r)}{H(r)*M(s)} * Cp (r) \dots(1.4)$$

Where:

$C_p(s)$: specific heat of the sample.

$C_p(r)$: specific heat of the reference.

$M(s)$: mass of the sample.

$M(r)$: mass of the reference.

$H(s)$: differential potential (in μV) of the signal between the base line and the sample.

$H(r)$: differential potential (in μV) of the signal between the base line and reference.

Heat capacity is the fundamental property from which all thermodynamic quantities may be derived, and this is central to DSC measurements and to the fundamental underlying thermodynamics^[99].

Enthalpy (ΔH_{trs}) is a measure of the net flow of energy, as heat, during a chemical reaction. Reactions in which heat is produced have a negative ΔH and are called exothermic. Endothermic reactions absorb heat from their surroundings and have a positive (ΔH_{trs}). The enthalpy value (ΔH_{trs}), calculated from the area under the transition peak. The ΔH value is actually a net value from a combination of endothermic contributions^[91,100].

$$\Delta H = KA/m \dots(1.5)$$

Where K is calorimetric constant and A is area under the transition peak and m is the mass of the sample. Another thermodynamic property is Entropy (ΔS ; a measure of the disorder) calculated from change in enthalpy at its transition temperature:

$$\Delta S = \Delta H/T \quad \dots(1.6)$$

If the phase transition is exothermic ($\Delta H_{\text{trs}} < 0$, as in freezing or condensing), then the entropy change is negative. This decrease in entropy is consistent with localization of matter and energy that accompanies the formation of a solid from a liquid or a liquid from a gas. If the transition is endothermic ($\Delta H_{\text{trs}} > 0$, as in melting and vaporization), then the entropy change is positive, which consistent with dispersal of energy and matter in the system^[84,100].

1.6 Aim of the work

Renewable energy sources are an alternative energy sources in natural oil sources providing energy for valuable applications. Therefore storing heat from the sun to be converted into electricity or used as such as challenged method. One promising media is ionic liquids which are liquid below 100 °C. The valuable properties of these ionic liquids (RTIL) open the door for this applications. Thus some room temperature ionic liquids of ASIL, USIL, ANIL, AN2IL and UNIL were investigated for their suitability of their thermophysical properties studied aims TGA/DTG and DSC from room temperature to 500 °C.

1. Preparation of new low temperature ionic liquids for sensible heat storage media.
2. Improvement thermophysical properties of some existent ionic liquids as a heat storage (heat capacity, C_p and thermal energy storage capacity, E).
3. Improvement of the thermophysical properties intended by adding some oxy anion compounds of alkali metal, alkaline earth metal and some transition metal compounds to some ILs.

Chapter Two
Experimental

Chapter Two

Experimental

2.1 Chemicals:-

All chemicals were used in current work with highest purity available and without further purification, as in Table (2-1) shows the reagents, their purities and suppliers:

Table (2-1): Specification of the chemicals.

Chemical compounds	Formula	Purity %	Company
Acetamide	CH_3CONH_2	98	Fluka
Aluminum Nitrate nanohydrate	$\text{Al}(\text{NO}_3)_3 \cdot 9\text{H}_2\text{O}$	99.3	MERCK
Ammonium aluminum sulfate dodecahydrate	$\text{NH}_4\text{Al}(\text{SO}_4)_2 \cdot 12\text{H}_2\text{O}$	99.5	BDH
Barium Oxide	BaO	99	BDH
Calcium Oxide	CaO	99	BDH
Cupric Oxide	CuO	99	MERCK
Magnesium Oxide	MgO	99	BDH
Nickel Oxide	NiO	99	MERCK
Potassium hydroxide	KOH	99	BDH
Sodium hydroxide	NaOH	99	BDH
Vanadyl sulfate pentahydrate	$\text{VO}(\text{SO}_4) \cdot 5\text{H}_2\text{O}$	99	MERCK
Urea	NH_2CONH_2	99.5	THOMAS BAKER
Zinc Oxide	ZnO	99	MERCK

2.2 Experimental Methods:-

2.2.1 Preparation of Room Temperature Ionic Liquids (RTILs):-

Ionic liquid was prepared by mixing a proper amount of aluminum nitrate nanohydrate $[\text{Al}(\text{NO}_3)_3 \cdot 9\text{H}_2\text{O}]$ or hydrated ammonium alum $[\text{NH}_4\text{Al}(\text{SO}_4)_2 \cdot 12\text{H}_2\text{O}]$ either with urea $[\text{NH}_2\text{CONH}_2]$ or acetamide $[\text{CH}_3\text{CONH}_2]$ were milled, mixed together and heated with gentle stirring until clear colorless liquids were obtained that left to cool and kept sealed in container for further use as follow:

2.2.1.1 Ionic liquid preparation with acetamide:

- Aluminum nitrate and acetamide were prepared in different mole ratios and among them two mole ratios of 1:2.4 and 1:22 were selected for the study due to their proper stability. The mixtures were heated at a temperature of 50 °C for 30 min and 80 °C for 1 hour respectively.

Aluminum nitrate:acetamide of 2:1 mole ratio showed melting point of 26 °C, while 1:1 mole ratio gave higher melting point of 50 °C. However, when the mole ratio of aluminum nitrate was less than acetamide gave much lower melting point of (-20 °C) for 1:1.5-1:2.65 mole ratios and (-25 °C) for 1:4 up to the liquid 1:22 mole ratios.

- Ammonium alum and acetamide in the mole ratio of 1:12 (ASIL) heat gradually from 25 °C to 80 °C for 10 hours produced colorless liquid^[78].

2.2.1.2 Ionic liquid preparation with urea:

- Hydrated aluminum nitrate and urea salts in the mole ratio of (1:1.2) (UNIL) were heated gradually from room temperature to 80 °C for 3 hours, to obtain colorless liquid^[80].

- Ammonium alum and urea in the mole ratio of (1:5) (USIL) were also heated gradually from room temperature to 80 °C for 3 hours producing colorless liquid [78].

2.2.2 Added salts to ionic liquids:-

- 0.1 M blue solution of vanadyl sulfate pentahydrate prepared in ammonium alum:urea (USIL) that heated to 80 °C for 2hrs.

- 0.1 M green solution of Nickel Oxide prepared in ammonium alum:urea (USIL) that heated to 80 °C for 2hrs.

- 10 ml of 0.1 M blue solution of Cupric Oxide prepared in ammonium alum:urea (USIL) that heated to 80 °C for 2hrs.

- 10 ml of 0.1 M colorless solution of Zinc Oxide prepared in ammonium alum:urea (USIL) that heated to 80 °C for 2hrs.

- 10 ml of 0.1 M colorless solution of Potassium hydroxide prepared in ammonium alum:urea (USIL) that heated to 80 °C for 2hrs.

- 10 ml of 0.1 M colorless solution of Magnesium Oxide prepared in ammonium alum:urea (USIL) that heated to 80 °C for 2hrs.

- 10 ml of 0.01 M colorless solution of Calcium Oxide prepared in ammonium alum:urea (USIL) that heated to 80 °C for 2hrs.

- 10 ml of 0.1 M colorless solution of Sodium hydroxide prepared in aluminum nitrate:acetamide (AN2IL) that heated to 80 °C for 2hrs.

- 10 ml of 0.1 M colorless solution of Sodium hydroxide prepared in aluminum nitrate:urea (UNIL) that heated to 80 °C for 2hrs.

- 10 ml of 0.1 M colorless solution of Barium Oxide prepared in aluminum nitrate:urea (UNIL) that heated to 80 °C for 2hrs.

2.3 Instruments and measurements:-

2.3.1 Simultaneous Thermal Analysis (STA):-

Thermal behavior of ionic liquids was investigated using LINSEIS Simultaneous thermal analyzer (STA PT1000), with platinum Evaluation V1.0.89 software. Ionic liquid samples were heated using alumina crucibles under air atmosphere with heating rate of 10 °C/min and sample weight of (23-25 mg) at room temperature up to 500 °C. The instrument was calibrated using melting points of Aluminum, Indium and Lead, that was performed in chemistry department of Al-Nahrain University.

2.3.2 X-Ray Diffraction (XRD):-

The crystalline and phase identification of samples were determined using X-ray Diffractometer (PAN analytical Philips, X Pert PRO MPD PW 3040) employing monochromatized radiation source of Cu-K α of 1.5408 Å. The voltage and current intensities were 8.5 kV*A. All samples were scanned in the range of 20° to 80° 2 θ with a step size of 0.01 and step time of 0.2 Sec. at room temperature 20 °C that was performed in physics department of Al-Nahrain University.

2.3.3 Fourier Transform Infra-Red Spectrophotometer (FTIR):-

The infrared spectra were measured using F.T.IR spectroscopy BRUKER, with ALPHA module, using attenuated total reflector (ATR) equipped with diamond composite crystal accessory. Each sample was scanned 25 times in the range of wave number (4000-400) cm⁻¹ at a resolution of 4 cm⁻¹, that was performed in chemistry department of Al-Nahrain University.

2.3.4 Conductivity, Density and Freezing Point measurements:-

The specific conductance was measured using HANNA instrument HI 9811 in (mS/cm), that was performed in chemistry department of Al-Nahrain University. Density was measured using gravimetric density bottle, (5 ml) in size at room temperature. Freezing temperatures obtained from a thermometer immersed inside the tube containing 1 ml of ionic liquid stored in deep freezing refrigerator and the temperature was recorded when the sample changed its state.

Chapter Three
Results &
Discussion

Chapter Three

Results and Discussion

Five room temperature ionic liquids; namely hydrated aluminum nitrate:acetamide in two mole ratios [(1:2.4, ANIL) and (1:22, AN2IL)], alum:acetamide, ASIL (1:12 mole ratio), alum:urea, USIL (1:5 mole ratio) and hydrated aluminum nitrate:urea, UNIL (1:1.2 mole ratio) were prepared for this study. They have the advantages of being stable towards air and moisture at room temperature. Thermal properties of these ionic liquids alone and with the additives have not yet been investigated; therefore thermal measurements and thermal properties have been covered by this work to establish their usefulness as thermal storage liquids.

Some thermo-physical properties such as melting point, decomposition temperature, density, conductivity, heat of fusion, entropy, heat capacity and thermal energy storage capacity were determined with and without the addition of some enhanced materials, such as alkali metal hydroxides NaOH and KOH, alkaline earth metal oxides MgO, CaO and BaO and transition metal oxides $\text{VOSO}_4 \cdot 5\text{H}_2\text{O}$, NiO, CuO and ZnO.

3.1 Thermal Analysis(TGA/DTG& DSC), ATR-FTIR spectroscopy and X-ray diffraction (XRD)of Ionic Liquids:-

These five RTILs: (ASIL, USIL, ANIL, AN2IL and UNIL) were heated to 500 °C. Thermal events are normally due to phase transition and decomposition is of two types either exothermic or endothermic according to the nature of the process and the material relied can be identified by appearance of exothermic and endothermic peaks that help to identify thermal changes occurred in ionic liquid. Thermogravimetric analysis and its derivative (TGA/DTG) and Differential Scanning Calorimetry (DSC); both

combined within single measurement through Simultaneous Thermal Analysis (STA).

3.1.1 ATR-FTIR spectroscopy, thermal decomposition behavior X-ray diffraction (XRD) of hydrated ammonium aluminum sulfate:acetamide (ASIL):-

The infrared spectrum of the ASIL Fig.(3-1), showed the appearance of characteristic absorption bands resembled its components acetamide and ammonium aluminum sulfate dodecahydrate [101-103]. Two strong stretching vibration bands at symmetric 3148 and asymmetric 3298 cm^{-1} of $\nu(\text{N-H})$ which attributed to $-\text{NH}_2$ vibration in acetamide were shifted to higher wave number (3191 and 3345) cm^{-1} respectively in AS ionic liquid. The stretching vibration band of $\nu(\text{C-H})$ appeared at (2817) cm^{-1} also shifted to higher frequency (2824) cm^{-1} . While stretching vibration bands of $\nu(\text{C=O})$ at (1671) cm^{-1} , $\nu(\text{C-N})$ at (1010 and 1144) cm^{-1} were shifted to lower wave numbers (1650) cm^{-1} and (1127) cm^{-1} respectively in ASIL. The bands related to hydrated ammonium aluminum sulfate showed the appearance of significant stretching vibration bands (3188 and 3321) cm^{-1} were shifted to higher frequencies (3121 and 3344) cm^{-1} in ASIL. The broad stretching vibration band of $\nu(\text{O-H})$, attributed to the H_2O molecules at (2884) cm^{-1} reduced in AS ionic liquid. The stretching vibration bands of $\nu(\text{S-O})$ attributed to $-\text{SO}_4$ at (1074) cm^{-1} shifted to higher frequency (1127) cm^{-1} , and the stretching vibration bands of $\nu(\text{Al-O})$ at (914 and 581) cm^{-1} [104-107] shifted to lower frequencies and (869 and 462) cm^{-1} respectively; as illustrated in Table (3-1).

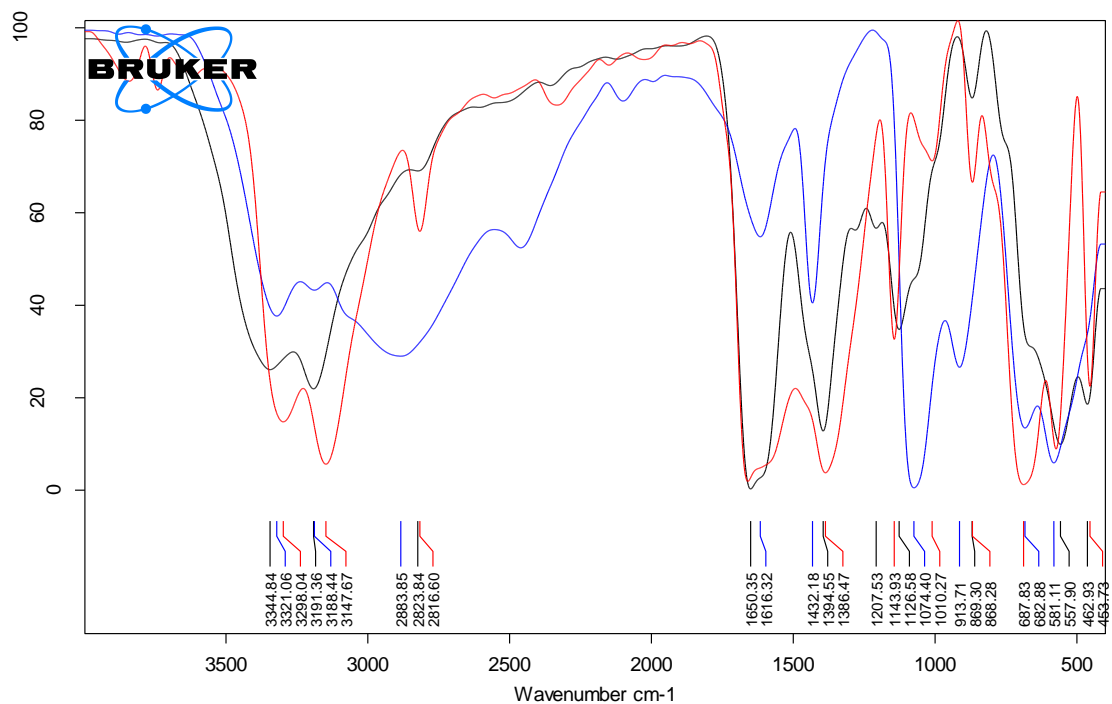


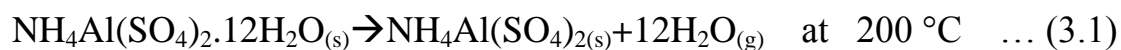
Fig.(3-1): FTIR of (hydrated ammonium aluminum sulfate: acetamide, ASIL with 1:12 mole ratio) (black line), hydrated ammonium aluminum sulfate (blue line) and acetamide (red line).

Table (3-1): FTIR vibration frequencies of hydrated ammonium aluminum sulfate:acetamide, ASIL with 1:12 mole ratio.

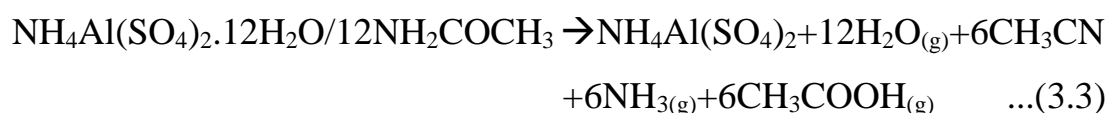
Compounds group	H ₂ NCOCH ₃	NH ₄ Al(SO ₄) ₂ .12H ₂ O	ASIL
ν (N-H)	3148 & 3298	3188 & 3321	3191 & 3345
ν (O-H)	-	2884	3000 - 3200
ν (C-H)	2817	-	2824
ν (S-O)	-	1074	1127
ν (C=O)	1671	-	1650
ν (C-N)	1144 & 1010	-	1127
δ (N-H)	1386	1432	1395
ν (Al-O)	-	914 - 581	869 - 462

Thermogravimetric measurements of ASIL (24.06 mg), Fig.(3-2) showed two decomposition stages started from 203 °C reached to 500 °C with total weight loss of (85.29 %, -20.52 mg) this weight loss was associated with

changes in heat through three endothermic peaks; the first was an endothermic peak with an enthalpy of -250.51 kJ/kg refer to the sensible heat stored in ASIL which in comparable with other thermal energy storage materials. Other ionic liquids show relatively small values of heat of fusion which are around 50 kJ/kg. On the other hand, the inorganic materials have a very high heat of fusion of around 200 to 500 kJ/kg and the organic materials including paraffins show these values around 100 to 200 kJ/kg. Thus ASIL can be enclosed between organic and inorganic material. The second/endothermic peak recorded an enthalpy of decomposition of -812.55 kJ/kg in a temperature range of 184 to 230 °C related to the decomposition of ASIL in the first stage in which (58.40 %, -14.05 mg) weight percent is lost in the temperature range of (203 to 235) °C that reached its maximum decomposition at 211 °C with the possible candidate evolution products from ASIL of $[\text{NH}_4\text{Al}(\text{SO}_4)_2 \cdot 12\text{H}_2\text{O} : 12\text{NH}_2\text{COCH}_3]$, including water molecules based on thermal decomposition of ammonium alum in which water evaporated around 100 °C as shown in equation (3.1), in addition to the partial decomposition of acetamide giving 6NH_3 and $6\text{CH}_3\text{COOH}$ based on the decomposition of acetamide^[108,109] at 425 °C (equation 3.2). These agreed with calculated weight loss of (58.40%), thus the first decomposition stage of ASIL was suggested as in equation (3.3):



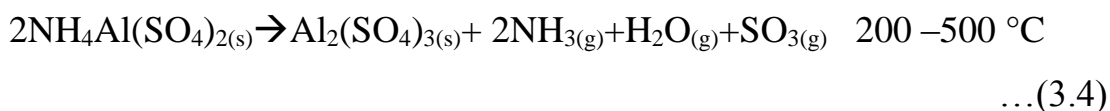
1. First decomposition stage was:



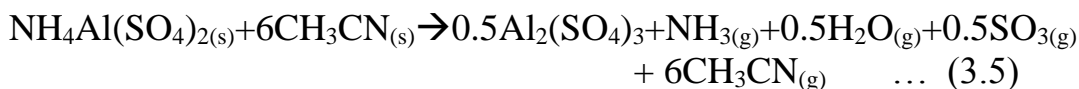
The initial decomposition temperature at 203 °C of the ionic liquid gave evidence to the new nature of interaction in ionic liquid differs from these experienced by its components ammonium alum and acetamide. As the above

temperature of water is much higher than the evaporation temperature of water from Ammonium aluminum sulfate (around 100 °C) and in the same sense much lower than the starting decomposition temperature of acetamide alone (425 °C).

The second decomposition stage with weight loss percent of (26.89 %, -6.47 mg) in temperature range of (235 to 475) °C showed small exothermic behavior between 240 °C to 250 °C could be referred to slow decomposition of ammonium aluminum sulfate and complete decomposition of acetamide. It's possible that the decomposition products of this stage were NH₃, H₂O, SO₃ and 6CH₃CN that evolved from ammonium aluminum sulfate decomposition^[104] as shown in equation (3.4) and acetamide decomposition (equation 3.2) that agreed with calculated weight loss percent 26.87 % as shown in equation (3.5):



2. Second decomposition stage was:



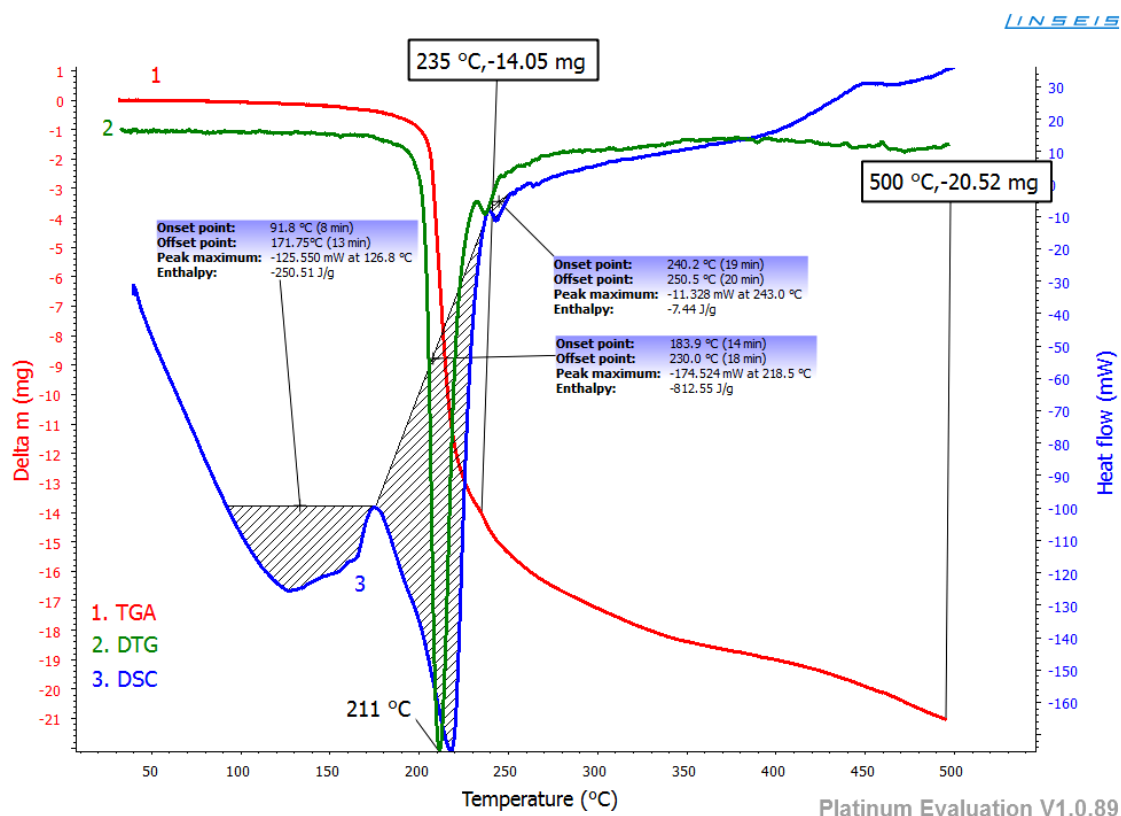


Figure (3-2): Thermogravimetric Analysis TGA (1), Differential Thermal Analysis DTG (2), Differential Scanning Calorimeter DSC (3) of (hydrated ammonium aluminum sulfate: acetamide, ASIL with 1:12 mole ratio) heated from room temperature to 500 °C at 10 °C/min.

The final decomposition products resulted from heating this ionic liquids to 500 °C was analyzed by X-ray diffraction Figure (3-3) and FTIR spectroscopy Figure (3-4) to identify the remaining white powder. The X-ray found the white powder to be pure crystalline rhombohedral aluminum sulfate as shown in Table (3-2) with crystallite size of 48.151nm calculated from Scherer equation [105]:

$$D = k \cdot \lambda / \beta \cdot \cos \theta \quad \dots \dots (3.6)$$

Where k is a constant ~0.9, λ is the wave length of X-ray (1.5406 Å), β is the full width of diffraction peak at half maximum (FWHM) intensity, 0.2952 and θ is the Bragg angle, (25.437/2). The calculated crystallite size of aluminum sulfate agreed with other report [105].

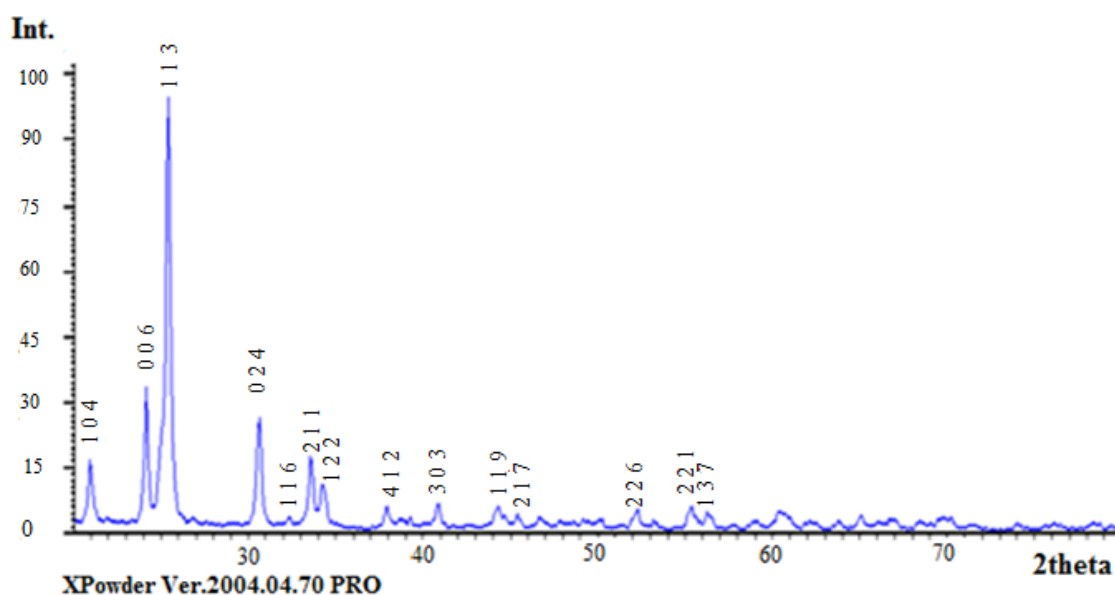


Fig.(3-3): X-ray diffraction of (hydrated ammonium aluminum sulfate: acetamide, ASIL with 1:12 mole ratio) after heating it to 500 °C.

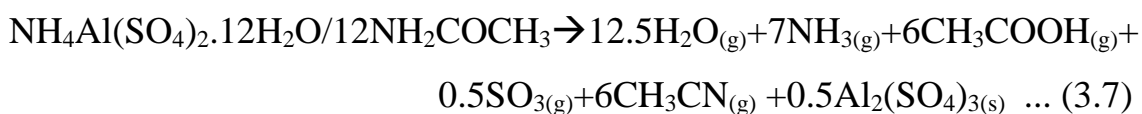
$$D = 0.9 \cdot 1.5406 \cdot 10 \text{ nm} / 0.2952 \cdot \cos(25.437/2) = 48.151 \text{ nm}$$

The vibrational frequencies of the white powder after heating ASIL to 500°C, (Fig.3-4) indicated the disappearance of amide and hydroxyl group bands with increased intensities of bands belong to sulfate (SO_4^{2-}) stretching vibration at 1178.32 cm^{-1} ^[106] and aluminum-oxide Al-O stretching vibration at 497.58 to 678.78 cm^{-1} ^[107]. This could be taken as further prove to decomposition of ASIL producing aluminum sulfate $\text{Al}_2(\text{SO}_4)_3$.

Table (3-2): X-ray data of the product of (hydrated ammonium aluminum sulfate:acetamide, ASIL with 1:12 mole ratio) heated up to 500°C compared with Al₂(SO₄)₃ standard data^[110].

2θ (measured)	2θ (reference)	Intensity (measured)	Intensity Al ₂ (SO ₄) ₃ (reference)	Miller indices h k l ^[110]
20.969	20.934	17	20	1 0 4
24.181	24.780	34	20	0 0 6
25.437	25.427	100	100	1 1 3
30.603	30.644	26	17	0 2 4
33.535	33.497	18	18	1 1 6
33.675	-	16	-	
34.233	34.222	11	10	2 1 1
34.373	35.036	11	2	1 2 2
37.910	37.933	6	5	2 1 4
40.889	40.777	7	7	3 0 3
44.333	44.118	6	6	1 1 9
45.403	45.545	4	6	2 1 7
52.291	52.222	5	5	2 2 6
55.363	55.549	6	4	2 1 1
56.247	56.139	5	6	1 3 7

The recorded weight of final product from TGA/DTG was (14.71 %, 3.54 mg) agreed with calculated weight percent of (14.73%) calculated on the bases of sample weight of ionic liquid if completely decomposed to Al₂(SO₄)₃ also supported the predicted final formation of aluminum sulfate from X-ray diffraction and FTIR spectroscopic measurements. The following equation (3.7) summarized the overall decomposition of ASIL:



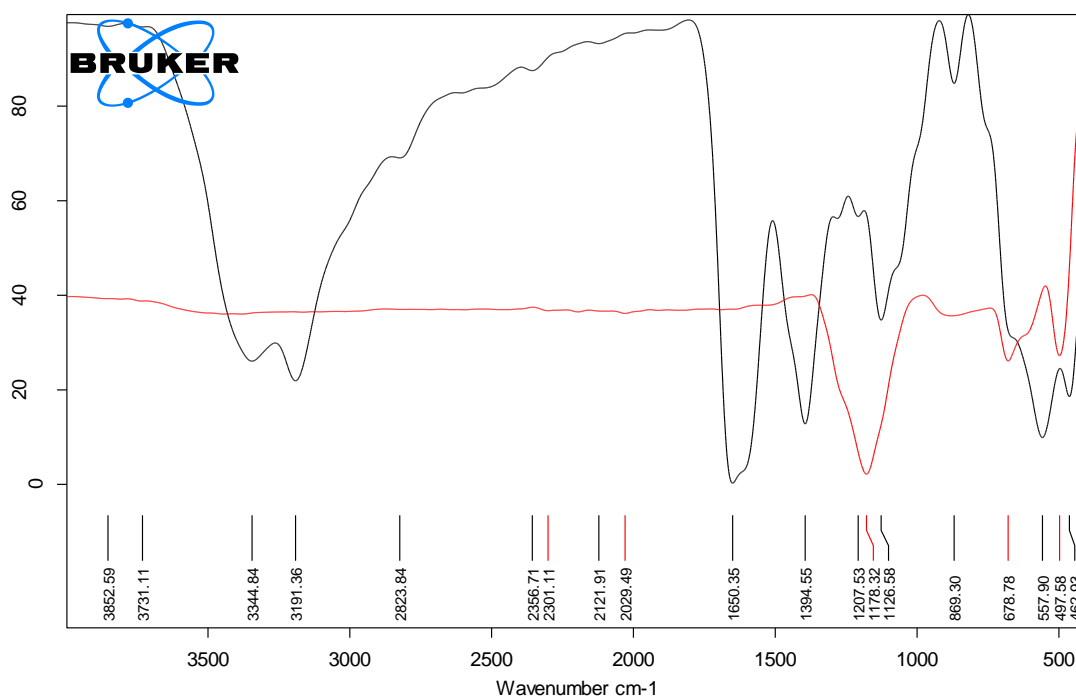


Fig.(3-4): FTIR of (hydrated ammonium aluminum sulfate: acetamide, ASIL with 1:12 mole ratio) (black line) and (red line) after heating it to 500 °C.

3.1.2 ATR-FTIR spectroscopy, Thermal decomposition behavior and X-ray diffraction (XRD) of hydrated ammonium aluminum sulfate: urea (USIL):-

Initial identification of the US room temperature ionic liquid by FTIR Fig.(3-5), showed the appearance of characteristic absorption bands resemble to its components urea and ammonium aluminum sulfate dodecahydrate^[101-103]. The two strong stretching vibration band of $\nu(\text{N-H})$ which attributed to $-\text{NH}_2$ either in urea at (3326 and 3342) cm^{-1} or attributed to $-\text{NH}_4^+$ in hydrated ammonium aluminum sulfate at (3188 and 3429) cm^{-1} were shifted to lower wave number (3199 and 3340) cm^{-1} in ionic liquid. But the stretching vibration band of $\nu(\text{O-H})$ either in urea at (3200) cm^{-1} or the broad stretching vibration band centered at (2884) cm^{-1} attributed to the H_2O molecules in hydrated ammonium aluminum sulfate that might made hydrogen bonding with (C=O) might be responsible for the viscose nature of US ionic liquid shifting to higher wave number (3400-2900) cm^{-1} in ionic

liquid effecting the stretching vibration bands $\nu(\text{C}=\text{O})$ at $(1593) \text{ cm}^{-1}$ to shift to lower wave number $(1591) \text{ cm}^{-1}$. The bands related to hydrated ammonium aluminum sulfate show the appearance of stretching vibration bands of $\nu(\text{S}-\text{O})$ attributed to $-\text{SO}_4$ at $(1074) \text{ cm}^{-1}$, and the stretching vibration bands of $\nu(\text{Al}-\text{O})$ at $(914 - 581) \text{ cm}^{-1}$ ^[104-107] which shifted in ionic liquid to lower frequencies $(1060) \text{ cm}^{-1}$ and $(771 - 537) \text{ cm}^{-1}$ respectively; as illustrated in Table (3-3).

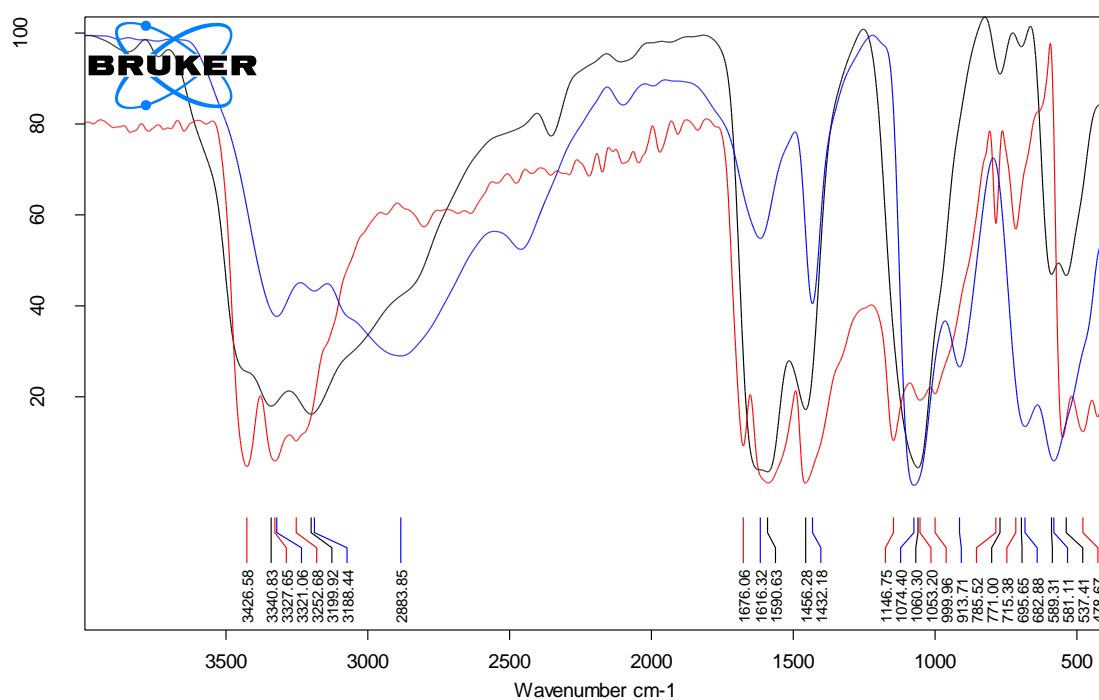


Fig.(3-5): FTIR of (hydrated ammonium aluminum sulfate:urea, USIL with 1:5 mole ratio) (black line), hydrated ammonium aluminum sulfate (blue line) and urea (red line).

Table (3-3): FTIR vibration frequencies of hydrated ammonium aluminum sulfate:urea, USIL with 1:5 mole ratio.

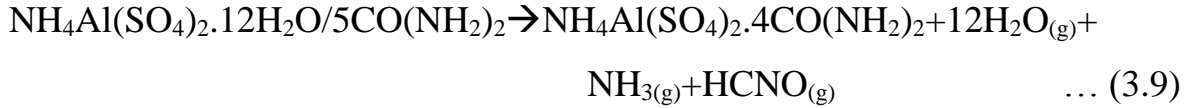
Compounds group	H ₂ NCONH ₂	NH ₄ Al(SO ₄) ₂ .12H ₂ O	USIL
v(N-H)	3326 & 3328	3188 & 3321	3199 & 3340
v(O-H)	3200	2884	3400-2900
v(S-O)	-	1074	1060
v(C=O)	1593	-	1591
v(C-N)	1142	-	1060
δ(N-H)	1442	1432	1456
v(Al-O)	-	914 - 581	771 - 537

Thermal analysis of USIL (20.06 mg) by TGA/DTG and DSC measurements, Fig.(3-6) showed high thermal stability reached 280 °C with large enthalpy value -2434.84 kJ/kg in which heat absorbed through two stages as a result of two endothermic peaks (-2216.83 and -218.01) kJ/kg at a temperature ranges of (109.6 – 163.5) °C and (200.2 – 238.8) °C respectively. These two endothermic peaks might be referred to solid to liquid transition due to non-eutectic mixture of USIL. Above 280 °C two decomposition stages appeared giving total weight loss (68.54%, -16.49 mg) up to 517 °C. The recorded weight lost in first decomposition stage was (36.66 %, -8.82 mg) at a temperature range 280-336 °C associated with first decomposition peak which include a complex decomposition process exothermal and endothermal resulted in small value of ΔH in endothermic value of -40.37 kJ/kg reached to maximum rate of decomposition at 296 °C characteristic with rapid gaseous evaporation of water, ammonia and isocyanic acid. Equation (3.9) was suggested that based on the calculated 36.66 % weight loss of decomposition of both ammonium alum as stated earlier

(equation 3.1) and urea which reported to evolve HNCO and NH₃ above its melting temperature to 360 °C^[111,112]:

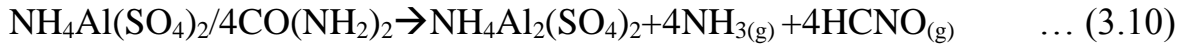


1. First decomposition step was:



The weight loss percent (31.88 %, -7.67 mg) of the second decomposition stage of USIL in the temperature range between 336 °C to 517 °C, was associated with liberation of heat in an endothermic peak with enthalpy of -51.19 kJ/kg with maximum rate of decomposition at 492 °C that attributed to decomposition of remaining urea evolving ammonia and isocyanic acid gases that agree with the calculated weight loss percentage of 31.87 % as illustrated in equation (3.10):

2. Second decomposition stage was:



In similar examination procedure, the final white powder obtained from the decomposition of USIL was also examined by X-ray diffraction (Fig.3-7 and Table 3-4) and was found to has similar diffraction data to hexagonal NH₄Al(SO₄)₂ with crystalline size of 36.023 nm calculated from equation (3.6) with the full width of diffraction peak at half maximum (FWHM) intensity, $\beta = 0.3936$ and 2θ of 24.134/2.

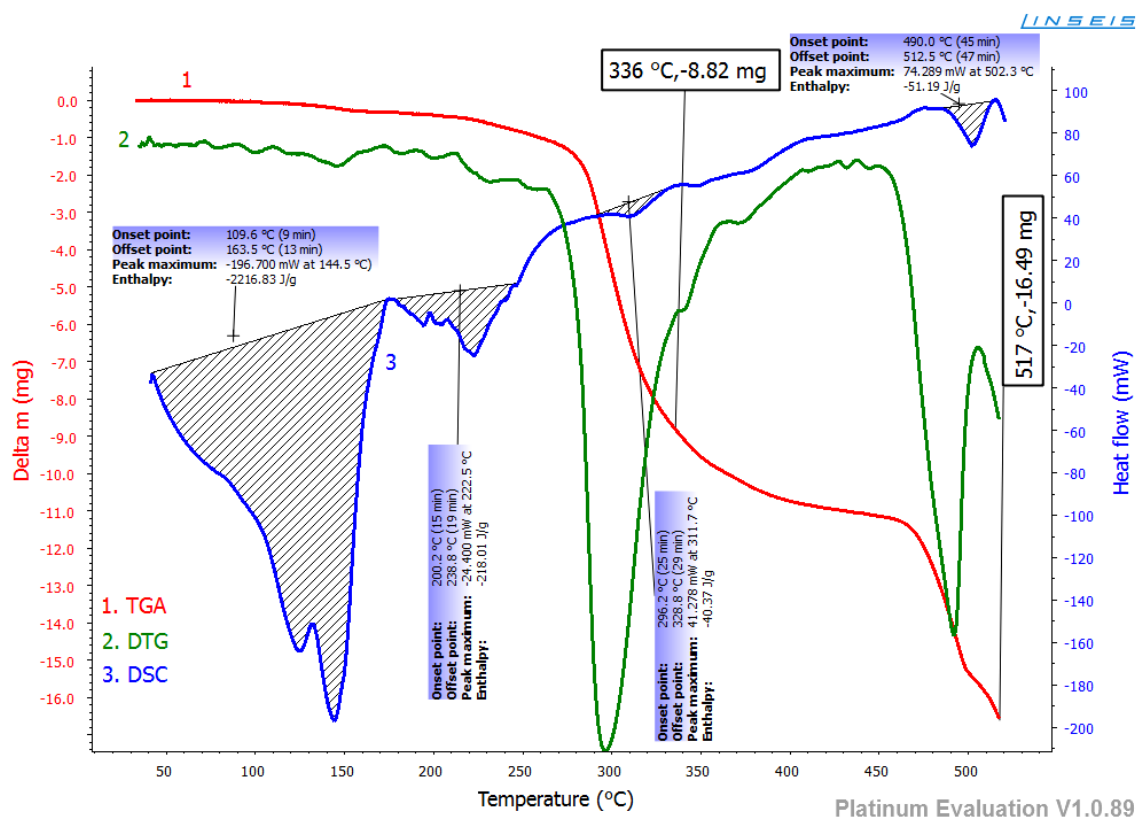


Figure (3-6): Thermogravimetric Analysis TGA (1), Differential Thermal Analysis DTG (2), Differential Scanning Calorimeter DSC (3) of (hydrated ammonium aluminum sulfate:urea, USIL with 1:5 mole ratio) heated from room temperature to 517 °C at 10 °C/min.

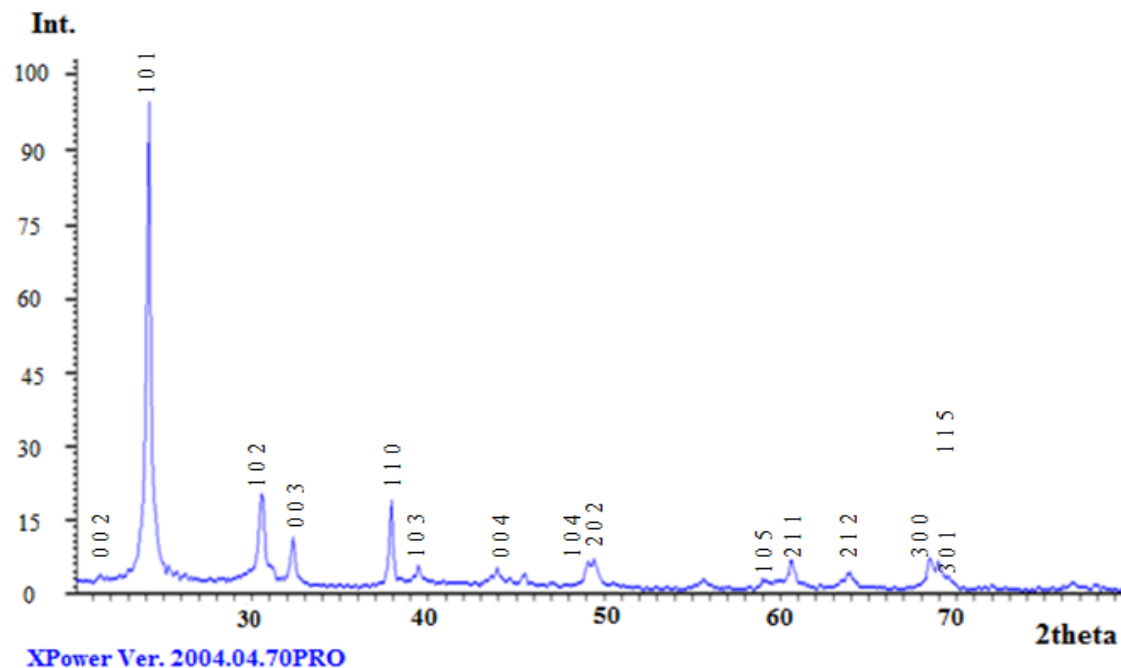


Figure (3-7): X-Ray diffraction of (hydrated ammonium aluminum sulfate:urea, USIL with 1:5 mole ratio) after heating up to 500°C.

However, FTIR vibrational bands Fig. (3-8) indicated, an intense sulfate vibrational frequency at maximum of 1171.17 cm^{-1} and Al-O stretching at $410.07\text{-}682.16\text{ cm}^{-1}$ amine vibrational bands at 1647.05 cm^{-1} with small intensity, in contrast to the completely disappearance of latter frequency in the white powder of final decomposition of ASIL at similar temperature of $500\text{ }^{\circ}\text{C}$.

Table (3-4): X-ray data of the product of (hydrated ammonium aluminum sulfate:urea, USIL with 1:5 mole ratio) heated up to $500\text{ }^{\circ}\text{C}$ compared with $\text{NH}_4\text{Al}(\text{SO}_4)_2$ standard data^[113].

2 θ (measured)	2 θ (reference)	Intensity (measured)	Intensity $\text{NH}_4\text{Al}(\text{SO}_4)_2$ (reference)	Miller indices h k l ^[113]
21.435	21.435	4	4	0 0 2
24.134	24.111	100	100	1 0 1
25.251	-	6	-	
30.557	30.591	20	28	1 0 2
30.650	-	19	-	
32.325	32.375	15	12	0 0 3
37.957	37.833	19	15	1 1 0
39.399	39.347	6	3	1 0 3
43.914	43.715	5	2	0 0 4
49.080	49.239	6	7	1 0 4
49.406	49.410	7	6	2 0 2
60.575	60.067	7	3	1 0 5
60.715	60.698	7	7	2 1 1
64.019	64.048	4	5	2 1 2
68.441	68.582	7	6	3 0 0
68.580	69.148	7	7	1 1 5
68.999	69.622	7	2	3 0 1

The recorded weight percent obtained from TGA/DTG of USIL final product was found to be (31.46%, 7.57 mg) which in agreement with calculated weight percent of 31.47% based on the formation of $\text{NH}_4\text{Al}(\text{SO}_4)_2$ as final product from USIL decomposition at 517 °C. Which support the $\text{NH}_4\text{Al}(\text{SO}_4)_2$ supported by X-ray diffraction and FTIR spectroscopic measurements.

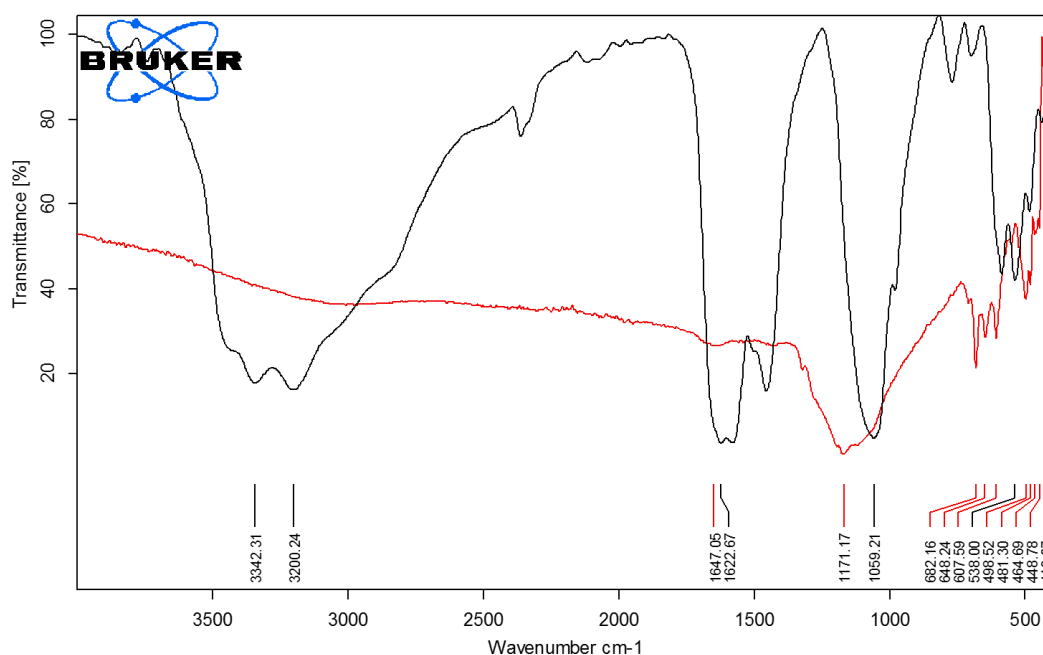


Fig.(3-8): FTIR of (hydrated ammonium aluminum sulfate:urea, USIL with 1:5 mole ratio) (black line), and (red line) after heating to 500°C.

3.1.3 ATR-FTIR spectroscopy, Thermal decomposition behavior and X-ray diffraction (XRD) of hydrated aluminum nitrate:acetamide (ANIL, 1:2.4 mole ratio) and (AN2IL, 1:22 mole ratio):-

The FTIR analysis of the ANIL Fig.(3-9a), showed the appearance of both characteristic absorption bands of its components (i.e. acetamide and aluminum nitrate nanohydrate)^[101-103] with noticeable shifting. The two strong stretching vibration band of $\nu(\text{N-H})$ which attributed to $-\text{NH}_2$ in acetamide at 3147 cm^{-1} and 3297 cm^{-1} shifted to higher frequency 3344 cm^{-1} in ionic liquid while stretching vibration band of $\nu(\text{C-H})$ at 2817 cm^{-1} that may be

overlapped with the broad band of $\nu(\text{O-H})$ started from 2700 cm^{-1} to 3500 cm^{-1} . Stretching vibration bands $\nu(\text{C=O})$ at 1671 cm^{-1} , $\nu(\text{C-N})$ at $1146 - 456\text{ cm}^{-1}$ and bending vibration band $\nu(\text{N-H})$ at 1392 cm^{-1} shifted to lower wave numbers 1330 cm^{-1} . The hydrated aluminum nitrate showed the appearance of significant broad stretching vibration band of $\nu(\text{O-H})$ centered at 2947 cm^{-1} attributed to the H_2O molecules that related to hydrogen bond formation with the oxygen of the carbonyl group of acetamide, shifting to higher frequency 3006 cm^{-1} in ionic liquid. Other frequencies of stretching vibration bands of $\nu(\text{N-O})$ resulted from $-\text{NO}_3$ group at 1334 cm^{-1} shifted to higher frequency 1387 cm^{-1} and 1335 cm^{-1} in ionic liquid and the stretching vibration bands of $\nu(\text{Al-O})$ at $880 - 685\text{ cm}^{-1}$ were shifted to lower frequency $886-586\text{ cm}^{-1}$ in ionic liquid as illustrated in Table (3-3) and Fig.(3-9a).

The shifting of FTIR either to lower or higher frequencies in ionic liquids compared to the frequencies of the ionic liquid components alone, taken as an indication to the chemical interaction between its components forming new coordination ions in the liquid state [78].

The infrared spectrum of the AN2IL Fig.(3-9b), showed different characteristic absorption bands compared with ANIL of same components [101-103] but with different mole ratios (1:2.4 compared to 1:22 respectively). The two strong stretching vibration band of $\nu(\text{N-H})$ which from $-\text{NH}_2$ in acetamide at (3147 and 3297) cm^{-1} were shifted to higher frequencies (3197 and 3342) cm^{-1} in ionic liquid with the disappearance of $\nu(\text{C-H})$ which showed appeared at (2817) cm^{-1} . The stretching vibration bands of $\nu(\text{C=O})$ at (1671) cm^{-1} and $\nu(\text{C-N})$ at ($1146-456$) cm^{-1} were shifted to lower wave numbers 1653 , 1124 cm^{-1} respectively yet appeared at the same positions as in ANIL with limited shifting. The bands related to $\nu(\text{O-H})$ of hydrated aluminum nitrate appeared at (2947) cm^{-1} with small intensity in AN2 ionic liquid in contrast to that in AN ionic liquid which showed broad band. The

stretching vibration bands of $\nu(\text{N-O})$ of $-\text{NO}_3$ at $(1334) \text{ cm}^{-1}$ shifted to higher frequency $(1387 \text{ and } 1335) \text{ cm}^{-1}$ respectively in ANIL and AN2IL and stretching vibration bands of $\nu(\text{Al-O})$ at $(880 \text{ to } 685) \text{ cm}^{-1}$ shifted to lower frequency of $870 \text{ to } 559 \text{ cm}^{-1}$ respectively as illustrated in Table (3-5).

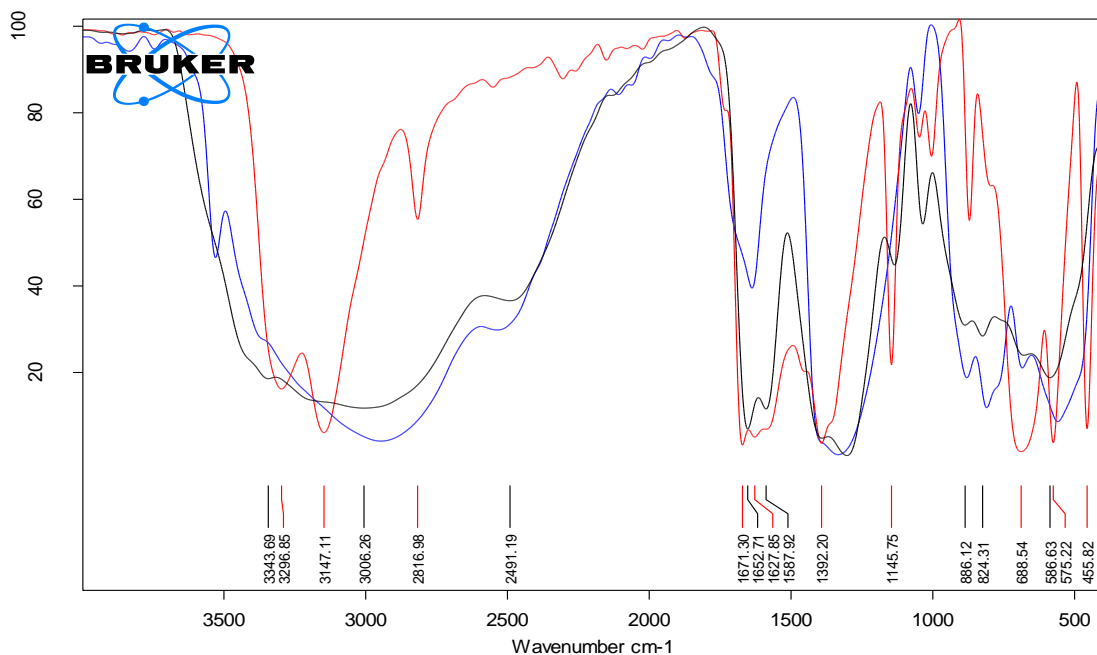


Fig.(3-9a): FTIR of (hydrated aluminum nitrate: acetamide, ANIL with 1:2.4) mole ratio (black line), hydrated aluminum nitrate (blue line) and acetamide in (red line).

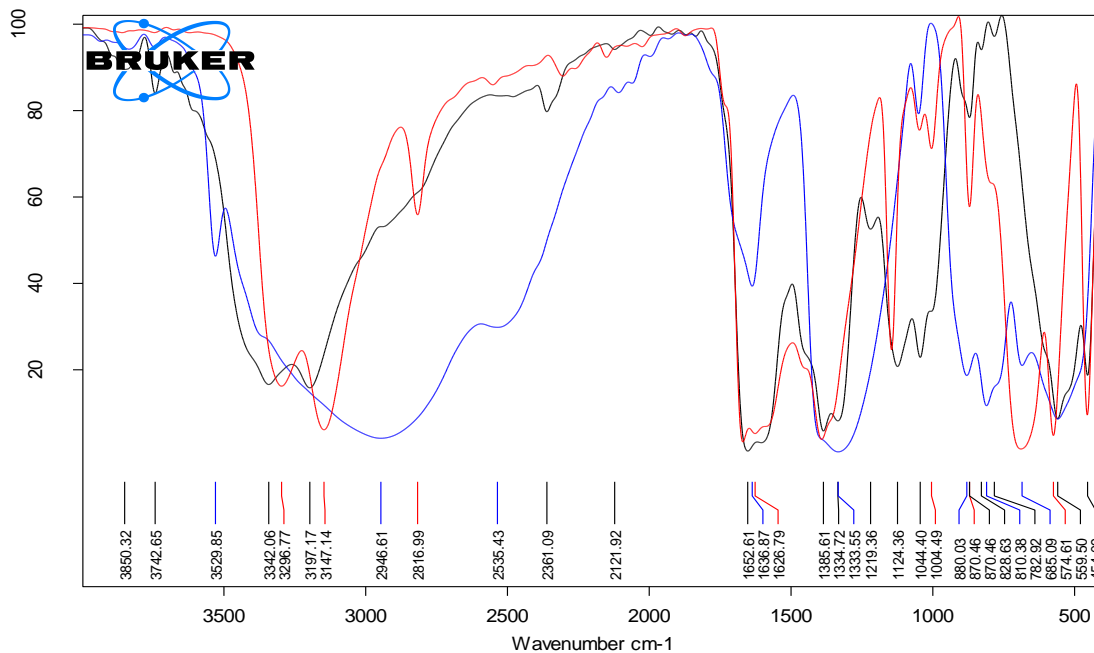


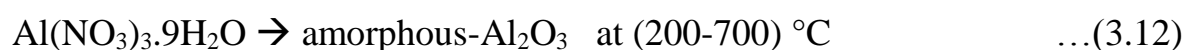
Figure (3-9b): FTIR of (hydrated aluminum nitrate: acetamide, AN2IL with 1:22 mole ratio) (black line), hydrated aluminum nitrate (blue line) and acetamide in (red line).

Table (3-5): FTIR vibration frequencies of hydrated aluminum nitrate: acetamide, ANIL with 1:2.4 and AN2IL with 1:22 mole ratios.

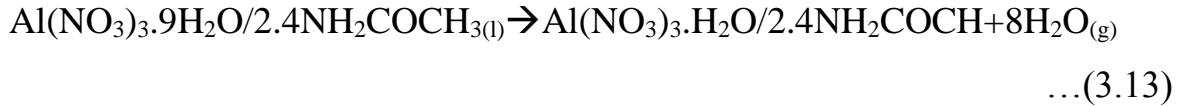
Compounds group	H ₂ NCOCH ₃	Al(NO ₃) ₃ ·9H ₂ O	ANIL (1:2.4)	AN2IL (1:22)
ν(N-H)	3147 & 3297	-	3344	3197 & 3342
ν(O-H)	-	2947	3006	3000 - 3200
ν(C-H)	2817	-	-	-
ν(N-O)	-	1334	1330	1386 & 1335
ν(C=O)	1671	-	1653	1653
ν(C-N)	1146 - 456	-	1140	1124
δ(N-H)	1392	-	1330	1386 & 1335
ν(Al-O)	-	880 - 685	886 - 586	870 - 559

However, ANIL (24.02 mg) appeared to have similar thermal behavior as AN2IL (24.22 mg), (Fig.3-10 and Fig.3-11) respectively in number of its

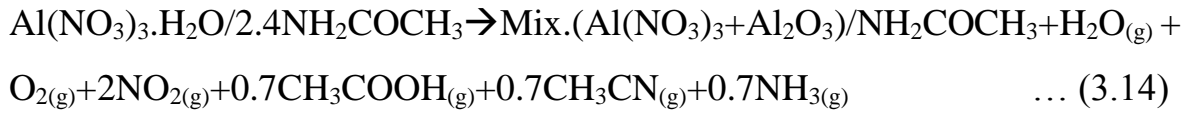
decomposition stages and endothermic /exothermic DSC peak with different weight lost percents at each stage and area under their curves related to different acetamide percent which increased from 2.4 to 22 causing such different interactions influencing not only the decomposition temperature but also further thermo-physical properties. Since ANIL and AN2IL were found to be stable until 232 °C and 276 °C respectively with two endothermic peaks in ANIL with negligible weight loss of an enthalpy value of -1536.4 kJ/kg, (Fig.3-10) compared to an enthalpy of -3697.02 kJ/kg in AN2IL (Fig.3-11). Both ANIL and AN2IL undergo three decomposition stages showing total weight loss percents of (78.56 %, -18.87 mg) and (79.85 %, -19.34 mg) respectively. ANIL decompose in temperature range of (232-254) °C as this first decomposition stage gives (27.89 %, -6.70 mg) with a significant amount of liberated heat with small enthalpy -1.56 kJ/kg referred to gaseous evaporation of water molecules through fast weight loss curve (i.e. fast decomposition rate) that reached its maximum rate at 241 °C which agreed with calculated weight loss percent of 27.87 % equation (3.13), followed by second decomposition step, equation (3.14) involve weight a loss percent (43.46 %, -10.44 mg) at temperature range of 254 to 351 °C reached its maximum rate of decomposition at 273 °C with endothermic peak of recorded enthalpy of -270.28 kJ/kg referred to the gaseous evaporation of water molecule, nitric dioxide, oxygen and pyrolysis of organic portion; acetamide giving ammonia, CH₃COOH and CH₃CN gases due to the calculated weight loss percent of 43.48 %, resemble to the decomposition of acetamide alone^[108,109] and thermal decomposition of pure aluminum nitrate^[104] as expressed in equation (3.12) that assists the suggestion of thermal decomposition of ANIL and AN2IL.



1. First decomposition stage of ANIL was:

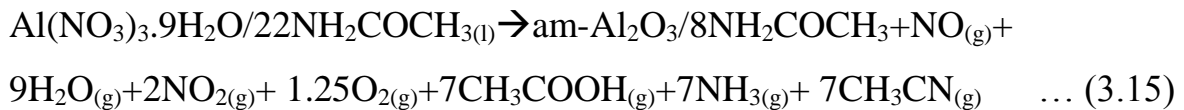


2. Second decomposition stage was:

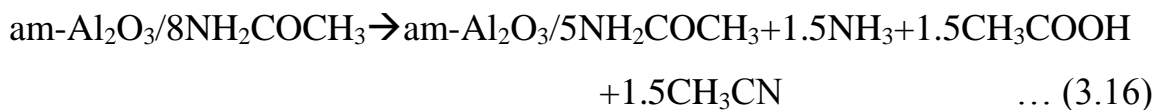


The first and second decomposition steps of ANIL appeared to merge in one step in AN2IL at a temperature between (276-332) °C with weight loss percent of (68.74 %, -16.65 mg) had an endothermic peak (Fig.3-11) with enthalpy of -302.70 kJ/kg reaching a maximum decomposition rate at 291 °C in which water molecules, NO, NO₂ and O₂ evaporated in addition to the excess acetamide that decomposing produce NH₃, CH₃COOH and CH₃CN gave calculated weight loss of 68.74 % as illustrated in equation (3.15). Decomposition of aluminum nitrate (equation 3.15) assisted with calculated weight loss percent of 68.74 % and with equation (3.12) in which amorphous alumina reported to be produced in temperature above 200 °C.

1. First decomposition stage of AN2IL:



and the second decomposition stage was:



The second decomposition stage of AN2IL gave (11.11 %, -2.69 mg) weight loss percent at a temperature range of (332-500) °C accompanied with an exothermic crystallization peak and exothermic peak with an enthalpy change of 101.07 kJ/kg referred to crystallization of the remaining product followed by endothermic peak with enthalpy of -12.93 kJ/kg resulted from decomposition giving calculated weight loss percent of 10.58 % as illustrated in equation (3.16). The third decomposition stage of ANIL with weight loss

percent of (7.20 %, -1.73 mg) produced in the temperature range of (350 to 500) °C accompanied with exothermic peak of enthalpy change of 106.62 kJ/kg at temperature range of 358.6 to 371.3 °C related to solid to solid crystallization transition reaching the maximum rate of weight loss at temperature 356 °C related to libration of nitrogen oxide and oxygen based on the calculated weight loss percent of 7.36 % as suggested in equation (3.17).

3. Third decomposition step of ANIL was:

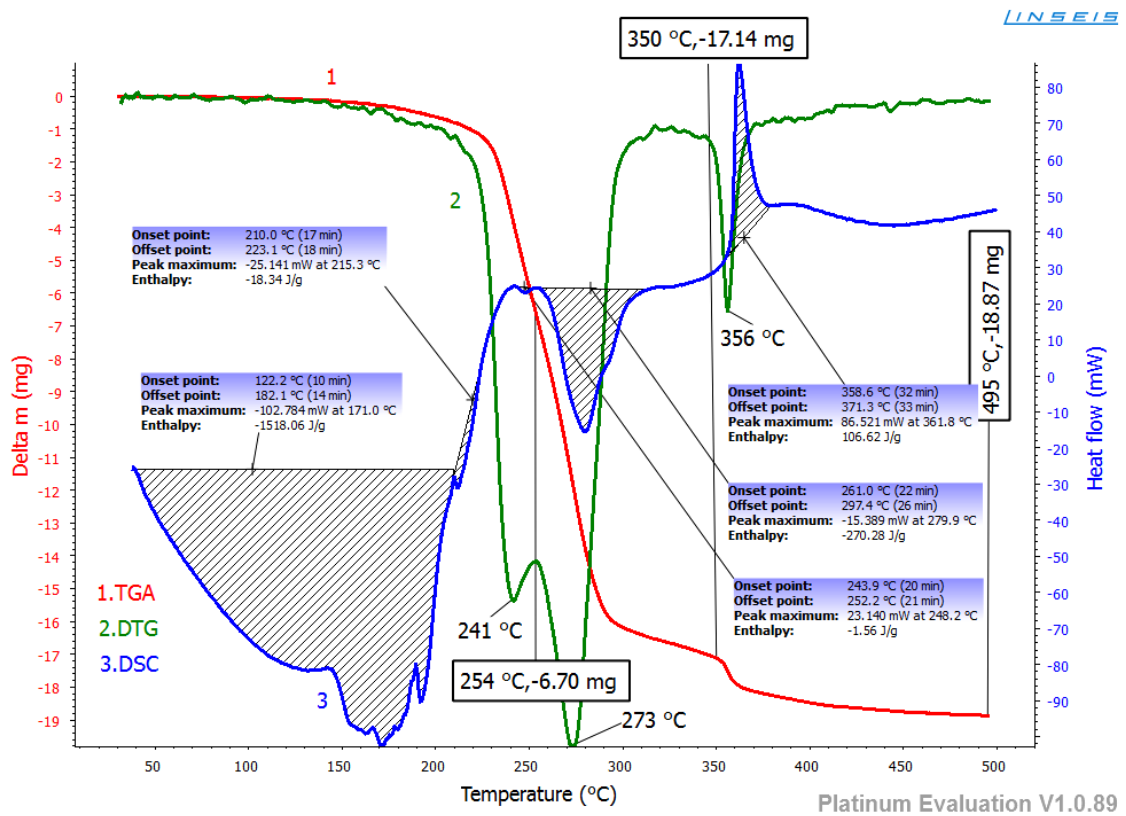
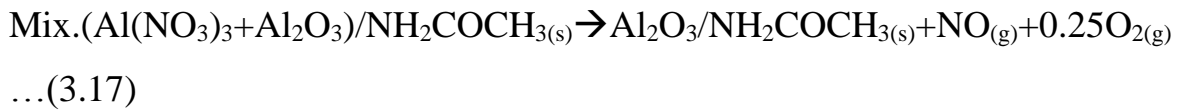


Fig.(3-10): Thermogravimetric TGA (1), Differential thermal Analysis DTG (2), Differential scanning calorimeter DSC (3) of (hydrated aluminum nitrate: acetamide, ANIL with 1:2.4 mole ratio) heated from room temperature to 495 °C at 10 °C/min.

The X-Ray diffraction of final decomposition products of ANIL showed an amorphous crystalline structure (Fig. 3-12) consisting only broad bands.

Not only high resolution of X-ray Diffractometer with a step size of 0.01 and step time of 0.2 Sec. which give minimum details, and the possibility of forming mixture of two compounds amorphous alumina and acetamide a final decomposing product, in addition to the expected structure of the product due to historical behavior of the starting material aluminum nitrate nanohydrate that form an amorphous alumina after heated it above 200 °C as illustrated in equation (3.12) leading to such bands (Fig. 3-12).

The FTIR spectra for final decomposition products of ANIL, Figure (3-13) showed the disappearance of amide and hydroxyl groups with small stretching vibration band at 1535.70 cm^{-1} that might be referred to the presence of carbonyl group of acetamide with shifting to higher stretching vibration band at 1653.80 cm^{-1} before heating ANIL to 500 °C. The stretching vibration bands at 556.28 to 771.25 cm^{-1} was related to aluminum-oxide.

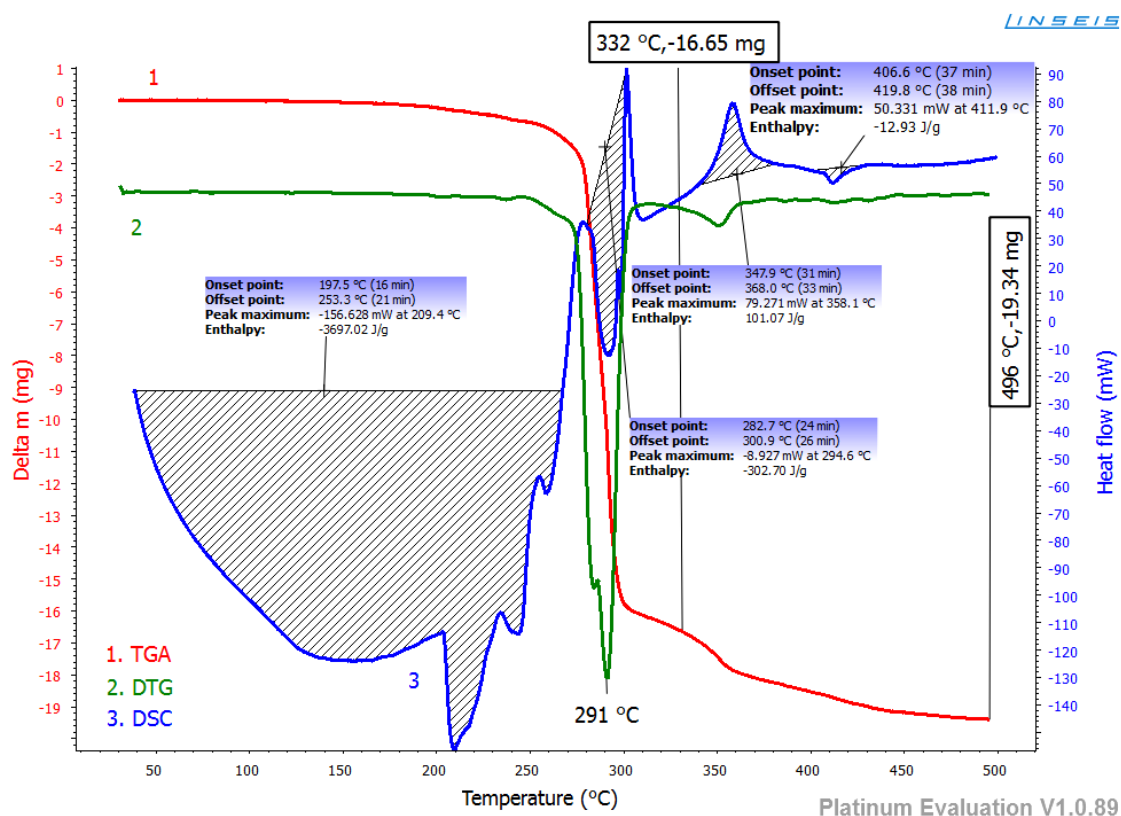


Fig.(3-11): Thermogravimetric Analysis TGA (1), Differential thermal Analysis DTG (2), Differential scanning calorimeter DSC (3) of (hydrated aluminum nitrate: acetamide, AN2IL with 1:22 mole ratio) heated from room temperature to 496 °C at 10 °C/min.

The FTIR of final product of heating AN2IL, Figure (3-14) gave different bands than that of ANIL. In general, most bands before heating AN2IL remained with lower intensities after heating. The stretching vibration did not show the bands at 2800-3500 cm^{-1} in which amine group has 2-peaks (3000 and 3400) cm^{-1} but only very broad band appeared from 2500 cm^{-1} to 3700 cm^{-1} . Vibration bands at 2361.09 cm^{-1} and 2121.92 cm^{-1} related to resonate ($\text{C}\equiv\text{N}$) bond in acetamide and the bands at around 1600 cm^{-1} was attributed to carbonyl of acetamide and the broad stretching vibration band in the range 870-454 cm^{-1} refer to (Al-O) while bands at 1385.61 and 1334.72 cm^{-1} related to nitrate group disappeared. The vibrational frequencies of nitrate group at

1385.61 cm^{-1} and 1334.72 cm^{-1} of ANIL and AN2IL was also completely disappeared after heating ionic liquids to 500 °C.

The obtained weight of final products of heating ANIL and AN2IL were (21.44 %, 5.15 mg) and (20.15 %, 4.88 mg) respectively of the original weight which were similar to those calculated for both liquids of 21.30% and 20.68% based on equation (3.17) and (3.16) respectively.

The presence of acetamide in the final product from heating ANIL and AN2IL could be due to non complete decomposition process of acetamide at 500 °C with short of experiment as the complete decomposition could be reached at 545 °C^[108,109].

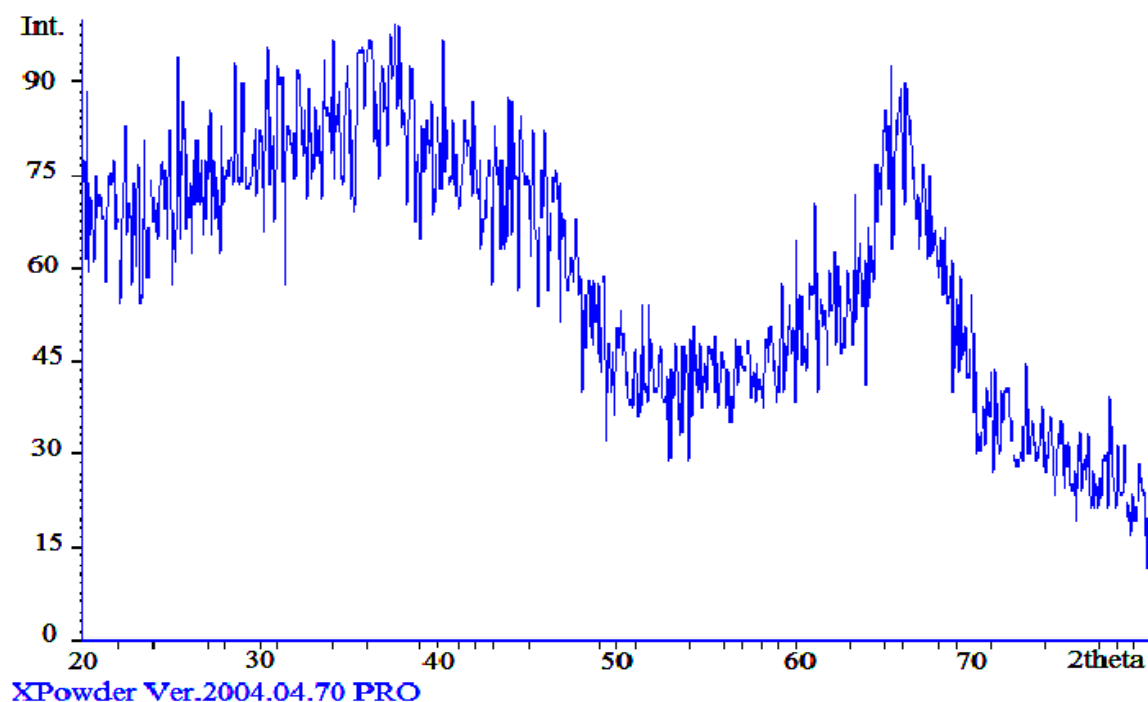


Fig.(3-12): X-ray diffraction of (hydrated aluminum nitrate: acetamide, ANIL with 1:2.4 mole ratio) after heating it to 500 °C.

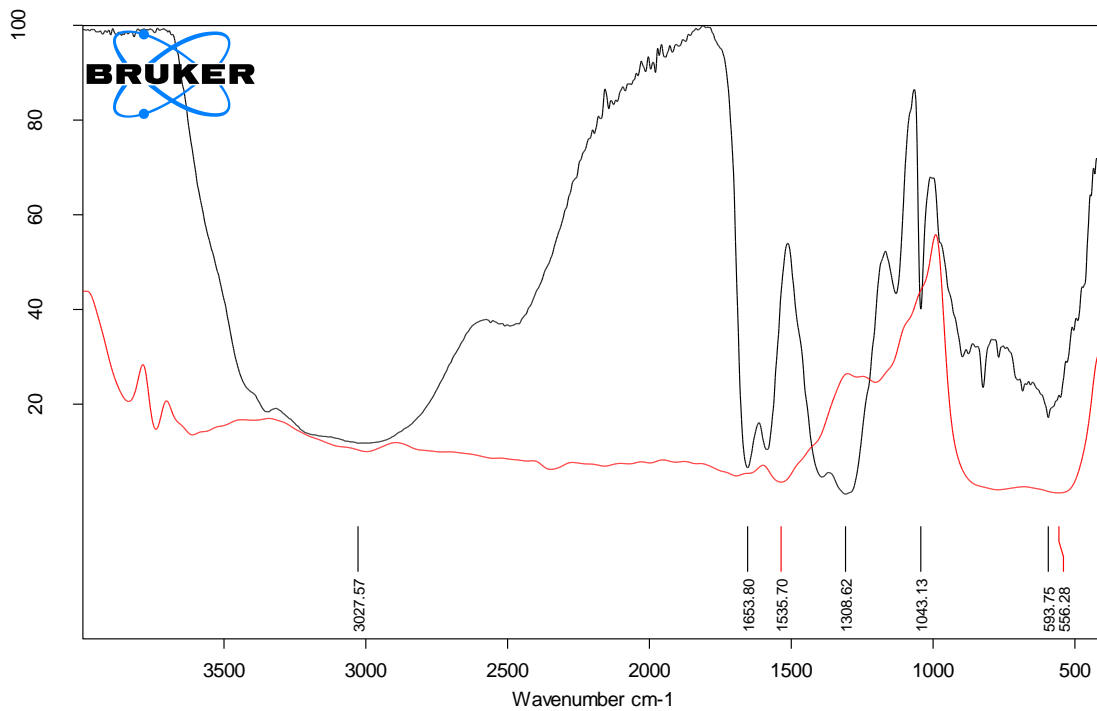


Fig.(3-13): FTIR of (hydrated aluminum nitrate: acetamide, ANIL with 1:2.4 mole ratio) (black line) and (red line) after heating it to 500 °C.

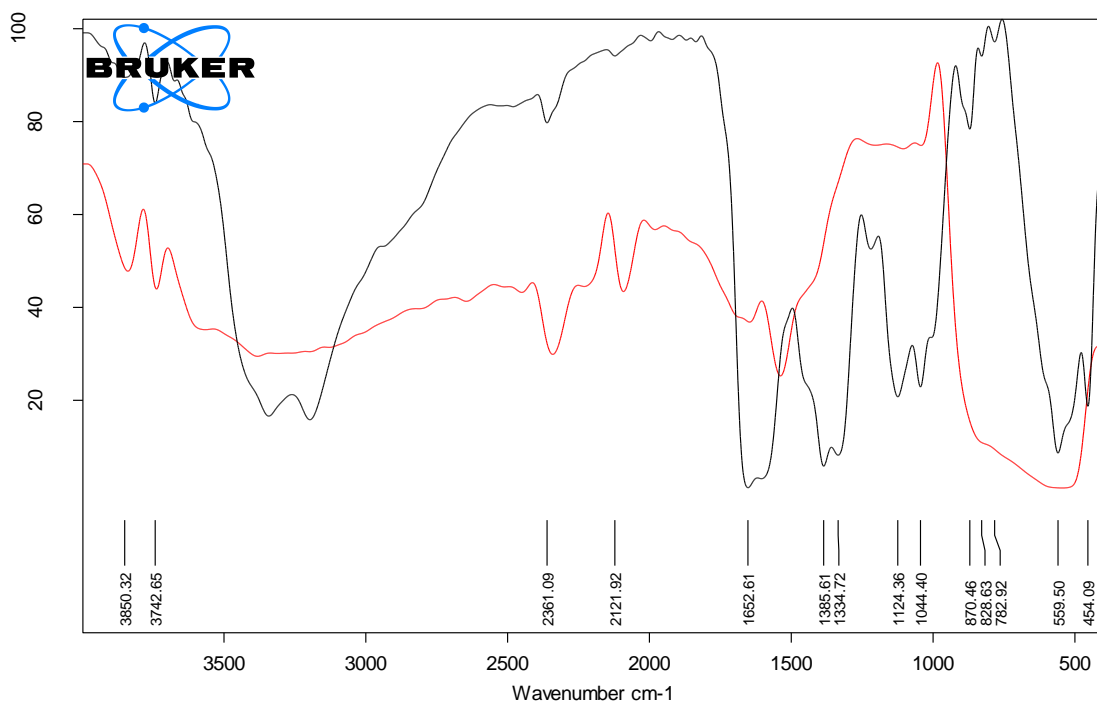


Fig.(3-14): FTIR of (hydrated aluminum nitrate: acetamide, AN2IL with 1:22 mole ratio) (black line) and (red line) after heating it to 500 °C.

3.1.4 ATR-FTIR spectroscopy, Thermal decomposition behavior and X-ray diffraction (XRD) of hydrated aluminum nitrate:urea (UNIL):-

The prepared UNIL^[80] was Analyzed by FTIR Fig.(3-15), that showed characteristic absorption bands of its components^[101-103] with small shifting. The two strong stretching vibration band of $\nu(\text{N-H})$ of $-\text{NH}_2$ in urea at (3328 and 3427) cm^{-1} were shifted to higher wave number (3352 and 3454) cm^{-1} respectively in UNIL. In addition the stretching vibration bands of $\nu(\text{C=O})$ at (1593) cm^{-1} was shifted to higher wave numbers (1693) cm^{-1} while bending vibration band $\delta(\text{N-H})$ at (1146) cm^{-1} was shifted to lower wave numbers (1036) cm^{-1} . Significant broad stretching vibration band centered at (2946) cm^{-1} of $\nu(\text{O-H})$, in H_2O molecules of hydrated UNIL may involved in hydrogen bonding with (C=O) and shifted to higher wave number of (2984) cm^{-1} in ionic liquid which might be responsible for the viscose nature of ionic liquid. Furthermore, the stretching vibration bands of $\nu(\text{Al-O})$ at (880 to 685) cm^{-1} shifted to lower frequency of (823 to 606) cm^{-1} , stretching vibration bands of $\nu(\text{N-O})$ in $-\text{NO}_3$ at (1334 and 1637) cm^{-1} shifted to lower frequency (1309) cm^{-1} ; as shown in Table (3-6).

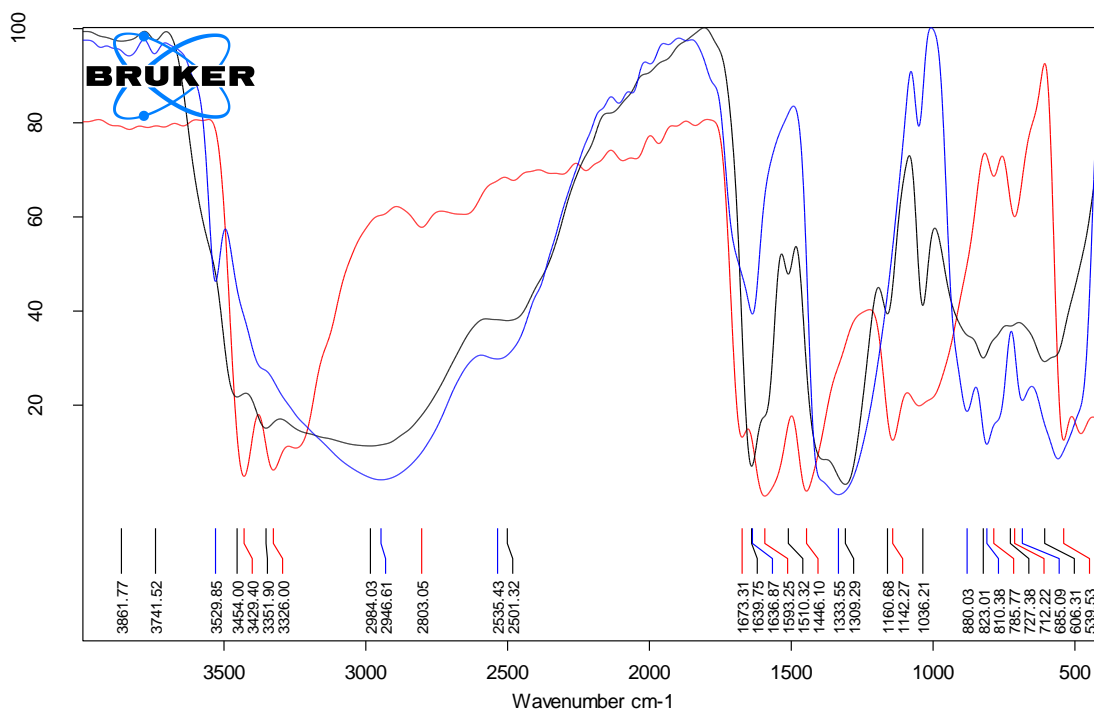


Fig.(3-15): FTIR of (hydrated aluminum nitrate: urea, UNIL with 1:1.2 mole ratio) (black line), hydrated aluminum nitrate (blue line) and urea (red line).

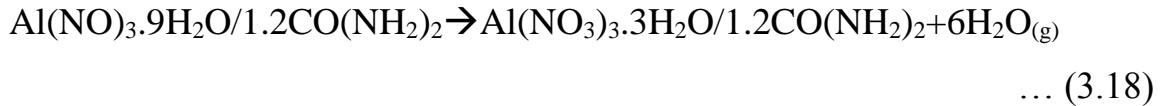
Table (3-6): FTIR vibration frequencies of hydrated aluminum nitrate: urea, UNIL with 1:1.2 mole ratio.

Compounds group	H ₂ NCONH ₂	Al(NO ₃) ₃ ·9H ₂ O	UNIL
ν(N-H)	3426 & 3429		3454 & 3352
ν(O-H).	3200	2946	2984
ν(N-O)	-	1637 & 1334	1309
ν(C=O)	1593		1639
ν(C-N)	1142		1161
δ(N-H)	1146		1036
ν (Al-O)		880 - 685	823 - 606

The TGA/DTG and DSC measurements of UNIL (23.84 mg) showed thermal stability up to 236 °C associated with an endothermic peaks refer to enthalpy value of -3319.94 kJ/kg followed by three decomposition stages until 500 °C with total weight loss percent of 56.59 % with changes in heat

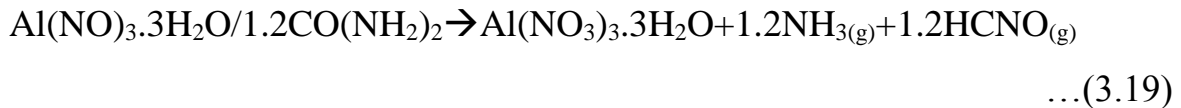
through two decomposition peaks as shown in Figure (3-16). First decomposition stage related to two endothermic peaks involve small weight loss of (3.23 %, -0.77 mg) indicated by loss of non interacted water molecule calculated to have 4.03 % weight loss percent and the recorded weight loss of (24.16 %, -5.76 mg) at a temperature range (236-271) °C might be related to rapid gaseous evaporation of water molecules which agree with calculated weight loss percent of 24.16 % related to the first decomposition endothermic peak with enthalpy value of -28.81 kJ/kg reached maximum rate of decomposition at 248 °C as shown in equation (3.18).

1. First decomposition stage:



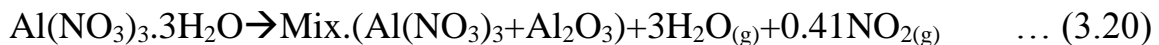
The second decomposition endothermic peak with weight loss percent of (16.11 %, -3.84 mg) related to an enthalpy of -216.85 kJ/kg referred to urea decomposition giving ammonia and isocyanic acid gases that agreed with calculated weight loss percent of 16.11 % as illustrated in equation (3.19).

2. Second decomposition stage:



The recorded weight loss percent in the slow third decomposition stage gave (16.32 %, -3.89 mg) weight loss referred to gaseous evaporation of water molecules and nitrogen dioxide due to the calculated weight loss percent of 16.30 % as explained in equation (3.20).

3. Third decomposition stage:



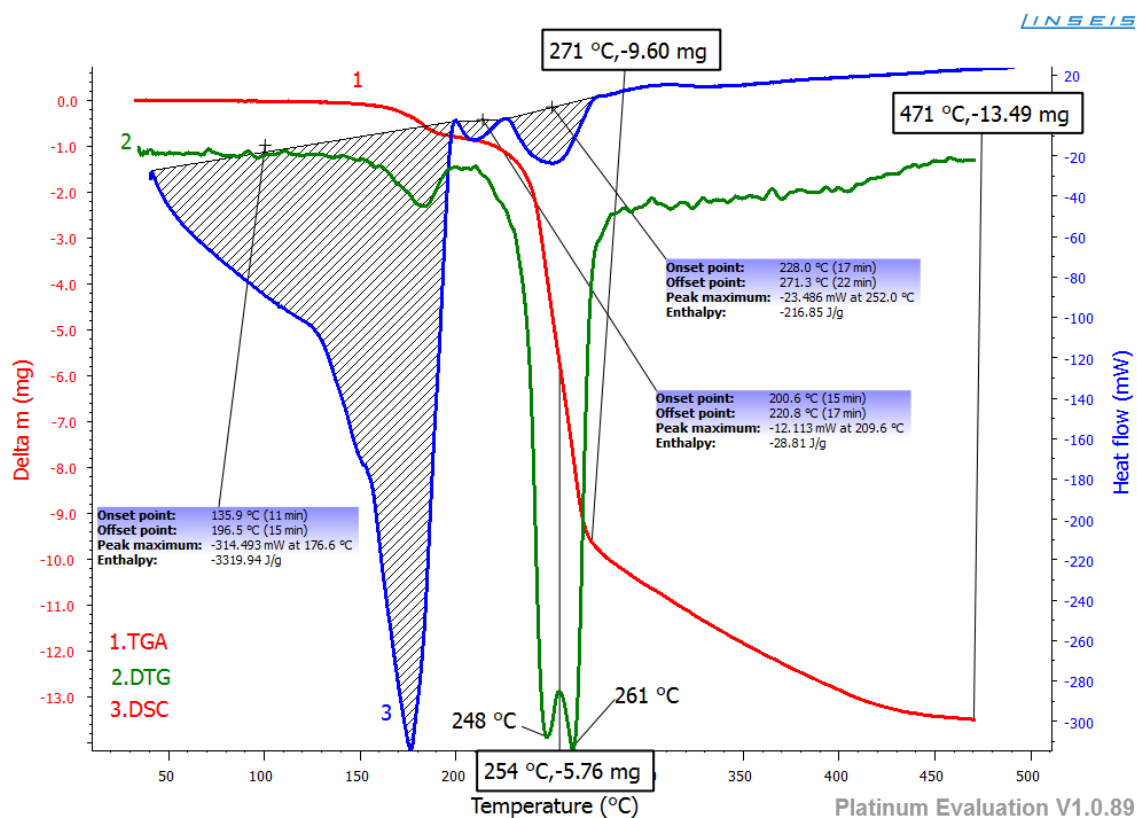
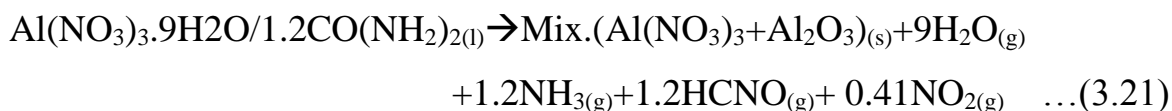


Figure (3-16): Thermogravimetric TGA (1), Differential thermal Analysis DTG (2), Differential scanning calorimeter DSC (3) of (hydrated aluminum nitrate: urea, UNIL with 1:1.2 mole ratio) heated from room temperature to 471 °C at 10 °C/min.

The X-Ray diffraction analysis of the final product of decomposition of UNIL at 500 °C consisting broad bands Figure (3-17) indicating an amorphous product.

The FTIR spectra for this remaining amorphous product of UNIL, Figure (3-18) showed, only one broad band from 3748 cm^{-1} and 2987 cm^{-1} to 821 cm^{-1} compared to multibands of original UNIL Fig.(3-17) which hardly to be analyze.



However, recorded weight obtained from TGA/DTG (43.41 %, 10.35mg) agreed with calculated weight percent of (43.42 %) based on equation (3.21).

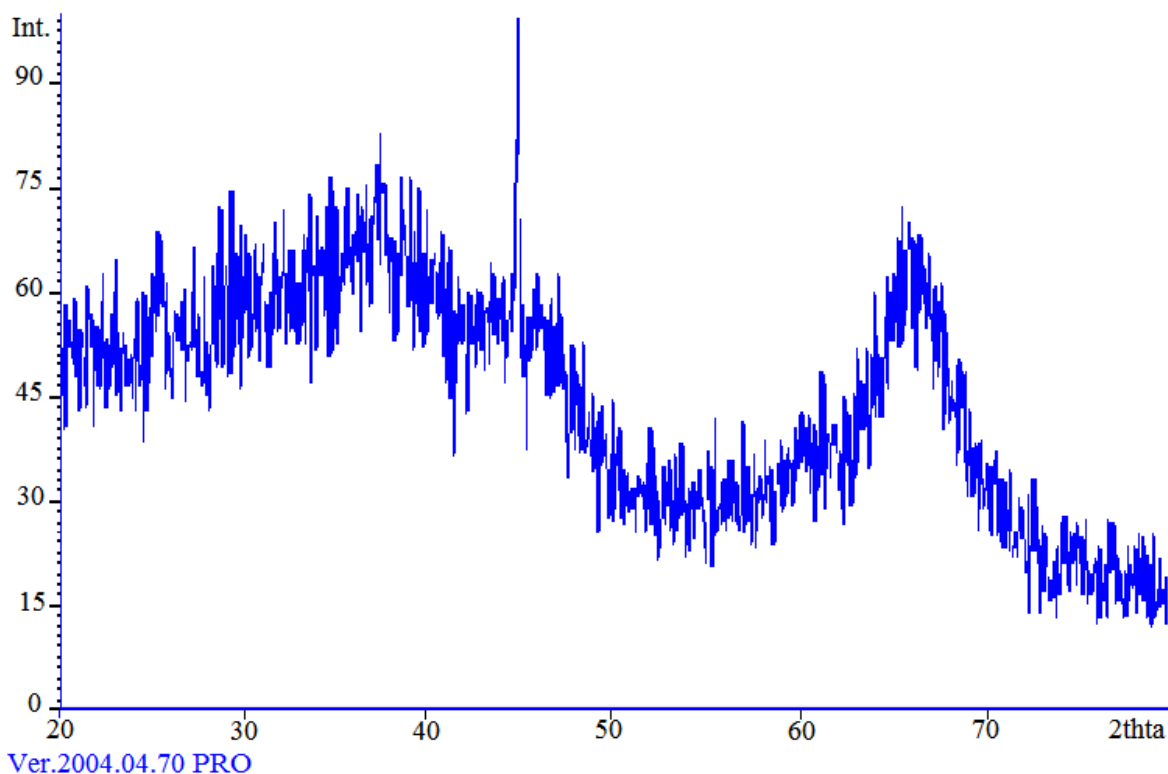


Fig.(3-17): X-Ray diffraction of (hydrated aluminum nitrate: urea, UNIL with 1:1.2 mole ratio) after heating to 500 °C.

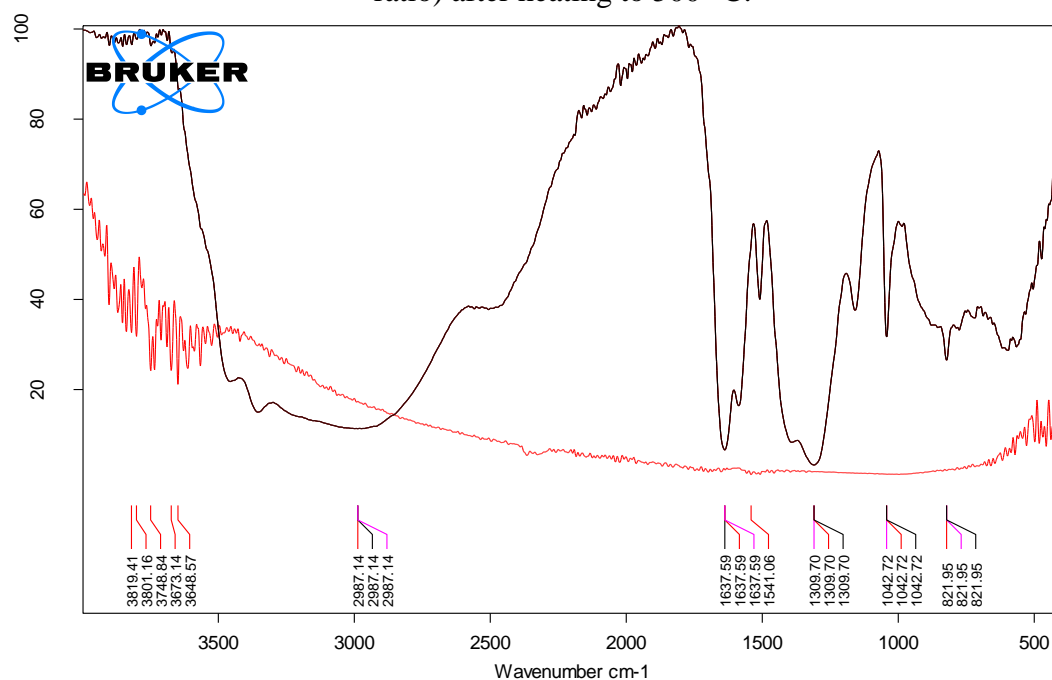


Fig.(3-18): FTIR of (hydrated aluminum nitrate: urea, UNIL with 1:1.2 mole ratio) (black line) and in (red line) after heating to 500 °C.

3.2 Thermo-physical properties of ionic liquids:-

Thermal data of ionic liquids of present investigation were done by TGA and DSC. The obtained data believed to be essential for both practical research and industrial application.

3.2.1 Thermal properties:

Thermal measurements of ionic liquids of present investigation are shown in Table (3-7) characterized by a wide range of freezing points (-25 to 50 °C) for different composition of these ionic liquids.

The lowest freezing temperature for the prepared these ionic liquids were -25 °C obtained for AN2IL in the mole ratios of (1:4 to 1:22) while the highest freezing point was 50 °C recorded for aluminum nitrate:acetamide ionic liquid of 1:1 mole ratio and 0 °C for ASIL with 1:12 mole ratio. The highest decomposition temperature of 280 °C was found for USIL and lower decomposition temperature of 203 °C was recorded for ASIL, but these temperatures indicated no relation between the melting point and decomposition temperature of these ionic liquids. However, it was expected that water would be evolved from these ionic liquids if heated to around 100 °C, but the absence of such evaporation indicated a strong bond of water molecules with species of ionic liquids as weight loss was only recorded around 203 °C. Such coordination was concluded in other work suggested from UV spectroscopic study of USIL^[79]. The ionic liquids stability may be arranged in the following order USIL > AN2IL > UNIL > ANIL > ASIL based on their decomposition temperatures.

Ionic liquid composed of sulfate and urea was found to be most stable liquid compared with other ionic liquids. This could be arise from stronger interaction of the constituent species of the cationic or anionic species formed from the original salts. Once the onset temperatures were reached for each ionic liquid the rate of decomposition of these ionic liquid was found to be very fast.

The different stability of these ionic liquids might also be related to the availability of amide groups coordinated with species in the liquid state. Other factor might be related to the two amide groups present in urea than in acetamide adding another coordination bond to the liquid containing urea than acetamide. If this was true then expected that urea containing ionic liquids have more thermal stability than acetamide containing ionic liquids. However, the AN2IL which is the second most stable as indicated in the above series could be related to the high mole ratio of acetamide percent in this liquid (i.e. 1:22) compared to other ionic liquids, Table (3-7), and acetamide known to have higher stability than urea (compare 425 °C with 132 °C respectively).

Acidity value, Table (3-8), of ionic liquids could be put in the order UNIL > ANIL > AN2IL > ASIL > USIL, which indicated the formation of acidic species of lewis type formed with cationic charges (e.g. for UNIL $[Al(NO_3)_2.n \text{ Urea}]^+ [Al(NO_3)_4]^-$) in analogous to those reported in aluminum chloride/urea ionic liquid^[114] which required additional identification to confirm its formula.

Table (3-7): Thermo-physical properties of five room temperature ionic liquids.

IL	T _m , °C	T _d , °C	ρ, kg/m ³	C _p , kJ/kg.°C)	E, kJ/m ³ *10 ⁵
ASIL (1:12)	0.0	203	1116	2.1	4.758
USIL (1:5)	-16	280	1460	2.2	9.508
ANIL (1:2.4)	-20	232	1405	1.6	5.665
AN2IL (1:22)	-25	276	1168	2.4	8.438
UNIL (1:1.2)	-20	236	1522	1.9	7.403

Ionic liquids containing acetamide as organic compound in the formation showed significant effect on liquid temperature range rather than inorganic salts, thus it was found that the temperature at which ANIL in the (1:2.4) mole

ratio remaining liquid down to -20 °C resulted from structural lattice deformation that was difficult to rearrange to its original structural solid lattice due to new ion formation. This resulted in freezing point reduction and a probable tendency for glass formation on cooling, rather than crystallization.

In the case ionic liquids containing urea showed that the effect of inorganic salts (hydrated ammonium aluminum sulfate and hydrated aluminum nitrate) more significant rather than urea liquid range reduction, since the presence of several different anions in these ionic liquids have the effect of significantly decreasing the freezing point and a pronounced possible tendency for glass formation on cooling, rather than crystallization. This would be an indicative of inefficient packing within the crystal structures.

3.2.2 Conductivity (k):

Conductivities of these ionic liquids have no relation with their pH values as the smaller pH value is not necessarily gave higher conductivity, Table (3-8). UNIL showed much higher conductivity than other ionic liquids while acetamide ionic liquids show lower conductivity than urea ionic liquids. Yet the presence of much higher mole ratio of acetamide of 22 in AN2IL did not show appreciable increase in conductivity. This may be related to the hindrance of ionic mobility in ionic liquids^[7].

The highest conductivity found was (9.09mS.cm⁻¹) for UNIL at 26 °C and reached 13.61 mS.cm⁻¹ at 70 °C as shown in Figure(3-19). Other ionic liquids have lower conductivities of 4.56 mS.cm⁻¹ at 26 °C for USIL down to 1.32 mS.cm⁻¹ at 30 °C for ASIL. The lowest conductivity value from these ionic liquids was much higher than reported ionic liquid of [C₂MIm][amino acids] (

$\lambda = 9.1 \times 10^{-6}$ to 0.65 mS.cm^{-1})^[115] and three times higher than [N₂₂₂₂][Pro] (0.46 mS.cm^{-1}) and eight times higher than [N₂₂₂₂][Ser] (0.16 mS.cm^{-1})^[116].

The conductivity of these ionic liquids was found to be directly proportional with temperature, Fig. (3-19). However, obtained conductivities were found to be small if compared to aqueous electrolyte solution due to the fact that conductivity depend on the mobility of ions and high concentration of ions in ionic liquid block the movement of ions^[8].

The temperature dependence of conductivity for ANIL, as in Figure (3-19) involved a complex interplay of short- and long-range forces that is strongly impacted by the type and character of the cation and anion^[20]. At our current level of understanding it is not possible to accurately predict how the conductivity of a given ionic liquid will vary with temperature. Since this conductivity reduction may be due to ion pairs or ion aggregation.

The proportion between conductivity and temperature is apply to some extent ; it was observed at a certain temperature the conductivity of USIL and UNIL ionic liquids become constant with temperature increase as in the figure (3-19) at temperature $65 \text{ }^\circ\text{C}$ and $50 \text{ }^\circ\text{C}$ respectively, result in smaller than expected conductivity of ionic liquids that can be attributed to the reduction of available charge carriers due to ion pairing and/or ion aggregation, and to the reduced ion mobility resulting from the large ion size found in many ionic liquids^[3].

Table (3-8): Conductivity (\bar{k}) and pH of five room temperature ionic liquids at $22 \text{ }^\circ\text{C}$.

IL	ASIL (1:12)	USIL (1:5)	ANIL (1:2.4)	AN2IL (1:22)	UNIL(1:1.2)
pH	2.3	4.2	0.8	1.8	0.5
\bar{k} (mS/cm)	1.32	4.56	4.10	3.72	9.09

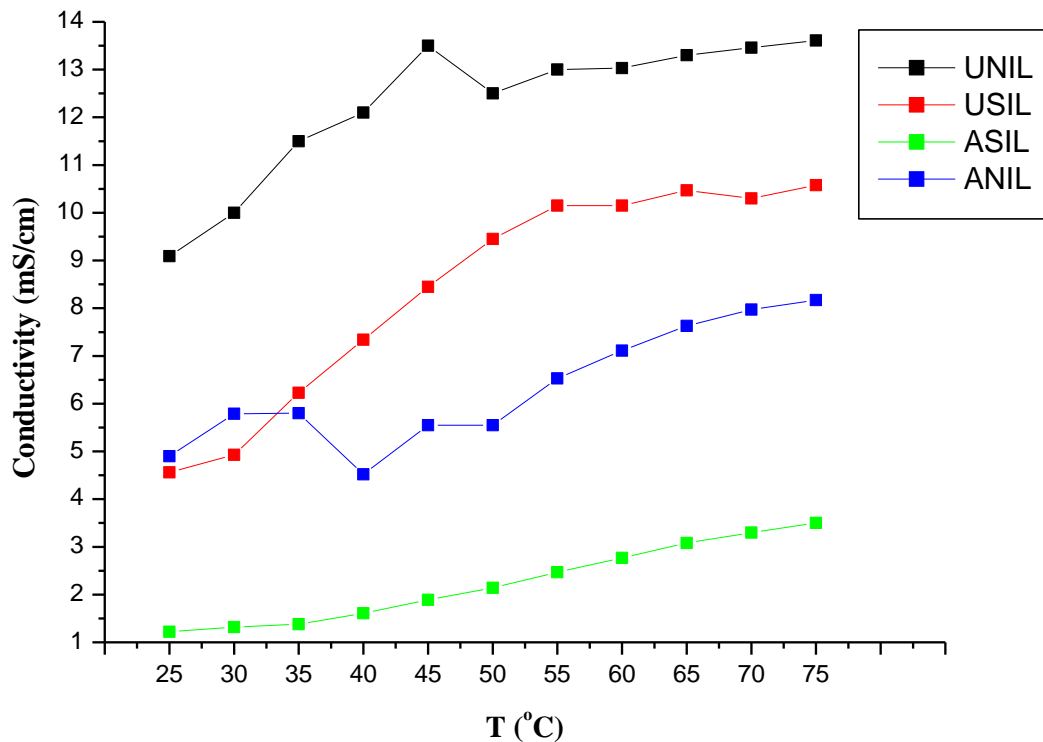


Figure (3-19): Conductivity (mS/cm) of (a): hydrated aluminum nitrate:urea, UNIL with 1:1.2 mole ratio, (b): hydrated ammonium aluminum sulfate:urea, USIL with 1:5 mole ratio), (c): hydrated ammonium aluminum sulfate:acetamide, ASIL with 1:12 mole ratio and (d): hydrated aluminum nitrate:acetamide, ANIL with 1:2.4 mole ratio versus temperature up to 70 °C.

3.2.3 Density:

Five ionic liquids are reviewed here on the basis of their density at room temperature 22 °C. Relatively small variation is observed in the density of the studied ionic liquids as shown in Table (3-7). Here, the density range from 1405 to 1522 kg/m³ for ionic liquids shown here which were higher than density value of water (998 kg/m³) as most ionic liquids, which are preferred density values of the common organic liquids used for thermal energy storage in the vicinity of 1100 kg/m³^[28]. Thus, Materials with higher density as these five ILs help to increase the energy storage capacity (E).

The linearity of this relation holds only up to some extent. Solid materials at room temperature with high density obviously possess higher energy storage capacity but many of them show a significant decrease in density in their molten state, the inorganic materials and their eutectic mixtures used for the same purpose have very high density ranging from 1440 to 2260 kg/m³.

Interestingly, ionic liquids being composed of organic portions exhibit density values 1320 kg/m³ for urea and 1159 kg/m³ for acetamide, and inorganic portions exhibit density values 1640 kg/m³ for hydrated ammonium aluminum sulfate and 1720 kg/m³ for hydrated aluminum nitrate had a density values lower than inorganic salts and higher than the corresponding organic compounds. Thus ionic liquids densities can be put between the densities of its components.

3.2.4 Enthalpy (ΔH):

Enthalpy is a state function that depending only on the initial and final point and independent in the path between them, here the measured enthalpy represent the energy stored in ionic liquid by heating it from room temperature to its decomposition point using DSC thermogram. Enthalpy is one of the most important properties for a potential thermal energy storage device. These values were calculated from the area enclosed in phase change endothermal DSC peaks.

It's found that the enthalpy of ASIL registered the lowest value (-250.51 kJ/kg) kJ/kg obviously appeared at the first endothermic DSC peak through temperature range (91.8-171.75) °C and the highest values found in urea based ionic liquids with an enthalpies of -2434.84 and -3319.94 kJ/kg recorded for USIL and UNIL respectively as shown in Table (3-9). ANIL exhibited an enthalpy value of -1536.4 kJ/kg and this value increased in significant amount with increasing acetamide ratio to 22 in AN2IL reaching to an enthalpy of -3697.02 kJ/kg.

Since large values of enthalpy leads to more efficient thermal energy storage in comparable with other thermal energy storage materials and other ionic liquids that show relatively small values of heat of fusion which are around 50 kJ/kg. On the other hand, the inorganic materials have a very high heat of fusion of around 200 to 500 kJ/kg and the organic materials including paraffins show these values around 100 to 200 kJ/kg. Thus ionic liquids of ASIL, USIL, ANIL, AN2IL and UNIL found to higher than most heat storage materials.

Table (3-9): Enthalpy (ΔH) and entropy (ΔS) of five room temperature ionic liquids.

IL	ASIL (1:12)	USIL (1:5)	ANIL (1:2.4)	AN2IL (1:22)	UNIL(1:1.2)
ΔS , kJ/kg. $^{\circ}C$	-1.976	-16.321	-8.963	-17.655	-18.799
ΔH , kJ/kg	-250.51	-2434.84	-1536.4	-3697.02	-3319.94
ΔG , kJ/kg	-201.11	-2026.82	-1312.33	-3255.65	-2849.97

3.2.5 Heat capacity (C_p) and thermal energy storage capacity (E):

The heat capacities (C_p), densities (ρ), and thermal energy storage capacities (E) of some heat storage materials are listed in Table (3-10).

Heat capacities of these ILs were elucidated from DSC thermograms, Fig. (3-20) using Al_2O_3 as reference material^[92] with $-7.6 \mu V$ heat flow and $0.80 \text{ kJ/kg.}^{\circ}C$ heat capacity, the average base line heat flow value was $-4.08 \mu V$ and the heat flow of ionic liquids in microvolt (μV) were obtained from DSC thermogram as showed in Figure (3-20), that can be calculated using equation(1.4) as illustrated previously in chapter one:

$$C_{p(\text{sample})} = (H_{(\text{sample})} - H_{(\text{baseline})}) * M_{(\text{ref.})} * C_{p(\text{ref.})} / (H_{(\text{ref.})} - H_{(\text{baseline})}) * M_{(\text{sample})} \dots (1.4)$$

$$1. C_p(\text{ASIL}) = (-15.2 + 4.08) \mu V * 19.9 \text{ mg} * 0.8 \text{ kJ/kg.}^{\circ}C / (-7.6 + 4.08) \mu V * 24.06 \text{ mg} \\ = 2.1 \text{ kJ/kg.}^{\circ}C \quad \text{heat capacity of ASIL.}$$

$$2. C_p(\text{USIL}) = (-15.8 + 4.08) \mu V * 19.9 \text{ mg} * 0.8 \text{ kJ/kg.}^{\circ}C / (-7.6 + 4.08) \mu V * 24.06 \text{ mg}$$

= 2.2 kJ/kg.°C heat capacity of USIL.

3. $C_p(ANIL) = (-12.5 + 4.08) \mu V * 19.9 \text{mg} * 0.8 \text{kJ/kg.}^\circ\text{C} / (-7.6 + 4.08) \mu V * 24.02 \text{mg}$
 = 1.6 kJ/kg.°C heat capacity of ANIL.

4. $C_p(AN2IL) = (-16.9 + 4.08) \mu V * 19.9 \text{mg} * 0.8 \text{kJ/kg.}^\circ\text{C} / (-7.6 + 4.08) \mu V * 24.22 \text{mg}$
 = 2.4 kJ/kg.°C heat capacity of AN2IL.

5. $C_p(UNIL) = (-14.2 + 4.08) \mu V * 19.90 \text{mg} * 0.8 \text{kJ/kg.}^\circ\text{C} / (-7.6 + 4.08) \mu V * 23.84 \text{mg}$
 = 1.9 kJ/kg.°C heat capacity of UNIL.

The values of heat capacity were found in the range of 1.6–2.4 kJ/kg °C for this work Table (3-10). These values were found to be higher in case of AN2IL, USIL, UNIL and ASIL. The ANIL showed the least value for heat capacity. Also was found that the lowest value of heat capacity of ionic liquids presented in this work still higher than those ionic liquids of $[N^{+4444}][BF_4^-]$, $[N^{+4444}][PF_6^-]$ and $[N^{+4444}][NO_3^-]$, Table (3-10).

The value of heat capacity was not significant as the most important property of thermal energy storage capacity depends on temperature range and density. Thus, thermal energy storage capacities calculated in the usable temperature range ($T_d - T_m$) of ionic liquid using the following equation [43]:

$E = \rho \cdot C_p (T_d - T_m) \dots\dots\dots (3.22)$

1. $E(ASIL) = 1116 \text{ kg/m}^3 * 2.1 \text{ kJ/kg.}^\circ\text{C} (203 - 0)^\circ\text{C} = 4.758 * 10^5 \text{ kJ/m}^3$
2. $E(USIL) = 1460 \text{ kg/m}^3 * 2.2 \text{ kJ/kg.}^\circ\text{C} (280 + 16)^\circ\text{C} = 9.508 * 10^5 \text{ kJ/m}^3$
3. $E(ANIL) = 1405 \text{ kg/m}^3 * 1.6 \text{ kJ/kg.}^\circ\text{C} (232 + 20)^\circ\text{C} = 5.665 * 10^5 \text{ kJ/m}^3$
4. $E(AN2IL) = 1168 \text{ kg/m}^3 * 2.4 \text{ kJ/kg.}^\circ\text{C} (276 + 25)^\circ\text{C} = 8.438 * 10^5 \text{ kJ/m}^3$
5. $E(UNIL) = 1522 \text{ kg/m}^3 * 1.9 \text{ kJ/kg.}^\circ\text{C} (236 + 20)^\circ\text{C} = 7.403 * 10^5 \text{ kJ/m}^3$

Table (3-10): A comparison of reported heat capacities (C_p), densities (ρ), temperature range ($^{\circ}\text{C}$) and thermal energy storage capacities (E) of some heat storage materials compared with ionic liquids present work.

<i>Heat storage materials</i>	C_p (kJ/kg. $^{\circ}\text{C}$)	ρ (kg/m ³)	<i>Temp. range</i> ($^{\circ}\text{C}$)	E , (kJ/m ³) *10 ⁵	<i>Ref.</i>
Water	1.60 at 100 $^{\circ}\text{C}$	1000	0 - 100	1.600*	[40]
Therminol VP-1	1.78 at 130 $^{\circ}\text{C}$	1060	-	1.887	[116]
Molten salt-Nitrate salts	1.45 at 300 $^{\circ}\text{C}$	1992	120- 500	-	[118]
[C ₂ MIm][BF ₄]IL	1.28 at 130 $^{\circ}\text{C}$	1253	-	1.609	[117]
[C ₄ MIm][BF ₄]IL	1.66 at 130 $^{\circ}\text{C}$	1175	-	1.949	[68]
[C ₁₆ CPTS]IL	2.85 at 145 $^{\circ}\text{C}$	922	-	2.628	[119]
[C ₈ MIm][PF ₆]IL	2.50	1400	-75 - 416	-	[40]
[N ⁺ ₂₂₂₂][IO ₃ ⁻]IL	1.70	1162	53 - 180	2.293	[43]
[N ⁺ ₄₄₄₄][BF ₄ ⁻]IL	1.00	1291	71 -	-	[69]
[N ⁺ ₄₄₄₄][PF ₆ ⁻]IL	0.40	1234	71 -	-	[69]
[N ⁺ ₄₄₄₄][NO ₃ ⁻]IL	1.50	1195	98 -	-	[69]
ANIL (1:2.4)	1.60	1405	-20 - 232	5.665	This work
AN2IL (1:22)	2.40	1168	-25 - 276	8.438	This work
ASIL (1:12)	2.10	1116	0 - 203	4.758	This work
USIL (1:5)	2.20	1460	-16 - 280	9.508	This work
UNIL (1:1.2)	1.90	1522	-20 - 236	7.403	This work

*calculated value from their reference information.

Most of ILs showed a significantly higher value of thermal energy storage capacity in the diversity of (4.758 to 9.508) $\times 10^5$ kJ/m³. As the other thermo-physical properties USIL, AN2IL, and UNIL exhibited the highest values of thermal energy storage capacity across the series.

As shown in the Table (3-10) thermal energy storage capacity (E) of ionic liquids presented in this work was much larger than many heat storage material except molten nitrate salts and [C₈MIm][PF₆] ionic liquid. High freezing points up to 120 $^{\circ}\text{C}$ of nitrate salts restrict their usage as heat storage

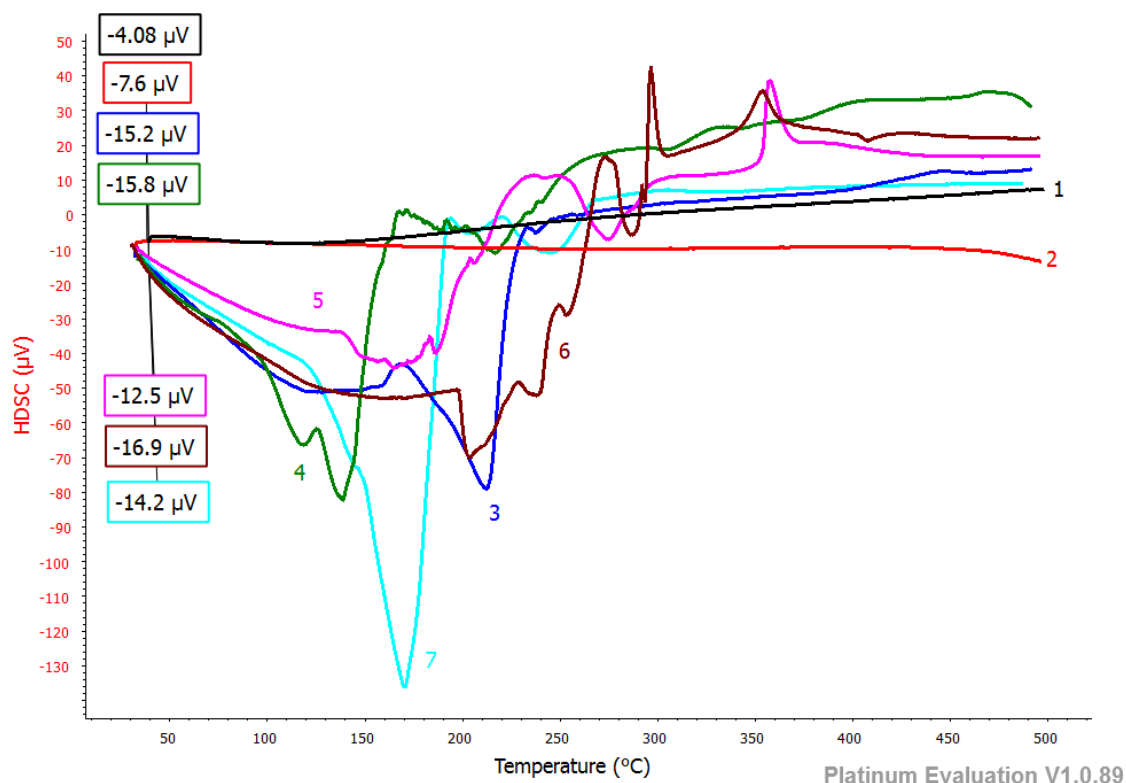


Figure (3-20): DSC thermogram in μV for; (1): baseline, (2): reference material (Al_2O_3), (3): hydrated ammonium aluminum sulfate:acetamide, ASIL with 1:12 mole ratio, (4): hydrated ammonium aluminum sulfate:urea, USIL with 1:5 mole ratio, (5): hydrated aluminum nitrate:acetamide, ANIL with 1:2.4 mole ratio, (6): hydrated aluminum nitrate:acetamide, AN2IL with 1:22 mole ratio, (7): hydrated aluminum nitrate:urea, UNIL with 1:1.2 mole ratio at $10\text{ }^\circ\text{C}/\text{min}$.

and transfer fluid that add complexity of design, operation, and maintenance of a trough plant^[116] and ionic liquids containing PF_6^- ions are hydrolytically unstable, have the propensity to decompose and release HPO_2F_2 , $\text{H}_2\text{PO}_3\text{F}$, H_3PO_4 , and highly corrosive HF ^[75]. It is worth mentioning that several ‘uncatalyzed’ reactions reported in $[\text{cation}][\text{PF}_6]$ ionic liquids that were, in fact, catalyzed by adventitious HF . Thus, a significant impact of IL anions is the release of HF containing compounds for which considerable care should be taken while using PF_6 containing ionic liquids. Thus, ILs should be treated with caution due to their unexplored toxicity and/or stability^[20]. Rogers et al.

identified 1-butyl-3-methylimidazolium fluoride hydrate crystallographically as a decomposition product that was obtained from hydrolytic degradation of $[\text{C}_4\text{MIm}][\text{PF}_6]$ during purification process. They observed the evolution of acidic HF white fumes, which are colorless, highly toxic and corrosive^[8].

Also it was found that the lowest value of heat capacity of ionic liquids presented in this work was higher than some ionic liquids i.e. $[\text{N}^+_{4444}][\text{BF}_4^-]$, $[\text{N}^+_{4444}][\text{PF}_6^-]$ and $[\text{N}^+_{4444}][\text{NO}_3^-]$, Table(3-10).

Moreover, the studied ionic liquids have some interesting and favorable properties, such as the higher enthalpies, higher specific heat capacities, and higher thermal energy storage capacity. In addition, ammonium alum or aluminum nitrate based RTILs could be considered safer than other ionic liquids $\{[\text{C}_4\text{MIm}][\text{BF}_4]$ and $[\text{C}_8\text{MIm}][\text{PF}_6]\}$ which are liable to release high toxic and corrosive product (HF)^[8]. On basis of safety, moisture stability and lower cost, these ionic liquids have the advantageous for usage in thermal applications such as thermal storage media.

3.4 Addition of some materials to ionic liquids:

Some alkali metal hydroxides, alkaline earth metal oxides and transition metal oxides were chosen according to their high temperature volatilization and their relative stability mainly above 1200 K ^[120] were added to some ionic liquids to investigate their ability to improve thermal characteristic of some ionic liquid, these material and their effect are outlined.

3.4.1 Addition of alkali metal hydroxide to ILs:

Potassium hydroxide was added to USIL, and sodium hydroxide to AN2IL and UNIL when their thermo-physical properties were investigated. It was found that both hydroxides have different behavior in ionic liquids. Thus addition of sodium hydroxide to UNIL increases storage capacity of UNIL,

despite the negligible change in the pH from 0.5 to 0.3 that eliminate the possibility of forming neutral mixture which would result from protonic acid-base reaction. In addition to the negligible effect on the liquid temperature range i.e. freezing point elevated from -20 to -17 °C and decomposition temperature reduced from 236 to 188 °C with increasing the rate of decomposition as shown in the (Fig.3-21). It had a significant effect on other thermo-physical properties such as visual observed decrease in viscosity. Despite the large decrease in enthalpy reached to 45 % from enthalpy of UNIL alone which decreased to -1824.44 kJ/kg at a maximum decomposition temperature of 188.3 °C with disappearance of second decomposition peak of UNIL and decrease enthalpy of decomposition related to the third decomposition step to -77.83 kJ/kg as shown in Figure (3-21). In addition to the significant increase in heat capacity, thermal energy storage capacity enhanced by 27 % and become 10.105×10^5 kJ/m³ as shown in Table (3-11).

Table (3-11): Thermal characteristics of ionic liquids with some alkali metal hydroxide.

Mixture	T _m , °C	T _d , °C	pH	$\bar{\kappa}$, mS/cm	ρ , kg/m ³	ΔS , kJ/kg.°C	ΔH , kJ/kg	ΔG , kJ/kg	C _p , kJ/kg.°C	E kJ/m ³ *10 ⁵
AN2IL	-25	276	1.8	3.72	1168	-17.655	-3697.02	-3255.65	2.4	8.438
AN2IL+ NaOH	-25	261	2.0	4.13	1140	-8.265	-2201.05	-1994.43	1.99	6.488
UNIL	-20	236	0.5	9.09	1522	-18.799	-3319.94	-2849.97	1.9	7.403
UNIL+ NaOH	-17	188	0.3	8.69	1512	-7.290	-1824.44	-1642.19	3.26	10.105
USIL	-16	280	4.2	4.56	1460	-16.321	-2434.84	-2026.82	2.2	9.508
USIL+ KOH	-15	264	3.1	6.80	1420	-14.325	-2202.04	-1843.92	2.94	11.648

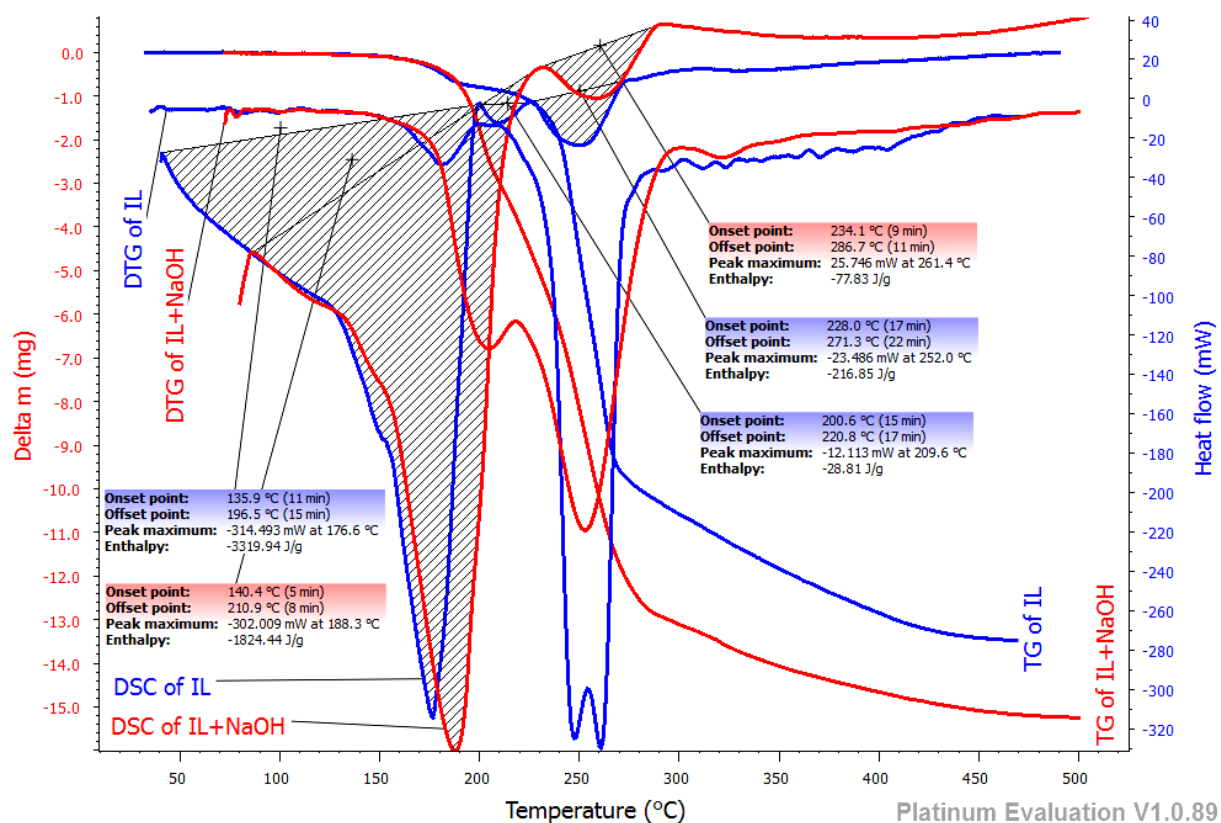


Figure (3-21): TGA/ DSC of (hydrated aluminum nitrate:urea, UNIL with 1:1.2 mole ratio) (blue color) and with addition of sodium hydroxide (red color) at 10 °C/min.

In contrast, sodium hydroxide decrease thermal stability of AN2IL in similar manner with UNIL (Fig. 3-22), eliminating the possibility of protonic acid-base reaction resulted from negligible change in the pH from 1.8 to 2, in addition to the small decrease in decomposition temperature which reduced from 276 °C to 261 °C and reducing in liquid temperature range and accelerate rate of the decomposition. The presence of NaOH decreased the enthalpy by 40 % in which enthalpy of AN2IL alone -3697.02 kJ/kg became -2201.05 kJ/kg with disappearance of second endothermic peak of the first decomposition stage of AN2IL alone. The two exothermic/endothermic peaks of the second decomposition stage of AN2IL alone were changed in which the enthalpy of 103.98 kJ/kg at a maximum decomposition temperature of 358.1 °C increased to 109.28 kJ/kg with a maximum decomposition temperature of

314.9 °C in liquid mixture of NaOH and AN2IL and the enthalpy of -9.63 kJ/kg changed to an exothermic peak with an enthalpy of 23.06 kJ/kg at maximum decomposition temperature of 348.8 °C might be associated with solid crystallization of the decomposition product of the liquid mixture producing during the decomposition process. A significant decrease in heat storage capacity of AN2IL by decreasing heat capacity and thermal energy storage capacity to lower value of 1.4 kJ/kg.°C and $6.565 \cdot 10^5$ kJ/m³ as shown in Table (3-11) thus thermal energy storage capacity was reduced by 23 %. From above results and behavior it could be concluded that the addition of sodium hydroxide to AN2IL reduced thermal stability and storage capacity of AN2IL alone and did not enhance heat storage capacity.

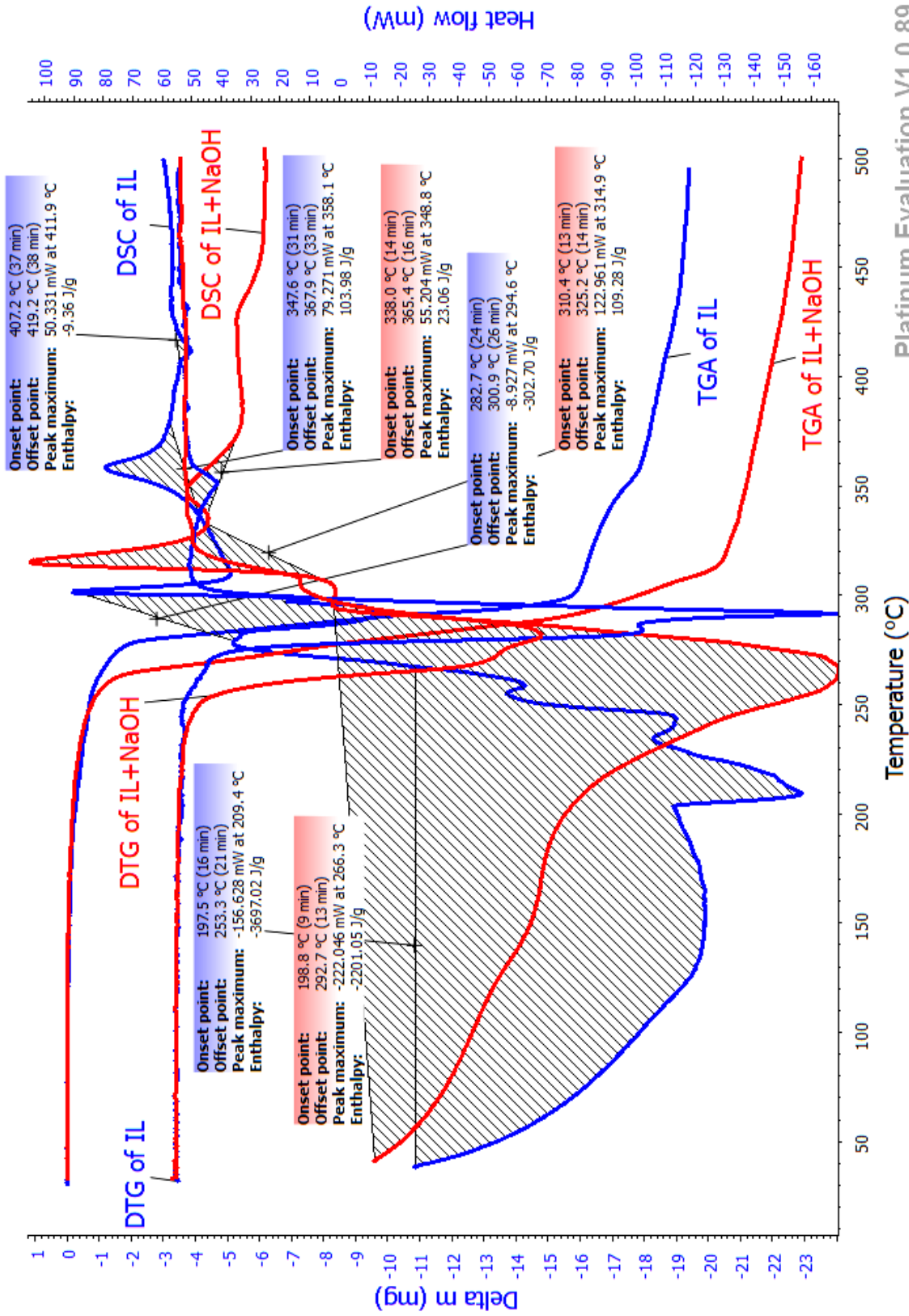


Figure (3-22): TGA/ DSC of hydrated aluminum nitrate:acetamide, AN2IL with 1:22 mole ratio) (blue color) and with addition of sodium hydroxide (red color) at 10 °C/min.

The addition of potassium hydroxide to USIL Fig. (3-23), it was found that potassium hydroxide reduced thermal stability of USIL alone and increased freezing point to higher temperature (from -20 to -15 °C) and decreased the decomposition temperature down to 264 °C. Although enthalpy of USIL alone was decreased by 10 % and second endothermic peak of USIL increased with an enthalpy of -52.37 kJ/kg at maximum decomposition temperature of 331.5 °C followed by exothermic enthalpy value of 193.07 kJ/kg as shown in the Figure (3-23) refers to solid crystallization of product through decomposition process. On the other hand, thermal energy storage capacity enhanced by 23 % due to significant increase in heat capacity and thermal energy storage capacity to $11.648 \cdot 10^5$ kJ/m³, in Table (3-11).

In General, Table (3-11) shows that the addition of NaOH or KOH to UNIL, AN2IL or USIL reduce decomposition temperature and density while they have variable effect on other thermo-physical properties, as KOH and NaOH increased thermal energy storage capacity of UNIL and USIL respectively, while NaOH decrease it with AN2IL.

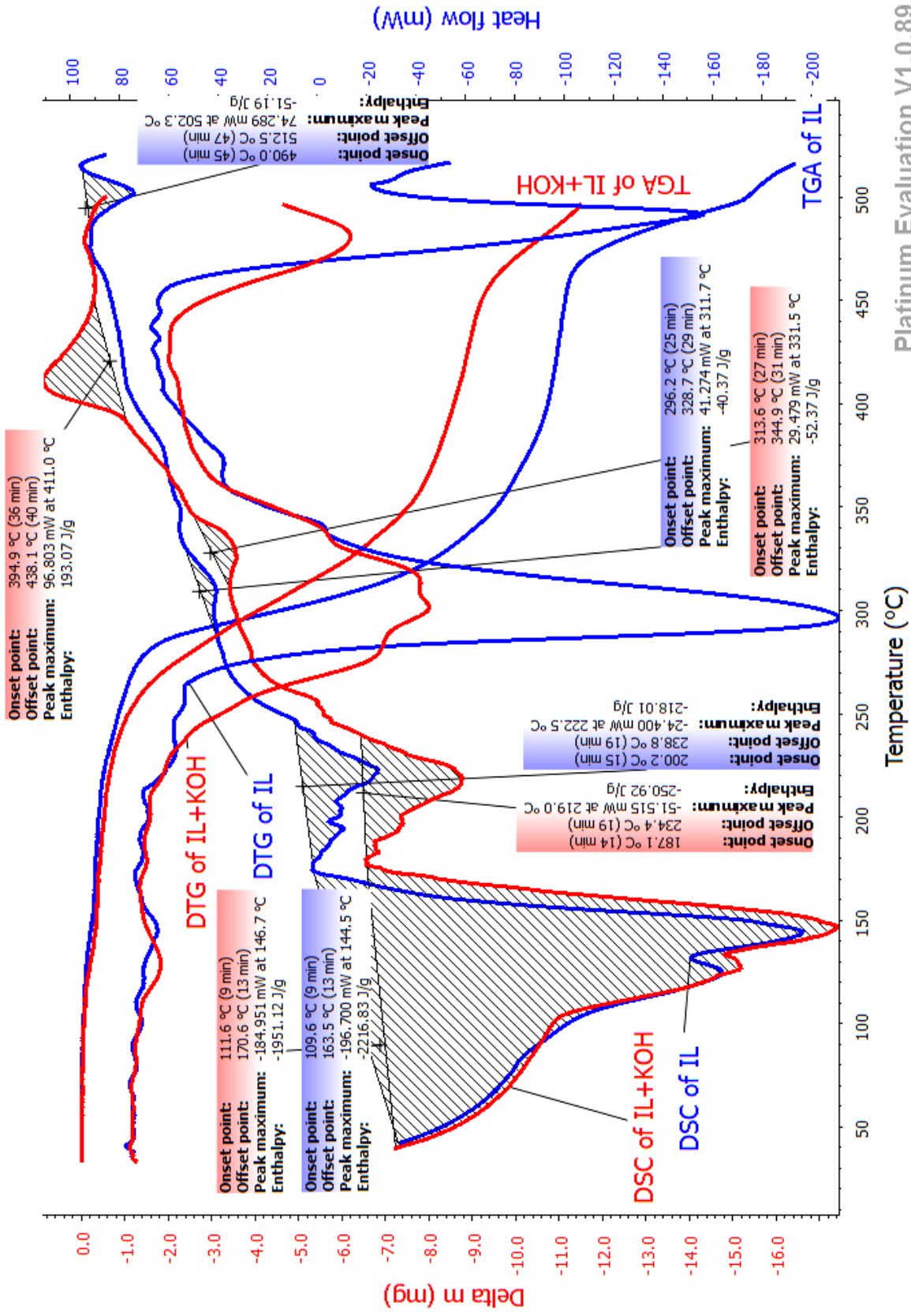


Figure (3-23): TGA/DSC of (hydrated ammonium aluminum sulfate:urea, USIL with 1:5 mole ratio) (blue color) and with addition of potassium hydroxide (red color) at 10 °C/min.

3.4.2 Addition of alkaline earth metal oxide to ILs:

Two alkaline earth metal oxides magnesium oxide and calcium oxide were added to USIL individually while BaO was added to UNIL to establish their behavior by TGA/DSC measurements. It was found that the addition of magnesium oxide to USIL caused in dramatic change on overall thermo-physical properties (Fig.3-24) resulted in reducing thermal energy storage capacity by 30 %, through reducing freezing point, decomposition temperature and heat capacity which became -14 °C, 230 °C and 1.93 kJ/kg.°C respectively, see Table (3-12). This resulted due to kind of interaction of magnesium oxide with water molecules in ionic liquids resulted in accelerating of decomposition process and evolving of water.

Table (3-12): Thermal characteristics of ionic liquids with some alkaline earth metal oxide.

Mixture	T_m , °C	T_d , °C	PH	κ , mS/cm	ρ , kg/m ³	ΔS , kJ/kg.°C	ΔH , kJ/kg	ΔG , kJ/kg	C_p , kJ/kg.°C	E kJ/m ³ *10 ⁵
USIL	-16	280	4.2	4.56	1460	16.321-	-2434.84	-2026.82	2.2	9.508
USIL+ MgO	-14	230	3.2	6.75	1420	-7.456	-1144.06	-957.66	1.93	6.687
USIL+ CaO	-15	117	3.5	6.91	1490	-6.541	-826.18	-662.66	1.71	3.363
UNIL	-20	236	0.5	9.09	1522	-18.799	-3319.94	-2849.97	1.9	7.403
UNIL+ BaO	-13	167	1.5	10.71	1472	-5.900	-988.89	-841.39	1.66	4.398

The enthalpy of USIL in presence of MgO decreased by 53% to a value of -1144.06 kJ/kg (the summation of enthalpies of the first two endothermic peaks) as shown in Figure (3-24), with small decrease in the third exothermic peak with respect to the first decomposition stage of USIL alone to 19.94 kJ/kg, with the disappearance of the fourth endothermic peak of USIL.

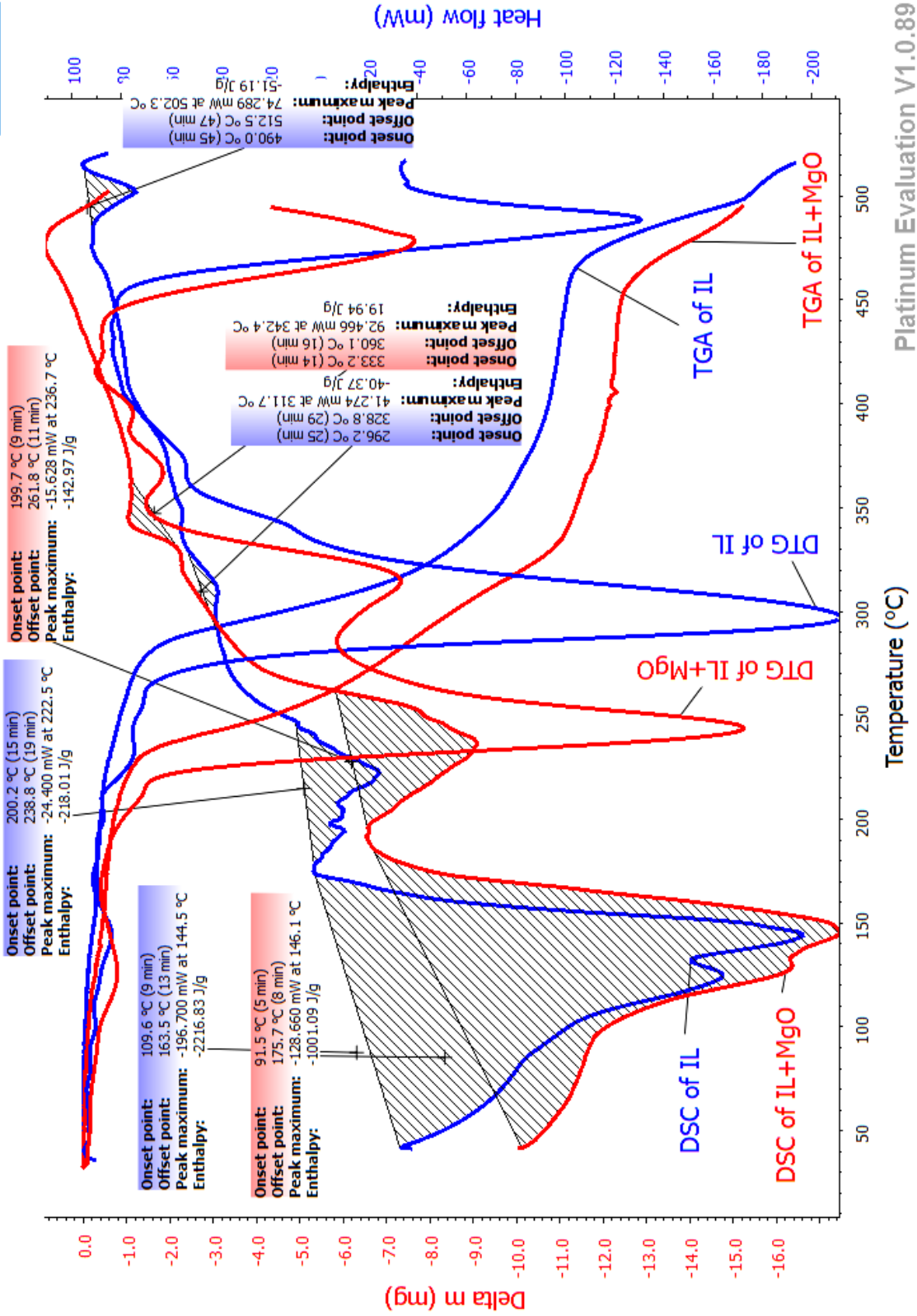


Figure (3-24): TGA/DSC of (hydrated ammonium aluminum sulfate:urea, USIL with 1:5 mole ratio) (blue color) and with addition of magnesium oxide (red color) at 10 °C/min.

The addition of calcium oxide showed the same reverse effect as shown in Figure (3-25) in which most thermo-physical properties such as freezing point elevation ($-15\text{ }^{\circ}\text{C}$), decomposition temperature ($117\text{ }^{\circ}\text{C}$), heat capacity and thermal energy storage capacity reduction ($1.4\text{ kJ/kg}\cdot^{\circ}\text{C}$) and (2.754 kJ/m^3) respectively as indicated in Table (3-12). The overall reduction effect in thermal energy storage capacity was 65 %. This unfavorable effect might be related to an interactions between soluble calcium oxide with water of USIL that weaken their attraction bond with ionic liquid ions leading to favorable decomposition at earlier stage as noticed with an acceleration in the rate of decomposition.

The effect of CaO present in USIL also appeared in reduction in the enthalpy to -826.18 kJ/kg and the successive endothermic peaks to -180.19 kJ/kg and -3.36 kJ/kg respectively. While crystallization peak was shifted to higher temperature and lower enthalpy value of decomposition ($362\text{ }^{\circ}\text{C}$, 19.52 kJ/kg) as shown in the Figure (3-25).

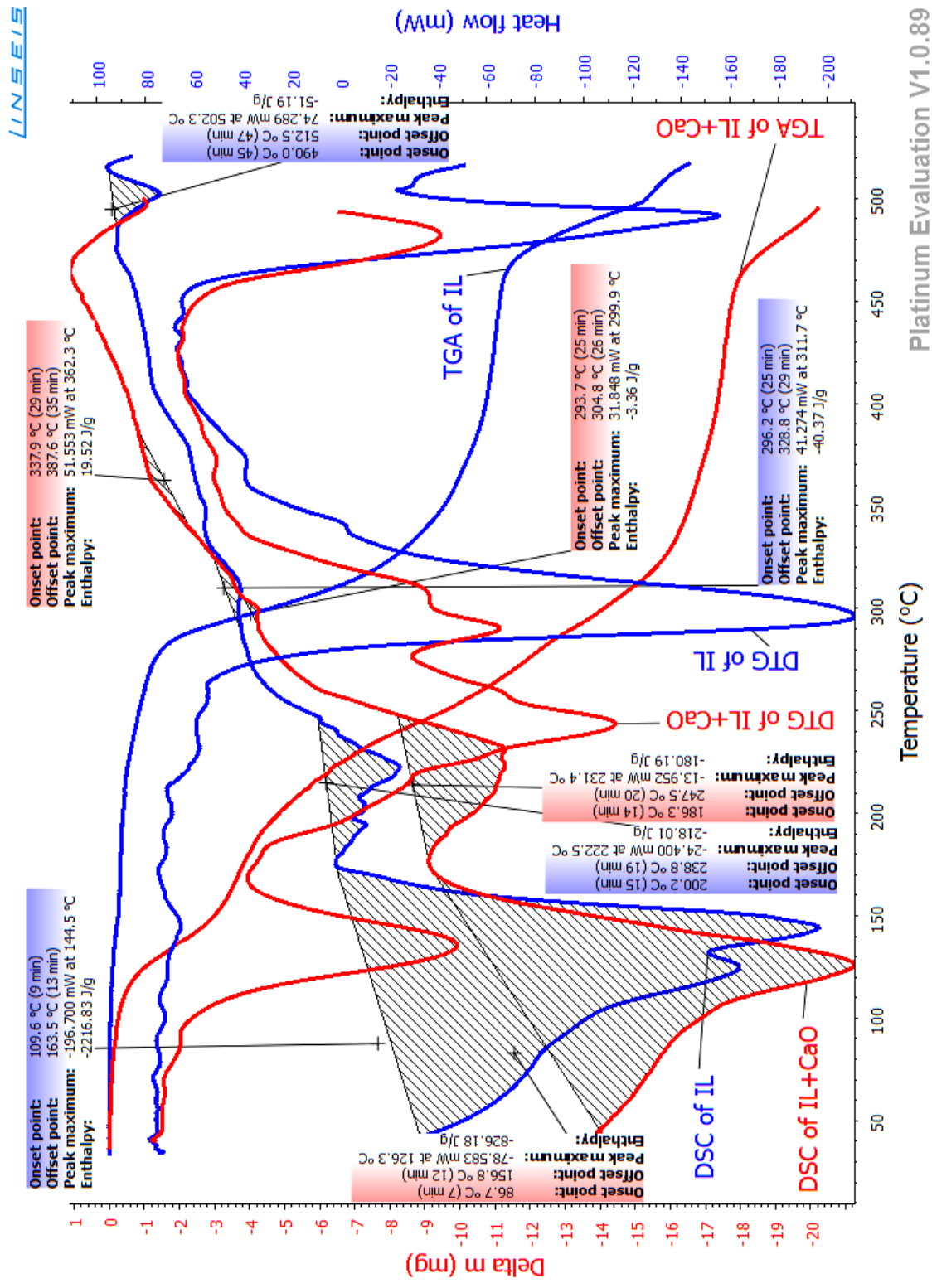


Figure (3-25): TGA/DSC of (hydrated ammonium aluminum sulfate:urea, USIL with 1:5 mole ratio) (blue color) and with addition of calcium oxide (red color) at 10 °C/min.

The effect of addition of barium oxide to UNIL (Fig.3-26), and Table (3-12) gave a small liquid temperature range due to the increase in the freezing point and decrease decomposition temperature. Put it in a reduced heat capacity and lowered thermal energy storage capacity by 41 %. This effect was synchronized as with MgO and CaO addition to USIL due to weakening the water molecules interaction with ionic liquid that leading to earlier release of water from the mixture of BaO with UNIL.

It was concluded that the addition of either MgO or CaO and BaO to USIL and UNIL respectively resulted in decreasing thermal stability of ionic liquids alone. Yet the oxides had similar reduction effect of conductivity, freezing point density, decomposition temperature, heat capacity and thermal energy storage capacity, see Table (3-12).

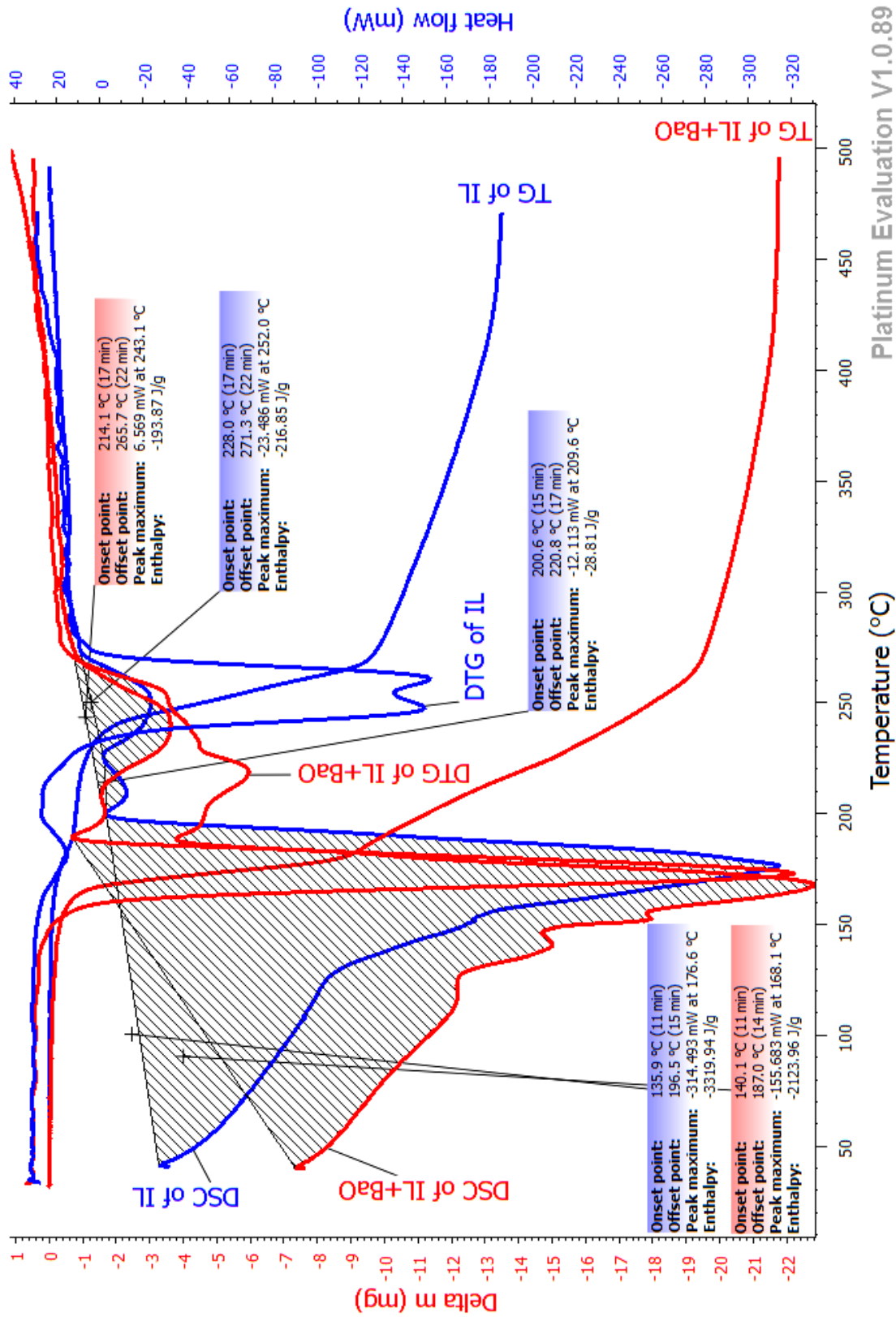


Figure (3-26): TGA/DSC of (hydrated aluminum nitrate:urea, UNIL with 1:1.2 mole ratio) (blue color) and with addition of barium oxide (red color) at 10 °C/min.

3.4.3 Addition of transition metal oxide to USIL:

Oxy vanadyl sulfate pentahydrate $\text{VO}_2\text{SO}_4 \cdot 5\text{H}_2\text{O}$ and transition metal oxides of NiO, CuO and ZnO were added to USIL to study some transition metal compounds on the thermal behavior of USIL. The addition of nickel oxide to USIL gives green liquid. Thermogravimetric analysis of NiO with USIL liquid mixture, Figure (3-27) showed noticeable increase in thermal stability by increasing decomposition temperature to 294 °C with low total weight loss percent. This might be referring to an interaction of nickel oxide with the ions of ionic liquid. On the other hand DSC analysis showed that the storage capacity decreased due to significant decrease in the heat capacity of USIL as shown in Table (3-13) by the effect of nickel oxide leading to reduction in thermal energy storage capacity by 24 % and the enthalpy decreased by 49% from -2434.84 kJ/kg to -1241.11 kJ/kg as shown in Table (3-13).

Table (3-13): Thermal characteristics of (hydrated ammonium aluminum sulfate:urea, USIL with 1:5 mole ratio) with some transition metal oxide.

Mixture	T_m , °C	T_d , °C	pH	κ , mS/cm	ρ , kg/m ³	ΔS , kJ/kg.°C	ΔH , kJ/kg	ΔG , kJ/kg	C_p , kJ/kg.°C	E kJ/m ³ *10 ⁵
USIL- alone	-16	280	4.2	4.56	1460	-16.321	-2434.84	-2026.82	2.2	9.508
USIL+ $\text{VO}_2\text{SO}_4 \cdot 5\text{H}_2\text{O}$	-15	332	2.8	8.33	1509	-16.023	-2423.26	-2022.69	3.03	15.86 6
USIL+ NiO	-10	294	3.1	4.42	1460	-8.331	-1241.11	-1032.84	1.63	7.235
USIL+ CuO	-14	320	3.4	5.72	1420	-8.132	-1216.76	-1013.46	2.40	11.38 3
USIL+ ZnO	-15	303	3.6	4.7	1390	-10.902	-1687.23	-1414.68	2.36	10.43 2

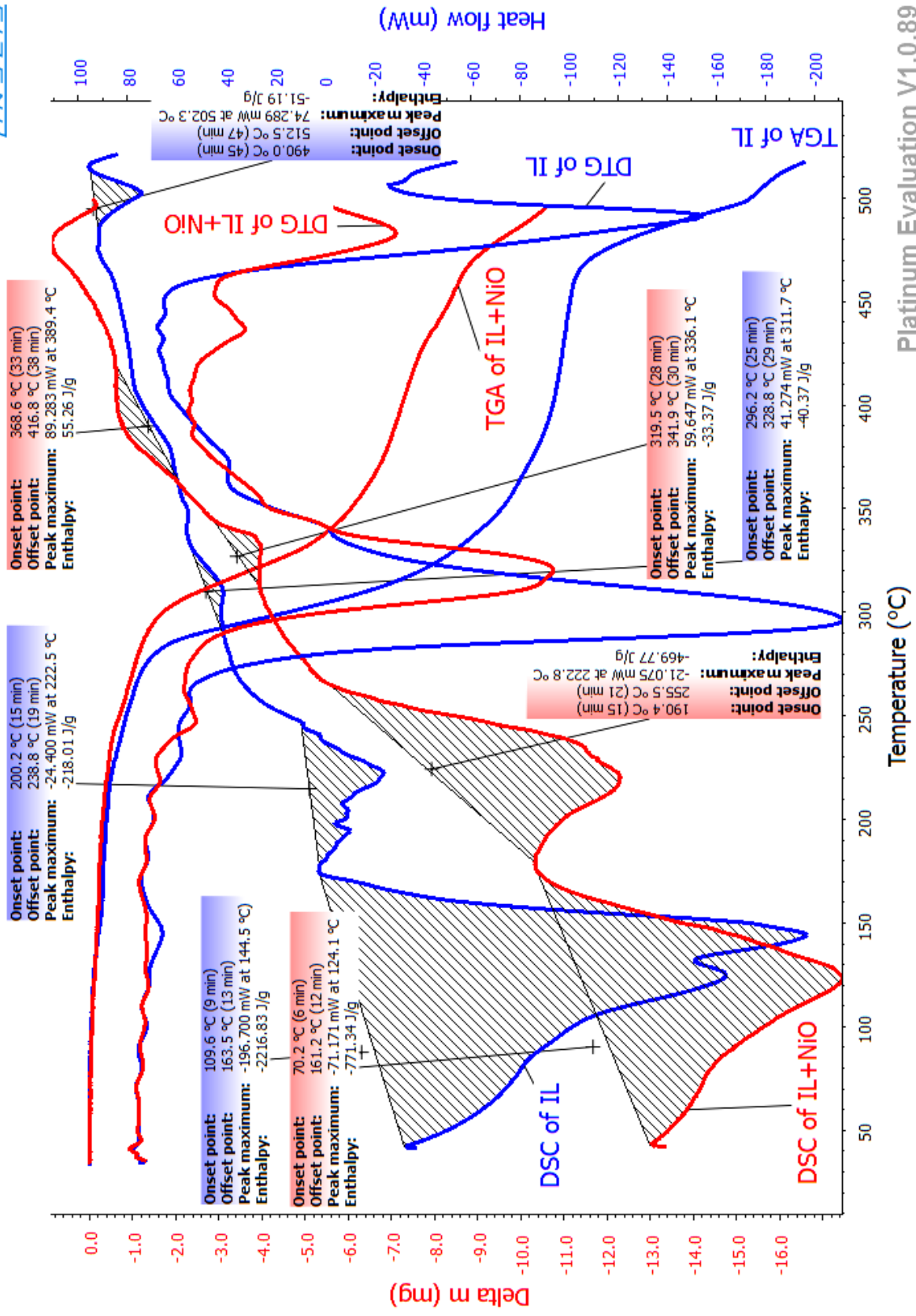


Figure (3-27): TGA/DSC of (hydrated ammonium aluminum sulfate:urea, USIL with 1:5 mole ratio) (blue color) and with addition of nickel oxide (red color) at 10 °C/min.

Thermal stability of USIL was increased by the addition of copper oxide to USIL that gave blue liquid mixture with improving thermo-physical properties of USIL despite a decrease in enthalpy of the mixture by 50 % from -2434.84 kJ/kg to -1216.76 kJ/kg. However, thermal stability and storage capacity were increased to significant values due to increase in decomposition temperature, heat capacity and thermal energy storage capacity by 20 % as shown in Table (3-13). This is might be refer to the interaction of copper oxide with ionic liquid species resulted in stronger and more complicated bonds make USIL liquid mixture more stable.

Like copper oxide, zinc oxide also had small enhancement of thermal stability and storage capacity of USIL in which thermal energy storage capacity only increased by 10 %. Beside that it showed slightly different behavior to DSC of USIL alone through decrease in enthalpy of USIL by 31 % from -2434.84 kJ/kg to -1684.23 kJ/kg as shown in the Figure (3-29).

Generally, the addition of transition metal oxides of NiO, CuO and ZnO to USIL changes in an enthalpy of first decomposition peaks from -40.37 kJ/kg at maximum decomposition temperature of 311.7 °C to -33.37 kJ/kg, -48.03 kJ/kg and -41.40 kJ/kg at maximum decomposition temperatures of 331.6 °C, 337.0 °C and 328.8 °C respectively, these include a complex decomposition process exothermal and endothermal resulted in small value of ΔH in endothermic value, while the second decomposition peaks of the liquid mixtures with an exothermic enthalpy values of 55.26 kJ/kg, 157.36 kJ/kg and 509.38 kJ/kg at a maximum decomposition temperatures of 389.4 °C, 394.3 °C and 403.6 °C respectively as shown in (Fig.3-37), (Fig.3-28) and (Fig.3-29) respectively could be related to a solid crystallization of the decomposition product of the liquid mixtures producing during the decomposition process.

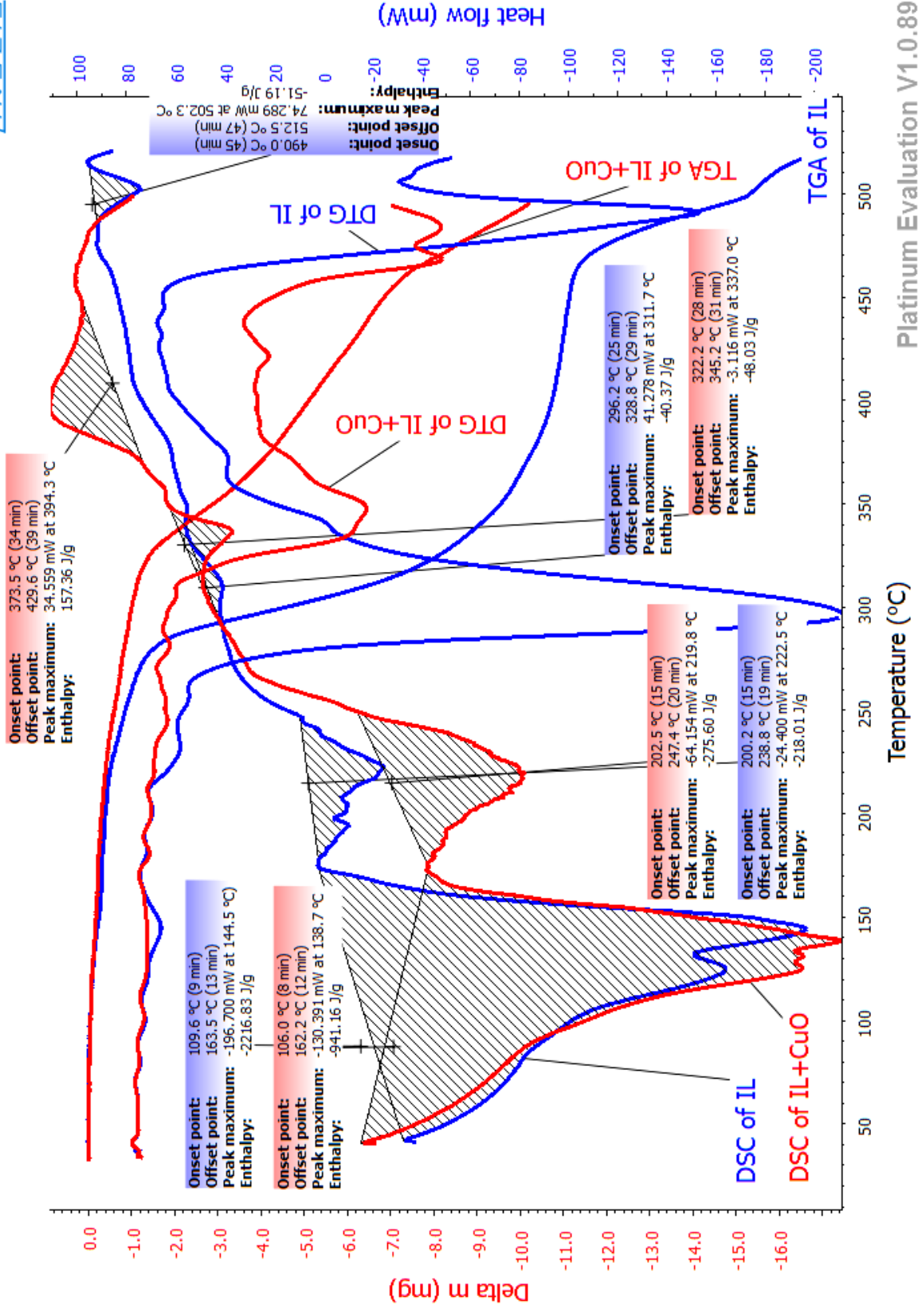


Figure (3-28): TGA/DSC of (hydrated ammonium aluminum sulfate:urea, USIL with 1:5 mole ratio) (blue color) and with addition of copper oxide (red color) at 10 °C/min.

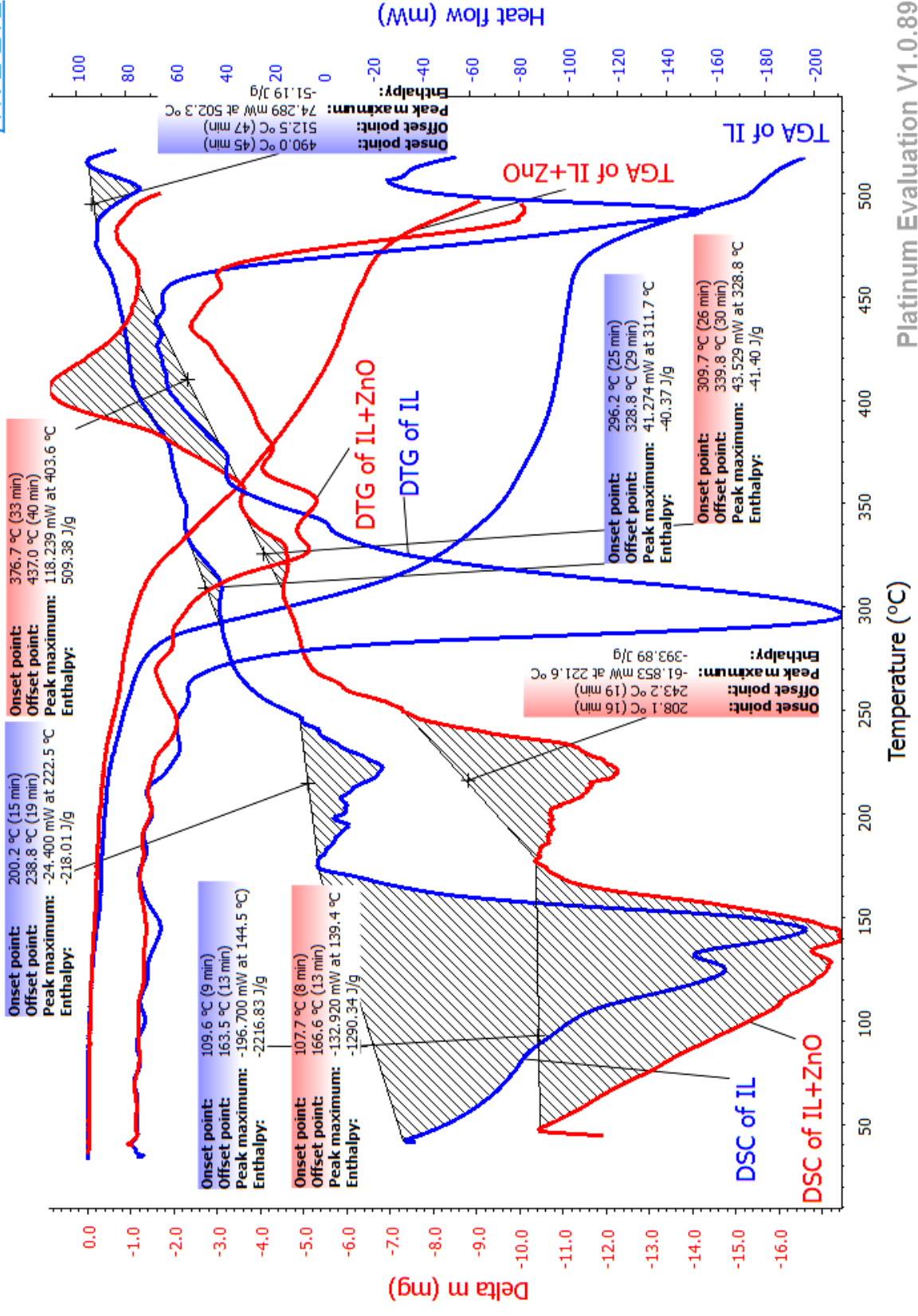


Figure (3-29): TGA/DSC of (hydrated ammonium aluminum sulfate:urea, USIL with 1:5 mole ratio) (blue color) and with addition of zinc oxide (red color) at 10 °C/min.

The large effect was noted with the addition of vanadyl sulfate pentahydrate to USIL, Figure (3-30), in which DSC of liquid mixture showed three peaks in which the first two endothermic peaks at maximum temperature of 143.6 °C and 219.7 °C related to an enthalpy of -2423.26 kJ/kg decreased by less than 0.5 % from enthalpy of USIL alone. Other thermo-physical properties of decomposition temperature, density, conductivity, heat capacity and thermal energy storage capacity were also improved due to the possibility of strong interaction of hydrated vanadyl sulfate with ionic species in USIL that responsible for this stability and hence increasing thermal energy storage capacity by 67 %, Table (3-13).

Generally, the addition of transition metal oxides ($\text{VO}_2\cdot 5\text{H}_2\text{O}$, CuO and ZnO) to USIL cause an improve in thermal stability temperature up to 300 °C and increase storage capacity, Table (3-13). This might be related to interaction of these metal ions with ionic liquid species. Since V^{+4} and Cu^{+2} had d^1 and d^9 electronic configuration respectively and these configurations known to undergo octahedral distortion geometry due to Jahn-Teller effect which might formed more stable complexes with ionic liquid compared with Ni^{+2} of d^8 electronic configuration with normal octahedral coordination geometry this also proved in electronic spectroscopy in other work^[81].

Then, the catalytically effect of these transition metal oxides on thermo-physical properties of USIL can be arranged in the following order:



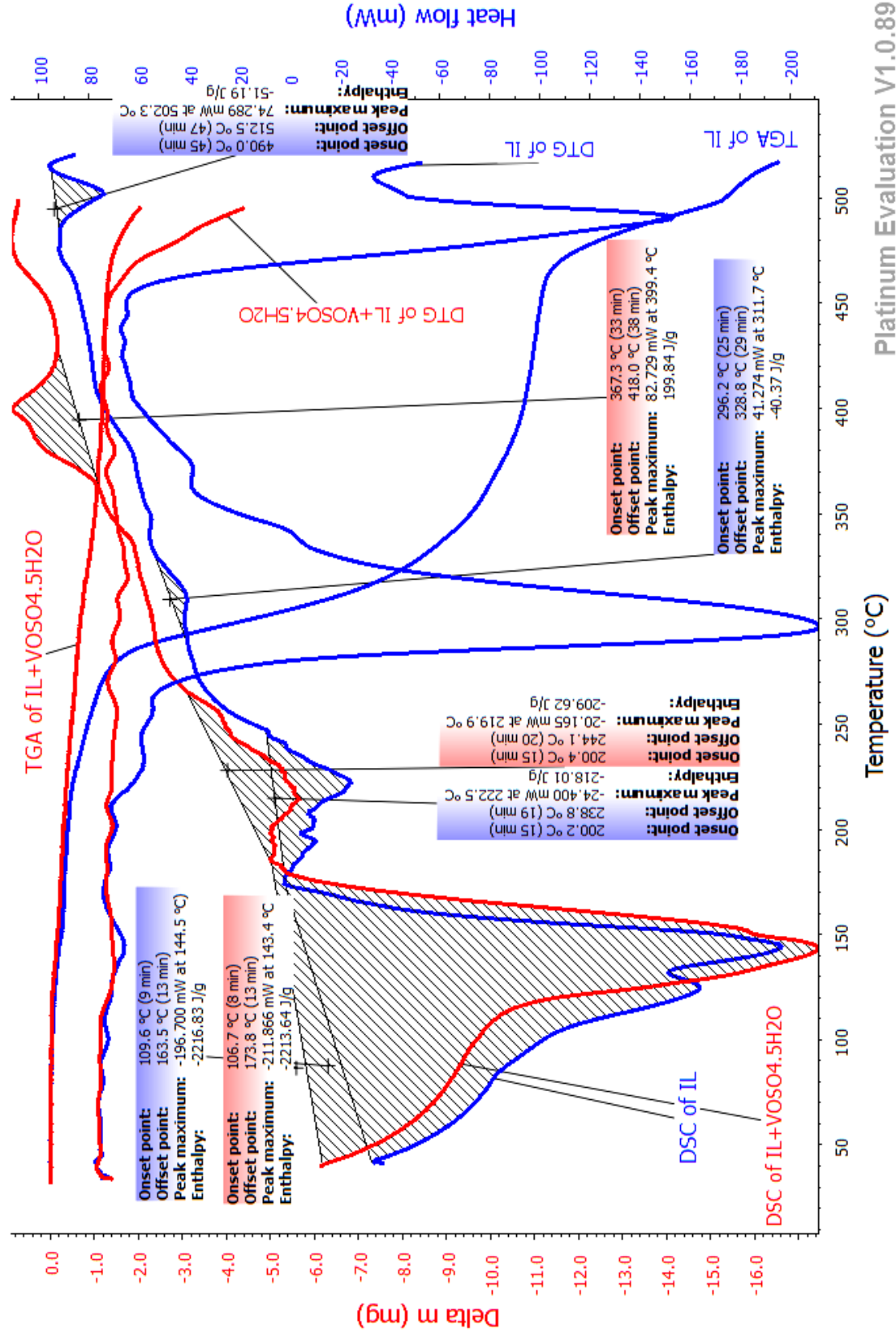


Figure (3-30): TGA/DSC of (hydrated ammonium aluminum sulfate:urea, USIL with 1:5 mole ratio) (blue color) and with addition of vanadyl sulfate pentahydrate (red color) at 10 °C/min.

Conclusions:

Ionic liquids deserve a consideration as valuable candidate with traditional materials used as thermal energy storage. These RTILs have unique properties of storing and releasing a significant amount of thermal energy with non volatile properties. Ionic liquids under the present study, of hydrated ammonium aluminum sulfate:urea, USIL in the mole ratio 1:5 and hydrated aluminum nitrate:acetamide, AN2IL in the mole ratio (1:22) offered thermal stability up to 280 °C and 276 °C respectively and working temperatures down to -16 and -25 °C respectively in addition to the high storage capacity by $9.508 \cdot 10^5$ kJ/m³ obtained for USIL.

The addition of KOH to USIL and NaOH to UNIL increase the storage capacity of these ionic liquids by increasing their thermal energy storage capacity up to $11.648 \cdot 10^5$ kJ/m³ and $10.105 \cdot 10^5$ kJ/m³ respectively. But the effect of NaOH on AN2IL proceed in reverse behavior i.e. thermal energy storage capacity was decreased to lower value $6.488 \cdot 10^5$ kJ/m³.

It was found that MgO and CaO inhibit the activity of hydrated ammonium aluminum sulfate:urea USIL as heat storage material through a significant reduction in the thermal energy storage capacity down to $6.687 \cdot 10^5$ kJ/m³ and $3.363 \cdot 10^5$ kJ/m³ respectively.

It was also found that vanadyl sulfate pentahydrate, copper oxide and zinc oxides enhanced thermal stability of hydrated ammonium aluminum sulfate:urea USIL by increasing decomposition temperature from 280 °C to 332 °C, 320 °C and 303 °C respectively and increasing heat capacity from 2.20 kJ/kg.°C to 3.03 kJ/kg.°C, 2.40 kJ/kg.°C and 2.36 kJ/kg.°C respectively and thermal energy storage capacity to $15.866 \cdot 10^5$ kJ/m³, $11.383 \cdot 10^5$ kJ/m³ and $10.432 \cdot 10^5$ kJ/m³ respectively. While NiO show reverse effect on heat

storage capacity through obvious decrease in heat capacity and thermal energy storage capacity to $1.63 \text{ kJ/kg}\cdot^{\circ}\text{C}$ and $7.235 \cdot 10^5 \text{ kJ/m}^3$ respectively.

Future work

The obtained result indicated a successful attempt to introduce these ionic liquids as suggested thermal storage liquids either alone or with some added materials. However, it was important to suggest further work:

1. Elaboration studying of the reaction mechanism of heating stage of ionic liquids either alone or with added materials with the aid of mass spectroscopy, NMR, CHN....etc.
2. Corrosion behavior of these liquids mixtures, to establish their effect on metal parts if applied in piping or pumps.

References

4. References

- [1] S. Gabriel and J. Weiner, "On some Derivatives of Propylamines", J. American Chemical Society, 21, 2669-2679, 1888.
- [2] P. Walden, "Ueber die Molekulargröße und elektrische Leitfähigkeit einiger geschmolzenen salze", J. Bull. Acad. Imper. Sci. St. Petersburg, 8, 405-422, 1914.
- [3] A. Mohammed and Inamuddin, "Properties and Applications of Ionic Liquids", Green Solvent 2nd edition, Springer Science and Business Media Dordrecht, 3–21, 2012.
- [4] J. S. Wilkes, "A Short History of Ionic Liquids- from Molten Salts to Neoteric Solvents"; J. Green Chemistry, 4, 73–80, 2002.
- [5] S. Geetha and D. C. Trivedi, "Properties and Applications of Chloroaluminate as Room Temperature Ionic Liquid", J. Bull. of Electrochemistry, 19(1), 37–48, 2003.
- [6] J. S. Wilkes, M. J. Zaworotko, "Air and water stable 1-Ethyl-3-Methyl imidazolium based ionic liquids", J. Chem. Soc. Chem. Comm., 1992, 965–967, 1992.
- [7] F. Endres and S. Zien El Abedien, "Air and Water Stable Ionic Liquids in Physical Chemistry" J. Phys. Chem. Chem. Phys., 8, 2101–2116, 2006.
- [8] P. Wasserscheid and T. Welton, "Ionic Liquids in Synthesis", 2nd edition, Wiley-VCH Verlag GmbH & Co. KGaA 1, 13–125, 2009.
- [9] H. Ohno, "Physical Properties of Ionic Liquids for Electrochemical Applications", in book of, F. Endres, D. MacFarlane and A. Abbott, "Electrodeposition from Ionic Liquids", Wiley-VCH Verlag GmbH & Co. KgaA, 47–82, 2008
- [10] D. R. MacFarlane, N. Tachikawa, M. Forsyth, J. M. Pringle, P. C. Howlett, G. D. Elliott, J. H. Davis, M. Watanabe, Patrice Simon and C. A.

- Angell, "Energy applications of ionic liquids", *J. Energy & Environmental Science*, 7, 232–250, 2014.
- [11] S. Zhang, N. Sun, Xuezhong He, Xingmei Lu, and X. Zhang, "Physical Properties of Ionic Liquids: Database and Evaluation", *J. Phys. Chem.*, 35(4), 1475–1517, 2006.
- [12] J. Jacquemin, P. Husson, A. A. H. Padua and V. Majer, "Density and Viscosity of several Pure and Water-Saturated Ionic Liquids", *J. Green Chem.*, 8, 172-180, 2006.
- [13] D. Urszula , "General review of ionic liquids and their properties", In: "Ionic Liquids in Chemical Analysis", Mihkel Koel editor, 2–57, 2009.
- [14] K. N. Marsh, J. A. Boxall and R. Lichtenthaler, "Room Temperature Ionic Liquids and their Mixtures- A review ", *J. fluid phase equilib.*, 219, 93–98, 2004.
- [15] P. Bonhôte, A. Dias, N. Papageorgiou, K. Kalyanasundaram and M. Grätzel, "Hydrophobic, Highly Conductive Ambient Temperature Molten Salts", *J. Inorg. Chem.*, 35(5), 1168–1178, 1996.
- [16] W. R. Pitner, P. Kirsch, K. Kawata, and H. Shinohara, "Applications of Ionic Liquids in Electrolyte Systems", In: *Hand book of Green Chemistry, Ionic Liquids*, P.Wasserscheid and A. Stark editors, 6, 191–203, 2010.
- [17] S. Carda-broch, A. berthod and D. W. Armstrong, "Solvent Properties of The 1-Butyl-3-Methylimidazolium Hexafluoro-phosphate Ionic Liquid", *J. Anal Bioanal Chem.*, 375, 9–191, 2003.
- [18] M. Kosmulski, J. Gustafsson and J. B. Rosenholm, "Thermal Stability of Low Temperature Ionic Liquids revisited", *J. Thermochim Acta*, 412, 47–53, 2004.

- [19] C. P. Fredlake, J. M. Crosthwaite, D. G. Hert, S. N. V. K. Aki and J. F. Brennecke, "Thermophysical properties of imidazolium-based ionic liquids", *J. Chem. Eng. Data*, 49, 954-964, 2004.
- [20] S. Sowmiah, V. Srinivasadesikan, M. C. Tseng and Y. H. Chu, "Review on the Chemical Stabilities of Ionic Liquids", *J. Molecules*, 14, 3780–3813, 2009.
- [21] T. J. Wooster, K. M. Johanson, K. J. Fraser, D. R. MacFarlane and J. L. Scott, "Thermal degradation of cyano containing ionic liquids", *J. Green Chem.*, 8, 691-696, 2006.
- [22] J. G. Huddleston, A. E. Visser, W. M. Reichert, H. D. Willauer, G. A. Broker and R. D. Rogers, "Characterization and Comparison of Hydrophilic and Hydrophobic Room Temperature Ionic Liquids incorporating the Imidazolium Cation", *J. Green Chem.*, 3, 156-164, 2001.
- [23] A. Heintz, "Recent developments in thermodynamics and thermo-physics of non-aqueous mixtures containing ionic liquids", *J. Chem. Thermodyn.*, 37, 525–535, 2005.
- [24] C. Chiappe and D. Pieraccini, "Ionic liquids: solvent properties and organic reactivity" *J. Phys. Org. Chem.*, 18, 275–297, 2005.
- [25] M. H. Joshipura, "Predictions of Vapor Pressures of Ten Ionic Liquids Using Patel Teja Equations of State", *Int. J. Research in Engineering and Technology (IJRET)*, 1(2), 49–54, 2013.
- [26] I. M. AL-Nashef, M. L. Leonard, M. C. Kittle, M. A. Matthews and J. W. Weidner, "Electrochemical Generation of Superoxide in Room-Temperature Ionic Liquids", *J. Electrochemical and Solid-State Letters*, 4(11), D16-D18, 2001.
- [27] U. Schroder, J. D. Wadhawan, R. G. Compton, F. Marken, P. A. Z. Suarez, C. S. Consorti, R. F. De Souza and J. Dupont, "Water-Induced

Accelerated Ion Diffusion: Voltammetric Studies in 1-Methyl-3-[2,6-(*S*)Dimethylocten-2-Yl] Imidazolium Tetrafluoro borate, 1-Butyl-3-Methyl Imidazolium Tetrafluoro borate and Hexafluoro phosphate Ionic Liquids", *New J. Chem.*, 24, 1009-1015, 2000.

- [28] V. D. Bhatt, K. Gohil and A. Mishra, "Thermal Energy Storage Capacity of some Phase changing Materials and Ionic Liquids", *Int. J. Chem. Technol.*, 2(3), 1771-1779, 2010.
- [29] M. E. Van Valkenburg, *et al.*, "Ionic liquid heat transfer fluids", 15th Symposium on Thermophysical Properties, Boulder, CO, USA, 2003.
- [30] M. Koel, "Ionic Liquids in Chemical Analysis", 2nd edition, by Taylor & Francis Group, 1-73, 2009.
- [31] V. D. Bhatt, K. Gohil and A. Mishra, "Thermal Energy Storage Capacity of some Phase changing Materials and Ionic Liquids", *Int. J. Chem. Technol.*, 2(3), 1771-1779, 2010.
- [32] S. Keskin, D. Kayrak-Talay, U. Akman and Ö. Hortaçsu, "A Review of Ionic Liquids towards Supercritical Fluid Applications", *J. of Supercritical Fluids*, 43, 150–180, 2007.
- [33] R. Morland, American Chemical Society Division of Industrial and Engineering Chemistry, in: *Proceedings of the 221st American Chemical Society National Meeting*, San Diego, 2001.
- [34] H. Zhao, S. Xia, P. Ma, "Review: use of Ionic Liquids as Green Solvents for Extractions", *J. Chem. Technol. Biotechnol.*, 80, 1089–1096, 2005.
- [35] D. Zhao, M. Wu, Y. Kou, E. Min, "Ionic Liquids: Applications in Catalysis", *J. Catalysis Today*, 2654, 1–33, 2002.
- [36] I. Yoritsugu, K. Yuki, N. Nobuhumi and Ohno Hiroyuki, "Design of Phosphonium-Type Zwitterion as an Additive to Improve Saturated Water Content of Phase-Separated Ionic Liquid from Aqueous Phase

toward Reversible Extraction of Proteins", *Int. J. Mol. Sci.*, 14, 18350–18361, 2013.

- [37] A. E. Visser, R. P. Swatloski, W. M. Reischert, R. Mayton, S. Sheff, A. Wierzbicki, J. H. Davis and R. D. Rogers, "Task-Specific Ionic Liquids Incorporating Novel Cations for the Coordination and Extraction of Hg^{2+} and Cd^{2+} : Synthesis, Characterization, and Extraction Studies", *J. Environ. Sci. Technol.*, 36, 2523–2529, 2002.
- [38] H. M. A. Abood and E. Akram, "FTIR Study of Carbon Dioxide Interaction with some Room Temperature Ionic Liquids", *J. Al-Nahrain University*, 17(4), 76–85, 2014.
- [39] L. M. Galán Sánchez, G. W. Meindersma and A. B. de Haan, "Solvent Properties of Functionalized Ionic Liquids for CO_2 Absorption", *Institution of Chemical Engineers IChemE*, 85 (A1), 31–39, 2007.
- [40] B. Wu, R. G. Reddy and R. D. Rogers, "Novel Ionic Liquid Thermal Storage for Solar Thermal Electric Power Systems", *Proceedings of Solar Forum*, 2001.
- [41] R. G. Reddy, "Novel Applications of Ionic Liquids in Materials Processing", *J. Physics: Conference Series*, 165, 012076, 2009.
- [42] A. Karapekli, A. Sari, K. Kaygusuz, "Thermal Properties and Thermal Reliability of Capric Acid/Stearic Acid Mixture for Latent Heat Thermal Energy Storage", *J. Energy Sources, Part A: Recovery, Utilization and Environmental Effects*, 31, 199–207, 2009.
- [43] V. D. Bhatt and K. Gohil, "Ion Exchange Synthesis and Thermal Characteristics of Some $[\text{N}^{+}_{2222}]$ Based Ionic Liquids", *J. Bull. Mater. Sci.*, 36, 1121–1125, 2013.
- [44] K. Nagano, T. Mochida, S. Takeda, R. Domański and M. Rebow, "Thermal Characteristics of Manganese Nitrate Hexahydrate as A Phase

- Change Material for cooling Systems", *J. Appl. Therm. Eng.* 23, 229–241, 2004.
- [45] M. Tesfay and M. Venkatesan, "Simulation of Thermocline Thermal Energy Storage System using C", *Int. J. Innovation and Applied Studies*, 3, 354–364, 2013.
- [46] G. Zanganeh, A. Pedretti, S. Zavattoni, M. Barbato, and A. Steinfeld, "Packed-Bed Thermal Storage for Concentrated Solar Power-Pilot-Scale Demonstration and Industrial-Scale Design", *J. Solar Energy*, 86, 3084–3098, 2012.
- [47] M. Hänchen, S. Brückner and A. Steinfeld, "High-Temperature Thermal Storage using a Packed Bed of Rocks - Heat Transfer Analysis and Experimental Validation", *J. Applied Thermal Engineering*, 31,1798–1806, 2011.
- [48] M. M. Farid, A. M. Khudhair, S. A. K. Razack and S. Al-Hallaj, "A Review on Phase Change Energy Storage: Materials and Applications", *J. Energy Conversion and Management*, 45, 1597–1615, 2004.
- [49] P. Pinel, C. A. Cruickshank, I. Beausoleil-Morrison and A. Wills, "A Review of Available Methods for Seasonal Storage of Solar Thermal Energy in Residential Applications", *J. Renewable and Sustainable Energy Reviews*, 15, 3341–3359, 2011.
- [50] T. Schmidt, D. Mangold, and H. Müller-Steinhagen, "Central Solar heating Plants with Seasonal Storage in Germany", *J. Solar energy*, 76(1-3), 165–174, 2004.
- [51] O. S. Lieberg, "High Temperature Water Systems", The Industrial Press, New York, N.Y, USA, 1-10, 1958.
- [52] A. Sharma, V. V. Tyagi, C. R. Chen and D. Buddhi, "Review on Thermal Energy Storage with Phase Change Materials and Applications" *J. Renewable and Sustainable Energy Reviews*, 13, 318–345, 2009.

- [53] M. Harald and C. Luisa F., "Heat and Cold Storage with Phase Change Material", *J. Industrial Chemistry and Chemical Engineering*, 21–27, 2008.
- [54] S. P. Jesumathy, M. Udayakumar and S. Suresh, "Heat Transfer Characteristics in Latent Heat Storage System using Paraffin Wax", *J. of Mechanical Science and Technology*, 26(3), 959–965, 2012.
- [55] C. Thirugnanam, P. Marimuthu, "Experimental Analysis of Latent Heat Thermal Energy Storage using Paraffin Wax as Phase Change Material", *Int. J. Engineering and Innovative Technology (IJEIT)*, 3, 372–376, 2013.
- [56] P. Fraas, "Heat Exchanger design", 2nd, New York Wiley, 337, 1989.
- [57] B. R. Nandi, S. Bandyopadhyay, R. Banerjee, "Analysis of High Temperature Thermal Energy Storage for Solar Power Plant", *J. Institute of Electrical and Electronic Engineers (IEEE), International Conference on Engineering and Technology (ICSET)*, 1, 438–444, 2012.
- [58] L. Moens, D. M. Blake, D. L. Rudnicki and M. J. Hale, "Advanced Thermal Storage Fluids for Solar Parabolic Trough Systems", *J. Solar Energy Engineering*, 125, 112–116, 2003.
- [59] W. E. Kirst, W. M. Nagle and J. B. Cartner, "A New Heat Transfer Medium for High Temperatures", *J. Trans. AIChE*, 36, 371-378, 1940.
- [60] D. A. Brosseau, P. F. Hlava and M. J. Kelly, "Testing Thermocline Filler Materials and Molten Salt Heat Transfer Fluids for Thermal Energy Storage Systems Used in Parabolic Trough Solar Power Plants", Sandia National Laboratories P.O., 11–54, 2004.
- [61] J. E. Pacheco, S. K. Showalter and W. J. Kolb, "Development of a Molten-Salt Thermocline Thermal Storage System for Parabolic Trough Plants", *J. Solar Energy Engineering*, 124, 153–159, 2002.

- [62] N. P. Siegel, R.W. Bradshaw, J. B. Cordaro, and A. M. Kruizenga, "Thermophysical Property Measurement of Nitrate Salt Heat Transfer Fluids", Int. Conference on Energy Sustainability, ASME, 1–8, 2011.
- [63] D. K. Bwambok, M. M. Thuo, M. B. J. Atkinson, K. A. Mirica, N. D. Shapiro, and G. M. Whitesides, "Paramagnetic Ionic Liquids for Measurements of Density Using Magnetic Levitation", J. Anal. Chem., 85, 8442–8447, 2013.
- [64] M. J. Earle and K. R. Seddon, "Ionic Liquid. Green Solvents for the Future", J. Pure Appl. Chem., 72, 1391–1398, 2000.
- [65] H. Zhao, S. Xia and P. Ma, "Review: use of Ionic Liquids as Green Solvents for Extractions", J. Chem. Technol. Biotechnol., 80, 1089–1096, 2005.
- [66] H. Noritomi, K. Minamisawa, R. Kamiya, and S. Kato, "Thermal Stability of Proteins in The Presence of Aprotic Ionic Liquids", J. Biomedical Science and Engineering, 4, 94–99, 2011.
- [67] C. Wang, J. Liu, W. Leng and Y. Gao, "Rapid and Efficient Functionalized Ionic Liquid-Catalyzed Aldol Condensation Reactions Associated with Microwave Irradiation", Int. J. Mol. Sci., 15, 1284–1299, 2014.
- [68] X. Jun He, Z. Lu Shen, W. Min Mo, B. Xiang Hu and N. Sun, "Asymmetric Glyoxylate-Ene Reactions Catalyzed by Chiral Pd(II) Complexes in the Ionic Liquid [bmim][PF₆]", Int. J. Mol. Sci., 8, 553–563, 2007.
- [69] V. D. Bhatt and K. Gohil, "Performance Evaluation of Solar Cooker using some [N⁺₄₄₄₄] based Ionic Liquids as Thermal Energy Storage Materials", J. Adv. Mat. Lett., 4, 277–282, 2013.
- [70] Di Wei, "Review Dye Sensitized Solar Cells", Int. J. Mol. Sci., 11, 1103–1113, 2010.

- [71] M. E. V. Valkenburg, R. L. Vaughn, M. Williams and J. S. Wilkes, "Thermochemistry of Ionic Liquid Heat Transfer Fluids", *J. Thermochim. Acta*, 425, 181–188, 2005.
- [72] L. Cammarata, S. G. Kazarian, P. A. Salter and T. Welton, "Molecular States of Water in Room Temperature Ionic Liquids", *J. Phys. Chem. Chem. Phys.*, 23, 5192–5200, 2001.
- [73] X. Jun He, Z. Lu Shen, W. Min Mo, B. Xiang Hu and N. Sun, "Asymmetric Glyoxylate-Ene Reactions Catalyzed by Chiral Pd(II) Complexes in the Ionic Liquid [bmim][PF₆]", *Int. J. Mol. Sci.*, 8, 553–563, 2007.
- [74] P. Wasserscheid, R. V. Hal, A. Bössmann, "1-N-Butyl-3-methylimidazolium ([BMIM]) octylsulfate—an even 'Greener' Ionic liquid", *J. Green Chem.*, 4, 400–404, 2002.
- [75] K. Ghandi, "A Review of Ionic Liquids, Their Limits and Applications", *J. Green and Sustainable Chemistry*, 4, 44–53, 2014.
- [76] C. D. Tran, S. H. D. P. Lacerda and D. Oliveira, "Absorption of Water by Room Temperature ILs: Effect of Anions on Concentration and State of Water", *J. Soc. Appl. Spectrosc.*, 57, 152–157, 2003.
- [77] M. G. Freire, P. J. Carvalho, R. L. Gardas, I. M. Marrucho, L. M. N. B. F. Santos and J. A. P. Coutinho, "Mutual Solubilities of Water and The [C_(n)MIm][Tf₍₂₎N] Hydrophobic Ionic Liquids", *J. Phys. Chem. B*, 112, 1604–1610, 2008.
- [78] H. M. A. Abood, "New ionic liquid made from hydrated aluminum sulfate with amide", Patent, Central Organization for Standardization and Quality, Property division, Iraq, Application no. 336, 3915, 2011.
- [79] Z. N. Al-Qudsi and H. M. A. Abood, "The Electronic Transition Behavior Cr (III), Fe (III), Fe (II) and Ni (II), Transition Metal Cations

- in Ammonium Alum-Urea Room Temperature Ionic Liquid", J. Al-Nahrain university, 16, 46–55, 2013.
- [80] N. M. Hasan, H. M. A. Abood and M. F. Alias, personal communication work pending for publication, 2015.
- [81] PerkinElmer, "Thermogravimetric analysis TGA", A Beginner's Guide, 2013.
- [82] R. Artiaga, S. Naya, A. García, F. Barbadillo and L. García, "Subtracting the Water effect from DSC Curves by using Simultaneous TGA Data", J. Thermochemica Acta, 428, 137–139, 2005.
- [83] G. Klančnik¹, J. Medved and P. Mrvar, "Differential Thermal Analysis (DTA) and Differential Scanning Calorimetry (DSC) as A Method of Material Investigation", J. Materials and Geoenvironment, 57(1), 127–142, 2010.
- [84] D. T. Harvey, "Modern Analytical Chemistry", 1st edition, The McGraw-Hill Companies, 136– 257, 2000.
- [85] M. E. Brown, "Introduction to Thermal Analysis Techniques and Applications", 2nd edition, Springer Science and Business Media, 1-5, 2001.
- [86] C. R. Navarro, E. R. Agudo, A. Luque, A. B. R. Navarro and M. O. Huertas, "Thermal Decomposition of Calcite: Mechanisms of Formation and Textural Evolution of CaO Nanocrystals", J. American Mineralogist, 94, 578–593, 2009.
- [87] S. Vyazovkin, "Thermal analysis", Anal. Chem., 16, 80–4301, 2008.
- [88] P. Budrugaec and E. Segal, "The Application of the Thermo-gravimetric Analysis (TGA) and of the Differential Thermal Analysis (DTA) for rapid Thermal Endurance Testing of Electrical Insulating Materials", Physical Chemistry, Faculty of Chemistry, University of Bucharest, Bd. Elisabeta. Romania, 1-2, 241–246, 2005.

- [89] H. A. Laitenen and G. W. Ewing, "A History of Analytical Chemistry", eds., The Division of Analytical Chemistry of the American Chemical Society: Washington, D.C., 103–445, 1977.
- [90] A. Cooper, M. A. Nutley and A. Wadood, "Differential Scanning Microcalorimetry" in S. E. Harding and B. Z. Chowdhry (Eds.), "Protein-Ligand Interactions: Hydrodynamics and Calorimetry", Oxford University Press, Oxford New York, 287–318, 2000.
- [91] W. J. Boettinger, U. R. Kattner, K. W. Moon and J. H. Perepezko, "DTA and Heat-flux DSC Measurements of Alloy Melting and Freezing", in "Methods for Phase Diagram Determination" edited by J. –C. Zhao, Elsevier, Oxford, 151–221, 2007.
- [92] R. Sabbah, A. Xu-Wu, J. S. Chickos, M. L. P. Leitão, M. V. Roux and L. A. Torres, "Reference materials for calorimetry and differential thermal analysis", *J. Thermochemica Acta* , 331, 93–204, 1999.
- [93] M. H. Chiu and E. J. Prenner, "Differential Scanning Calorimetry: An invaluable Tool for a detailed Thermodynamic Characterization of Macromolecules and their Interactions", *J. Pharm. Bioall. Sci.*, 3(1), 39–59, 2011.
- [94] G. Bruylants, J. Wouters and C. Michaux, "Differential Scanning Calorimetry in Life Science: Thermodynamics, Stability, Molecular Recognition and Application in Drug Design", *J. Current Medicinal Chemistry*, 12, 2011–2020, 2005.
- [95] B. Bilyeu, W. Brostow and K. P. Menard, "Epoxy Thermosets and their Applications in Thermal Analysis", *J. Materials Education*, 22(4-6), 107–129, 2000.
- [96] J. E. Daw, "Measurement of Specific Heat Capacity Using Differential Scanning Calorimeter", Idaho National Laboratory Idaho Falls, 8, 15056, 2008.

- [97] M. Pyda, Y. K. Kwon, B. Wunderlich, "Heat Capacity Measurement by Sawtooth Modulated Standard Heat-Flux Differential Scanning Calorimetry with Sample Temperature Control", *J. Thermochemica Acta*, 367-368, 217–227, 2001.
- [98] M. J. Onill, "Measurements of Specific Heat Functions by Differential Scanning Calorimetry", The Perkin-Elmer Corp., Norwalk, Conn., 38(10), 1331–1336, 1996.
- [99] R. B. M. T. Bldg, "Specific Heat Capacity measurements Using DSC I", SII NanoTechnology Inc, TA No.11, 1981.
- [100] P. Atkins, J. D. Paula, "Physical Chemistry", Oxford university press, 8th edition, 78–100, 2006.
- [101] F. A. Carey, "Organic Chemistry", 4th edition, The McGraw-Hill Companies, Printed in the United States of America, 487-523, 2000.
- [102] J. Clayden, N. Greevs and Stuart Warren, "Organic Chemistry", 2nd edition, Oxford university press, 65-78, 2012.
- [103] R. T. Morrison, "Organic chemistry", 3rd edition, Universal Library, 410-1151, 2005.
- [104] T. Sato, "Thermal Decomposition of Inorganic and Organic Salts of Aluminum and Thermal Transformation of Formed Aluminas", *J. Netsui Sokutei*, 13(3), 113–122, 1986.
- [105] F. Bustanafruz, M. Jafar-Tafreshi and M.Fazil, "Studies on Thermal Decomposition of Aluminum Sulfate to Produce Alumina Nano Structure", *J. of Nano Structures*, 2, 463–468, 2013.
- [106] G. Lefèvre, "In situ Fourier-transform infrared spectroscopy studies of inorganic ions adsorption on metal oxides and hydroxides", *J. Advances in Colloid and Interface Science*, 107, 109–123, 2004.
- [107] D. N. Goldstein, J. A. McCormick and S. M. George, "Al₂O₃ Atomic Layer Deposition with Trimethylaluminum and Ozone Studied by in

- Situ Transmission FTIR Spectroscopy and Quadrupole Mass Spectrometry", *J. Phys. Chem.*, 112, 19530–19539, 2008.
- [108] A. Maccoll, J. Aspden and R. A. Ross, "Homogeneous Gas-Phase Pyrolysis of Acetamide", *J. Trans. Faraday Soc.*, 64, 965–976, 1968.
- [109] M. Okazaki and T. Funazukuri, "Decomposition of Acetamide and Formamide in Pressurized Hot Water", *J. Mat. Sci.*, 41, 1517, 2006.
- [110] International Center of Diffraction Data (ICDD), 81-1835. Holzar J., McCarthy G., North Dakota State University, Fargo, North Dakota, USA, Grant-in-Aid, 1991.
- [111] I. V. Tokmakov, S. Alavi and D. L. Thompson, "Urea and Urea Nitrate Decomposition Pathways: A Quantum Chemistry Study", *J. Phys. Chem. A*, 8, 2759–2770, 2006.
- [112] J. P. Chen, and K. Isa, "Thermal Decomposition of Urea and Urea Derivatives by Simultaneous TG/(DTA)/MS", *J. Mass Spectrom. Soc. Jpn.*, 46(4), 299–303, 1998.
- [113] International Center of Diffraction Data (ICDD), 42-1429. Zacek, V., *Acta Univ. Carol., Geol.*, 315, 1988.
- [114] H. M. A. Abood, A. P. Abbott, A. D. Ballantyne and K. S. Ryder, "Do All Ionic Liquids need Organic Cations? Characterisation of $[\text{AlCl}_2 \cdot n\text{Amide}]^+ \text{AlCl}_4^-$ and Comparison with Imidazolium based Systems", *J. Chem. Commun.*, 47, 3523–3525, 2011.
- [115] K. Fukumoto, M. Yoshizawa and H. Ohno, "Room Temperature Ionic Liquids from 20 Natural Amino Acids", *J. Am. Chem. Soc.*, 127(8), 2398–2399, 2005.
- [116] M. B. Abdul Rahman, K. Jumbri, M. Basri, E. Abdulmalek, K. Sirat and A. B. Salleh, "Synthesis and Physico-Chemical Properties of New Tetraethylammonium-based Amino Acid Chiral Ionic Liquids", *J. Molecules*, 15(4), 2388–2397, 2010.

- [117] H. Ohno, "Physical Properties of Ionic Liquids for Electrochemical Applications", in book of, F. Endres, D. MacFarlane and A. Abbott, "Electrodeposition from Ionic Liquids", Wiley-VCH Verlag GmbH & Co. KGaA, 47–82, 2008.
- [118] R. W. Bradshaw and N. P. Siegel, "Molten Nitrate Salt Development for Thermal Energy Storage in Parabolic Trough Solar Power Systems", *J. of Energy Sustainability*, 1–7, 2008.
- [119] J. Yang, Q. Zhang, L. Zhu, S. Zhang, J. Li, X. Zhang and Y. Deng, "Novel Ionic Liquid Crystals based on N-Alkylcaprolactam as Cations", *J. Chem. Mater.*, 19(10), 2544–2550, 2007.
- [120] A. K. Galwey and M. E. Brown, "Thermal Decomposition of Ionic Solid", In series of studies in physical and theoretical chemistry 86, Amsterdam-Lausanne- New York- Oxford- Shannon- Singapore-Tokyo, 1st edition, 291–308, 1999.

الملخص:

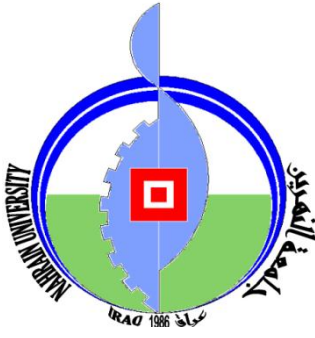
درست خواص بعض السوائل الايونية بدرجة حرارة الغرفة لترشيحها في التطبيقات الحرارية كوسائط خازنة للحرارة وموانع ناقلة للحرارة لخمسة سوائل أيونية حضرت من شب الامونيوم كملح لاعضوي مع اليوريا أو الاستمايد كمركبات عضوية, و نترات الالمنيوم المائية مع مركبات اليوريا او الاستمايد بنسب مولية مختلفة, لوحدها او مع إضافة بعض المواد المحسنة لدراسة التأثير التآزري باستخدام التحليل الحراري الوزني, المسعر الحراري التفاضلي, حيود الأشعة السينية, وطيف الأشعة تحت الحمراء ومقياس التوصيلية الكهربائية. كما تمت دراسة الخواص الفيزيائية الحرارية مثل الانتالبي, الحرارة النوعية وسعة خزن الطاقة الحرارية. وإمتازت السوائل الايونية لنترات الالمنيوم-أستمايد بالنسبة المولية (22:1) وشب الامونيوم-يوريا بالنسبة المولية (5:1) لوحدها أو بأضافة بعض المواد بكثافة عالية وأستقرارية كيميائية عالية وحرارة نوعية عالية و مدى حراري واسع. النتائج تشير الى أن السوائل الايونية لوحدها او بأضافة بعض المواد من الممكن اعتبارها كمرشحات واعدة لأستخدامها كوسائط خازنة للحرارة وموانع ناقلة للحرارة.

من جهة أخرى, هيدوكسيد الفلز القلوي (هيدوكسيد الصوديوم) مع نترات الالمنيوم المائية-يوريا بالنسبة المولية (1.2:1) وهيدروكسيد الكالسيوم مع كبريتات الامونيوم الالمنيوم المائية-يوريا بالنسبة المولية (5:1) ساهمت في زيادة سعة خزن الطاقة الحرارية لهذه السوائل الايونية. في حين أن إضافة هيدوكسيد الصوديوم الى نترات الالمنيوم المائية-استمايد بالنسبة المولية (22:1) اعطت أستقرارية حرارية وسعة خزن للطاقة الحرارية أقل لهذا السائل الايوني.

لتحسين الخصائص تم إضافة بعض الاكاسيد الفلزية من أجل بيان التأثير التآزري لهذه المركبات, حيث أن إضافة الفلزات القلوية الترابية (أوكسيد المغنيسيوم وأوكسيد الكالسيوم) الى كبريتات الامونيوم الالمنيوم المائية-يوريا بالنسبة المولية (5:1) وأوكسيد الباريوم الى نترات الامنيوم المائية-يوريا بالنسبة المولية (1.2:1) قد قللت من الاستقرارية الحرارية والحرارة النوعية وسعة خزن الطاقة الحرارية بالمقارنة مع السائل الايوني لوحده.

علاوة الى ذلك, إضافة بعض أكاسيد العناصر الانتقالية (أوكسيد كبريتات الفناديوم المائية وأوكسيد النحاس وأوكسيد الزنك) الى كبريتات الامونيوم الالمنيوم المائية-يوريا بالنسبة المولية (5:1) زادت من الاستقرارية الحرارية و سعة خزن الطاقة الحرارية للسائل الايوني الاصلي, بينما أضاف اوكسيد

النكل الى السائل الايوني كبريتات الامونيوم الالمنيوم المائية-يوريا بالنسبة المولية (5:1) حسنت من
الاستقرارية الحرارية له فقط.



جمهورية العراق
وزارة التعليم العالي والبحث العلمي
جامعة النهرين
كلية العلوم
قسم الكيمياء

تحري الخواص الحرارية لبعض السوائل الايونية الحاوية على اليوريا والاستمايد

رسالة
مقدمة إلى كلية العلوم/ جامعة النهرين
كجزء من متطلبات نيل درجة الماجستير في علوم الكيمياء

من قِبَلِ
هدى سلام عبد
بكالوريوس 2012

إشراف
الاستاذ المساعد الدكتور
هادي محمد علي عبود

أيار
2015 م

رجب
1436 هـ